2018

COLONIZATION OF AND ADAPTATION TO TIDAL MARSHES IN THE SAVANNAH SPARROW (PASSERCULUS SANDWICHENSIS)

Phred M. Benham

Let us know how access to this document benefits you.

COLONIZATION OF AND ADAPTATION TO TIDAL MARSHES IN THE SAVANNAH

SPARROW (*PASSERCULUS SANDWICHENSIS*)

By

PHRED M. BENHAM

M.S. Biology, University of New Mexico, Albuquerque, NM, 2012
B.S. Biological Sciences, Louisiana State University, Baton Rouge, LA, 2006

Dissertation

presented in partial fulfillment of the requirements
for the degree of

Doctor of Philosophy
in Organismal Biology, Ecology, and Evolutuon

The University of Montana
Missoula, MT

May 2018

Approved by:

Scott Whittenburg, Dean of The Graduate School
Graduate School

Zachary A. Cheviron, Chair
Division of Biological Sciences

Creagh Breuner
Division of Biological Sciences

Douglas J. Emlen
Division of Biological Sciences

Jeffrey M. Good
Division of Biological Sciecnes

Andrew Whitehead
Department of Environmental Toxicology, University of California Davis

i

Benham, Phred M., PhD, Spring 2018   Organismal Biology, Ecology, and Evolution

Colonization of and adaptation to tidal marshes in the Savannah Sparrow (*Passerculus sandwichensis)*

Chairperson: Dr. Zachary A. Cheviron

ABSTRACT: Intraspecific patterns of geographic variation reflect a dynamic history of colonization and divergence in response to spatially varying selective pressures. Analysis of this phenotypic variation has long stimulated biological thought*,* yet many outstanding questions remain regarding the ecological and evolutionary mechanisms driving patterns of geographic variation. In my dissertation, I collected data on demographic history, physiological traits contributing to salinity tolerance, and acclimation responses to different salinities to elucidate the mechanisms shaping colonization and adaptive divergence in tidal marsh populations of Savannah Sparrows (*Passerculus sandwichensis*). Specifically, I addressed two main questions related to adaptive divergence in this species: (1) how do demographic and ecological forces interact to shape spatial patterns of local adaptation? And (2) what role does ancestral plasticity play in adaptation to new environments?

In Chapter 1, phylogeographic analyses of a population genomic dataset revealed that tidal marshes have been colonized twice by Savannah Sparrows and include a younger, less isolated tidal marsh lineage from the California coast, and an older, more isolated lineage from northwest Mexico. In the second chapter, I assessed how variation in demographic history and environmental factors interacted to shape patterns of divergence in physiological traits associated with salinity tolerance across multiple tidal marsh populations. Finally, in Chapter 3, I compared acclimation responses to salinity in freshwater-adapted and tidal marsh Savannah Sparrows to test whether ancestral plasticity may have contributed to tidal marsh adaptation in this species. The outcomes of adaptation to spatially varying selective pressures will be contingent on many interacting ecological, demographic, and evolutionary processes. The results of my dissertation show that demographic history, variation in selective pressures, and plasticity all contributed to patterns of adaptive divergence within tidal marsh Savannah Sparrows. This underscores the necessity of considering multiple interacting processes to thoroughly understand the evolution of geographic variation.

Finally, a huge thank you to Libby Beckman who has been a constant companion throughout my graduate career. Reveling in the wonders of the natural world with her has helped make the whole process fun and exciting.

TABLE OF CONTENTS

OVERVIEW:

Intraspecific patterns of geographic variation reflect a dynamic history of colonization and divergence in response to spatially varying selective pressures. Analysis of this phenotypic variation has long stimulated biological thought (Bergmann 1847, Darwin 1859, Dobzhansky 1937, Mayr 1963), yet many outstanding questions remain regarding the ecological and evolutionary mechanisms driving patterns of geographic variation (Kawecki & Ebert 2004; Savolainen et al. 2013). For instance, how does population history interact with selective pressures to shape local adaptation? Under what contexts does gene flow promote versus constrain adaptive divergence? What role does plasticity play in adaptive divergence between environments? What is the genetic architecture underpinning locally adapted traits? Theoretical explorations provide valuable insights into these questions (e.g. Lenormand 2002; Lande 2009), however, empirical examples from a diversity of natural systems will be essential for evaluating these insights in light of different ecological, functional, and demographic contexts. In my dissertation, I collected data on demographic history, physiological traits contributing to salinity tolerance, and acclimation responses to different salinities to elucidate the mechanisms shaping colonization and adaptive divergence in tidal marsh populations of Savannah Sparrows (*Passerculus sandwichensis*). Specifically, I addressed two main questions related to adaptive divergence in this species: (1) how do demographic and ecological forces interact to shape spatial patterns of local adaptation? And (2) what role does ancestral plasticity play in adaptation to new environments?

In Chapter 1, I characterized the phylogeographic and demographic history of Savannah Sparrows across their entire North American distribution to provide demographic context for interpreting results in subsequent chapters. A mtDNA-based phylogeography of the Savannah

1

Sparrow previously identified two sympatric, but divergent (~2%) mitochondrial haplotype clades within the widespread, nominate subspecies group and a third clade that consisted of birds sampled from northwest Mexico. I revisited this phylogeography using a population genomic dataset to better resolve the demographic and phylogeographic history of Savannah Sparrows. Two genetic clusters were identified in the genomic dataset corresponding to (1) the nominate subspecies group, which includes tidal marsh populations from coastal California, and (2) birds from northwest Mexico that are entirely restricted to tidal marsh environments. Following divergence, the nominate clade seems to have maintained a large, stable population, indicating that divergent mitochondrial lineages arose within a panmictic population. Simulations based on parameter estimates from this model further confirmed that this demographic history could produce observed levels of mtDNA diversity. Results also show that tidal marshes have been colonized twice by Savannah Sparrows and include a younger, less isolated tidal marsh lineage along the California coast, and an older, more isolated lineage from northwest Mexico.

A persistent challenge in making phenotype-environment associations in analyses of geographic variation is understanding how ecological and demographic factors interact to shape adaptive outcomes. In Chapter 2, I tackled this issue by analyzing patterns of divergence in physiological traits associated with salinity tolerance across replicate tidal marsh populations of the Savannah Sparrow. I collected data on six osmoregulatory traits from 10 tidal marsh and 3 interior populations and compared patterns of trait divergence between interior and tidal marsh populations within the context of ecological and demographic variation among tidal marsh populations. Based on these analyses, variation in divergence in four osmoregulatory traits, kidney mass, medulla volume, plasma osmolality, and total evaporative water loss (TEWL), was best explained by variation in genetic divergence (Fst) from interior populations. In contrast, two

other traits, urine osmolality and urine:plasma osmolality ratio (measures of salt excretion ability), were best explained by environmental variation (May-June maximum temperature) among the different sampling sites.

The role ancestrally plastic responses play in adaptation to new environments remains a heavily debated question in evolutionary biology. In Chapter 3, I assessed support for a series of predictions consistent with the hypothesis that selection on ancestral plasticity can facilitate colonization of new environments. These predictions included: (1) that ancestral populations will exhibit acclimation responses in the adaptive direction; (2) there will be evidence for evolutionary divergence in reaction norms in the derived population; and (3) selection has canalized acclimation responses resulting in reduced variance around environmentally induced phenotypic means. I evaluated each of these predictions across an integrated suite of behavioral and physiological traits that contribute to osmoregulatory performance in tidal marsh environments. I found that evidence for accommodation of ancestral plasticity in adaptation to tidal marshes appears to be highly trait specific. Specifically, I found support for all three predictions in some traits (e.g. plasma volume, drinking responses), while other traits provided only mixed support (e.g. medulla volume), and still others did not exhibit any evidence that ancestral plasticity contributed to divergence between environments (e.g. maximum urine concentration). Variable evolutionary responses across these different traits that contribute to osmoregulatory performance suggest different evolutionary mechanisms can shape divergence in different components of the same integrated system.

The outcomes of adaptation to spatially varying selective pressures will be contingent on a number of interacting ecological and evolutionary processes. In my dissertation, I demonstrate that understanding patterns of geographic variation requires simultaneous consideration of both

population history and ecological variation. Secondly, that adaptive plasticity in an ancestral population can play an important role in facilitating colonization and adaptation to different environments. In addressing both questions I found that the conclusions were dependent on the traits being analyzed. In many cases the answers to outstanding questions in local adaptation will be similarly context dependent. This underscores the necessity of considering multiple interacting processes to thoroughly understand how patterns of geographic variation evolve.

REFERENCES:

Bergmann, C. 1847. Über die Verhältnisse der Wärmeökonomie der Thiere zu ihrer Grösse. *Göttinger Studien,* 3: 595-708

Darwin, C. 1859. *On the origin of species.* John Murray, London, UK.

Dobzhansky, T. 1937. *Genetics and the origin of species.* Columbia University Press, New York, NY.

Kawecki, T. J., & Ebert, D. 2004. Conceptual issues in local adaptation. *Ecology Letters*, 7: 1225-1241.

Lande, R. 2009. Adaptation to an extraordinary environment by evolution of phenotypic plasticity and genetic assimilation. *Journal of Evolutionary Biology* 22: 1435-1446.

Lenormand, T. 2002. Gene flow and the limits to natural selection. *Trends in Ecology and Evolution*, 17: 183-189.

Mayr, E. 1963. *Animal species and evolution.* Harvard University: Belknap Press, Cambridge, MA.

Savolainen, O., Lascoux, M., & Merilä, J. 2013. Ecological genomics of local adaptation. *Nature Reviews. Genetics*, 14: 807-20.

CHAPTER 1:

Divergent mitochondrial lineages arose within a large, panmictic population of the

Savannah Sparrow (*Passerculus sandwichensis*).

Phred M. Benham, Zachary A. Cheviron

Division of Biological Sciences, University of Montana, 32 Campus Dr. HS104, Missoula, MT
59812

ABSTRACT: Unusual patterns of mtDNA diversity can reveal interesting aspects of a species'
biology. However, making such inferences requires discerning among the many alternative
scenarios that could underlie any given mtDNA pattern. Next-generation sequencing methods
provide large, multi-locus datasets with increased power to resolve unusual mtDNA patterns. A
mtDNA-based phylogeography of the Savannah Sparrow previously identified two sympatric,
but divergent (~2%) clades within the nominate subspecies group and a third clade of northwest
Mexico birds. We revisited the phylogeography of this species using a population genomic
dataset to resolve the processes leading to the evolution of sympatric and divergent mtDNA
lineages. We identified two genetic clusters in the genomic dataset corresponding to (1) the
nominate subspecies group, and (2) Mexican birds. Following divergence, the nominate clade
maintained a large, stable population, indicating that divergent mitochondrial lineages arose
within a panmictic population. Simulations based on parameter estimates from this model further
confirmed that this demographic history could produce observed levels of mtDNA diversity.
Patterns of divergent, sympatric mtDNA lineages are frequently interpreted as admixture of
historically isolated lineages. Our analyses reject this interpretation for Savannah Sparrows and

underscore the need for genomic datasets to resolve the evolutionary mechanisms behind

anomalous, locus-specific patterns.

KEYWORDS: *Passerculus,* Passerellidae, phylogeography, genotyping-by-sequencing,

mitochondrial DNA

INTRODUCTION:

The early reliance on mtDNA in phylogeographic studies has uncovered a litany of

mtDNA patterns that are anomalous when compared to other loci. Prominent examples include

mtDNA haplotype sharing among divergent species (e.g. Andersson 1999; Weckstein et al.

2001; Beckman & Witt 2015; Good et al. 2015; Sloan et al. 2016), and deeply divergent, but

sympatric mtDNA lineages within a single species (e.g., Quinn et al. 1992; Spottiswoode et al.

2011; Hogner et al. 2012; Xiao et al. 2012; Giska et al. 2015). Determining the processes that

give rise to these discordant mtDNA patterns can point to intriguing aspects of the species'

biology (e.g. Spottiswoode et al. 2011), but doing so requires the consideration of several

alternative demographic histories. Unfortunately, in most cases, data are not available to tease

apart different demographic hypotheses, and we are left to speculate about the potential

evolutionary drivers of these unusual mtDNA patterns. As genomic datasets become the norm

for phylogeographic inference, new opportunities are arising to revisit these unexpected and

apparently anomalous phylogeographic patterns revealed by earlier single locus studies. The

scale of these population genomic datasets promises to provide unparalleled resolution for

demographic inference. This will enable rigorous tests of competing hypotheses and a deeper

understanding into the evolutionary mechanisms that underlie discordant patterns in heavily used

loci, such as mtDNA.

One such discordant pattern is the presence of broadly sympatric, but deeply divergent (>2% sequence divergence) mtDNA clades within an otherwise panmictic species. This pattern is widely encountered in mtDNA studies of animals (e.g. Quinn 1992; Hoelzer et al. 1994 Spottiswoode et al. 2011; Hogner et al. 2012; Xiao et al. 2012; Block et al. 2015; Giska et al. 2015), and it is most frequently interpreted as evidence for the merger of historically isolated lineages (e.g. Quinn 1992; Avise 2000; Hogner et al. 2012). The lack of recombination in the mitochondrial genome, allows for the persistence of divergent mtDNA haplotypes that arose in isolation even as rampant gene flow erodes genetic structure across the nuclear genome (Block et al. 2015). A recent and well-supported example can be found in a Madagascar bird species, the spectacled tetraka (*Xanthomixis zosterops*). Although this species does not exhibit any evidence of population structure in the nuclear genome, it harbors several divergent and sympatric mitochondrial haplotypes (~5% sequence divergence) (Block et al. 2015). Importantly, the authors also found evidence of associations between mtDNA haplogroups and lineages of host-specific chewing lice, corroborating the hypothesis that this species experienced a history of isolation followed by recent merger. Although this represents one empirical example supporting a history of recent admixture between historically isolated mtDNA lineages, many studies lack sufficient corroborating evidence to exclude other potential explanations (e.g. Quinn et al. 1992; Hogner et al. 2012; Giska et al. 2015).

Historical isolation is not always necessary to generate divergent mtDNA lineages within a population. Due to characteristics of the mitochondrial genome, several alternative population histories could also result in divergent, but sympatric mtDNA lineages. First, the reduced recombination rate of the mitochondrial genome can result in presence of multiple mtDNA haplotypes that arose within a large panmictic population and transiently persist through

stochastic lineage sorting processes (Slatkin & Hudson 1991; Hudson & Turelli 2003). Similarly, this process can lead to mtDNA geographic structure in the absence of a barrier (Irwin 2002). Second, the thirteen protein-coding genes found in the animal mitochondrial genome encode subunits of key proteins within the electron transport chain, which may be a frequent target of selection (Ballard & Whitlock 2004). Experimental evolution studies have shown that selection on mitochondrial function can lead to sympatric, but divergent mtDNA haplotypes through processes such as negative frequency dependent selection (e.g., Kazancioğlu & Arnqvist 2014). Third, uniparental inheritance of the mitochondrial genome can also lead to discordant mitochondrial and autosomal genealogies in cases where the sexes differ in life history attributes (e.g., Spottiswoode et al. 2011). Finally, the mitochondrial genome has been found to be highly susceptible to introgression among populations relative to elements of the nuclear genome, resulting in discordance between mitochondrial and nuclear structure (Bachtrog et al. 2006, Currat et al. 2008; Mims et al. 2010; Good et al. 2015; Sloan et al. 2016). Sympatric and divergent mtDNA patterns have been documented in a wide range of taxa, but in most instances, independent datasets to discern among these alternative hypotheses are lacking. Demographic analysis of population genomic datasets presents a promising opportunity to explicitly test competing hypotheses of the processes that give rise to this anomalous mtDNA pattern.

The Savannah Sparrow (*Passerculus sandwichensis*) is one example where previous mtDNA phylogeographic analyses uncovered a pattern of deeply divergent and broadly sympatric mitochondrial lineages, but the initial study lacked any corroborating evidence to understand how this pattern arose (Zink et al. 2005). The Savannah Sparrow is one of the most widespread North American songbirds with populations found in a range of environments spanning tundra, prairie, meadow, and salt marsh habitats (Wheelwright & Rising 2008). The 18

subspecies currently recognized (Dickinson & Christidis 2014) are often classified into several subspecies groups that have been treated as distinct species by some authors (e.g. Rising 2017). The subspecies groups include: (1) the largely migratory nominate group found across most of the breeding range; (2) the *beldingi* group that is resident along the Pacific coast of southern California and the Baja peninsula; (3) the *rostratus* group of coastal Sonora, Mexico; and (4) *P. s. sanctorum* of Isla San Benito off the west coast of Baja California (Fig. 1). Despite this ecological and taxonomic diversity, the previous survey of mtDNA found little evidence for significant population structure across the species' distribution, however, the nominate subspecies group contained two broadly sympatric mtDNA clades that exhibited approximately 2% sequence divergence (Fig. 2; Zink et al. 2005). A third clade, sister to one of the nominate clades (B), included salt marsh residents from the *beldingi, rostratus* and *sanctorum* subspecies groups of northwestern Mexico. The authors did not find evidence for selection in the two clades based on MacDonald-Kreitman tests, and it is unlikely that savannah sparrows exhibit sex-based differences in life history (Wheelwright & Rising 2008). This leaves three potential explanations of the observed mtDNA patterns in the nominate group: **(1)** introgression of mitochondrial haplotypes exceeds rate of nuclear introgression between two historically isolated populations; **(2)** the two independently sorting haplotype groups arose in a large, panmictic population; **(3)** complete admixture of two historically isolated populations gave rise to the existence of divergent sympatric mtDNA clades. Hypotheses one and three are distinguished by the presence or absence of differential introgression of mitochondrial and nuclear loci. Hypothesis two differs from the others by not invoking a period of historical isolation.

To tease apart these three hypotheses we generated a large SNP dataset with dense geographic sampling across the Savannah Sparrow range using a genotyping-by-sequencing

(GBS) approach (Parchman et al. 2012). We analyzed this dataset using several methods to assess patterns of geographic structure, and infer the historical demography of Savannah Sparrows. To distinguish the three competing hypotheses, we made the following predictions. The first hypothesis of extensive, bidirectional mtDNA introgression with reduced nuclear introgression would be supported by evidence of nuclear population structure and a reduction of historical introgression of nuclear loci among populations within the nominate subspecies group. Conversely, a lack of population structure in the nuclear genome would either point to the second hypothesis of mtDNA haplotypes arising within a large, panmictic population, or to the third hypothesis of complete admixture of historically isolated lineages. To discern the second and third hypotheses, we fit variations on these two demographic models to the site frequency spectrum (SFS), and used population genetic parameter estimates from the best-fit models to parameterize coalescent simulations. The output of these simulations was then used to determine which models could give rise to the observed patterns of mtDNA diversity. This study represents the first attempt to understand the evolution of divergent, sympatric mtDNA lineages using a genomic dataset. Our approach should be broadly applicable to a range of taxa providing deeper insights into the evolution of anomalous locus-specific patterns.

METHODS:

Sampling:

We obtained tissue or blood samples from 191 individual Savannah Sparrows, including 15 of the 18 currently recognized subspecies (Wheelwright & Rising 2008; Dickinson & Christidis 2014; Appendix 1: Table 1.1). We selected four outgroups based on a recent phylogeny of the family Passerellidae (Klicka et al. 2014): Henslow's Sparrow (*Ammodramus*

henslowii), Le Conte's Sparrow (*Ammodramus leconteii*), Song Sparrow (*Melospiza melodia*), and Vesper Sparrow (*Pooecetes gramineus*). For all samples, we extracted whole genomic DNA from muscle tissue or whole blood using a Qiagen DNeasy Blood & Tissue extraction kit following the manufacturer's protocols (Valencia, CA).

mtDNA sequencing and analysis:

To more broadly assess the geographic distribution of the two previously identified mtDNA haplogroups, we sequenced the mtDNA gene NADH dehydrogenase subunit 2 (*ND2*) from 102 individuals of the nominate subspecies that were not previously included in any study (see Appendix 2 for sequencing details). We also obtained *ND2* sequence data from 110 individuals previously sequenced by Zink et al. (2005) and accessioned in GenBank (AY584869.1-AY584980.1) and *Ammodramus henslowii* (AY584982.1) served as an outgroup (as in Zink et al. 2005). Sequences were manually assembled and edited using Geneious v. 10.0.6 (Biomatters, Auckland, NZ) and aligned using MUSCLE v. 3.7 (Edgar 2004).

We used BEAST v. 1.8.4 (Drummond et al. 2012) to estimate phylogenetic structure and divergence times within the *ND2* dataset. The TN93 model of substitution and partitioning by codon position was identified as the best partitioning scheme, using PartitionFinder2 (Lanfear et al. 2016). We generated input files using BEAUti v. 1.8.4 (Drummond et al. 2012) with a relaxed lognormal clock model (Drummond et al. 2006), a mean substitution rate of 0.0125/myr for *ND2* (Smith & Klicka 2010), and a standard deviation of 0.4 (Walstrom et al. 2011). We ran two independent MCMC chains for 200 million generations each, sampling every 20,000 steps on the CIPRES science portal (Miller et al. 2010). We ensured priors all had an ESS >200 using TRACER v. 1.6.0 (Rambaut et al. 2014). Trees were merged in LogCombiner v. 1.8.4 (Drummond et al. 2012) and 10% of trees were removed in TreeAnnotator v. 1.8.4 (Drummond

et al. 2012). Based on the resulting phylogenetic structure, individuals were assigned to different mtDNA clades and the proportion of individuals in each clade per sampling locality were mapped in R (https://www.r-project.org/) to visualize their geographic distribution.

Genotyping-by-sequencing methods:

Genotyping-by-sequencing (GBS) libraries were prepared following Parchman et al. (2012). Briefly, we digested whole genomic DNA with two restriction enzymes (*Eco*RI and *Mse*1), ligated adaptor sequences with unique barcodes for each individual, and performed a PCR amplification. We then performed a gel extraction to select 500-600 bp fragments and purified extracts using a Qiagen Gel Extraction kit (Valencia, CA). Libraries were submitted to the W. M. Keck Sequencing Center at the University of Illinois, Urbana-Champaign for sequencing on an Illumina HiSeq 2500 platform. Individuals were sequenced on three separate flow-cell lanes, each resulting in over 200 million, 100-nt single-end reads with quality scores greater than 30, and a mean of 1,794,006 reads per individual.

Reads were demultiplexed and barcodes removed using process_radtags in STACKS (Catchen et al. 2011). This resulted in final reads 89bp in length, which were assembled *de novo* using the STACKS pipeline (Catchen et al. 2011; 2013). 89 bp reads that have been aligned and assembled into overlapping 'stacks' are referred to as loci for the rest of the paper. The minimum depth of coverage (m), maximum distance between stacks (M), and the maximum distance to align secondary reads to primary stacks (n) can significantly impact the resulting number of loci and the total number of SNPs identified within them (Catchen et al. 2011; Mastretta-Yanes et al. 2014; Paris et al. 2017). To address this issue, we performed multiple runs of STACKS on a subset of our data (n=24 individuals) while varying m from 2-10 (with M=2, n=2), M from 2-8 (with m=3, n=2), and n from 1-5 (with m=3, M=2). We compared the influence of parameter

variation on the number of loci and the total number of SNPs called in the STACKS pipeline, and on patterns of genetic structure (see Appendix 2 for further details). We found that the number of loci and SNPs decreased sharply with increasing m, increased and plateaued with $M \geq$ 3, and n had little influence (Appendix 3: Fig. 3.1). All datasets resulted in similar patterns of genetic structure (Appendix 3: Fig. 3.2). Based on these results, STACKS analysis of the full dataset was performed with the following parameter settings: m=3, M=3, and n=3. Once within individual reads are assembled into loci, the STACKS pipeline then matches loci across individuals to assemble a catalog of loci that are shared across all individuals (Catchen et al. 2011). Given the computational costs of building a catalog with all 195 individuals, we produced a catalog using 73 individuals total derived from 30% of individuals from each sampling locality plus the four outgroup species. This design should ensure that we include all common variants in the catalog. Once the catalog was assembled, loci from all 195 individuals were matched against the catalog in sstacks and genotyped at this panel of loci. Finally, a number of output files were generated for downstream analyses using the populations module of STACKS. For all population structure analyses (see next section) four output files were generated using a single, randomly-sampled SNP per locus and the minimum proportion of individuals genotyped at each locus (–r parameter) was set to 0.75, 0.8, 0.9, or 0.95. These different output files are referred to as our 25%, 15%, 10%, and 5% missing datasets, respectively. The four categories represent arbitrary levels of missing data selected to determine whether patterns of population structure were robust to different levels of missing data. These four datasets included 13,058 to 200,791 SNPs (including outgroups) depending on the level of allowed missing data (5-25%), and without outgroups the datasets varied from 6,709 to 66,705 SNPs (Appendix 3: Table 3.1).

Population structure analyses:

We evaluated range-wide population structure using several complimentary methods. First, we performed principal components analysis on the SNP dataset for all 191 Savannah Sparrows using the function glPca in the r-package Adegenet 1.3-1 (Jombart & Ahmed 2011). To assess the influence of missing data on population structure we performed this analysis with 5%, 10%, 15%, and 25% missing data. We also divided the full dataset into Mexican (n=56) and nominate (n=135) groups and performed similar PCAs in Adegenet with these subsets to test for more subtle structure within these groups. Second, we evaluated genetic structure using the program fastSTRUCTURE (Raj et al. 2014). We performed several structure analyses that varied the setting for K from 1-10 on the full, Mexican, and nominate datasets for each level of missing data (5%, 10%, 15%, and 25%). We also explored how setting a simple or logistic allele frequency prior would impact our results as the logistic prior may perform better in cases with subtle structure (Raj et al. 2014). We used the chooseK.py tool within fastSTRUCTURE to determine the best-supported number of clusters (K) for each dataset. Finally, we performed phylogenetic analyses using RAxML v. 8.2.4 (Stamatakis 2014) on the CIPRES webportal (Miller et al. 2010). Again, these phylogenetic analysis were performed on SNP datasets with 5%, 10%, 15%, and 25% missing data. We accounted for biases due to using only variant sites with the Felsenstein correction (Leaché et al. 2015), which corrects the likelihood for the number of invariant sites present in the data (read length*number of loci – number of SNPs). All analyses were run using an ASC_GTRCAT model with 100 rapid bootstrap replicates to assess topological support.

Demographic analysis:

Our first hypothesis, introgression of mitochondrial haplotypes between clades in spite of reduced nuclear introgression, would be supported by an obvious pattern of population structure

in the nuclear genomes of the nominate subspecies group. However, a lack of nuclear structure could point to either our second hypothesis of mtDNA clades arising within a large, panmictic population or our third hypothesis of complete admixture of historically isolated lineages. To distinguish between these two latter hypotheses, we took a two-pronged approach. First, we fit a range of demographic models that encompass these two scenarios to the site frequency spectrum (SFS) of our SNP data in $\partial a \partial$i v. 1.7 (Gutenkunst et al. 2009). Second, we performed a series of coalescent simulations to determine whether parameter estimates from the best-fit models in $\partial a \partial$i could generate observed levels of mtDNA diversity. We repeated these two steps for both the SFS of the nominate population only and the joint SFS of the Mexican and nominate populations. The latter analysis was performed to account for any gene flow between Mexican and nominate populations, which if unaccounted for could bias the single population analyses.

The program $\partial a \partial$i does not handle missing data (Gutenkunst et al 2009). To account for this issue, we generated a SFS for our dataset based on a restricted number of individuals (Mexican=16; nominate=25) to maximize the number of loci that were shared across all individuals (see Appendix 2). This 41-individual dataset was further filtered to remove reads aligning to the z-chromosome, due to its smaller effective population size, and to only include loci with read depth $\geq$ 10 that were in Hardy-Weinberg equilibrium (α set to 0.05), to minimize the influence of sequencing errors (see Appendix 3: Fig. 3.3). This resulted in a final dataset of 24,382 SNPs from 8,614 loci. $\partial a \partial$i input files were created using the vcf2dadi function in the R package stackr v. 0.2.6 (Gosselin & Bernatchez 2016). Analyses were based on a folded SFS given high levels of missing data in outgroups sequenced for phylogenetic analyses, which makes them unsuitable for polarizing the SFS.

Analysis of the SFS:

We fit the following demographic models to the SFS of the nominate group (Appendix 3: Fig. 3.4) that would be consistent with our second hypothesis (history of panmixia): a constant population size, exponential growth, a bottleneck, and bottleneck followed by exponential growth (Appendix 3: Fig. 3.5). We also fit models related to our third hypothesis where a history of isolation was followed by admixture using two different approaches. First, we modeled an initial population split, allowed populations to evolve in isolation, the two populations then merged via admixture, and finally, following admixture one of the nominate populations is removed (the "ghost" population). Second, we divided the SFS into two populations based on their mitochondrial haplotype (A or B; see Fig. 2) and fit the SFS to an identical admixture model as above. These two separate approaches to model historical isolation followed by admixture were necessary as mitochondrial and nuclear genomes are unlinked making it difficult to assume that mtDNA divergence will also be reflected in the nuclear genome following secondary contact. Modeling a "ghost" lineage allows for introgression to occur from a second lineage without requiring an explicit assignment of certain individuals to either mtDNA lineage. We next ran a similar series of models in ∂a∂i on the joint SFS of the nominate and Mexican Savannah Sparrows (Appendix 3: Fig. 3.6). These models all involve a split between these two populations and model the various demographic scenarios with and without gene flow between populations. As for the single population analyses we ran a series of models consistent with a history of panmixia in the nominate population (second hypothesis) or secondary contact and admixture (third hypothesis).

For all models, 10 optimizations were run from different starting parameters using the perturb function in ∂a∂i with max number of iterations set to 10. To ensure that a global optimum for a given model had been reached we ran one final optimization with 50 iterations using the

16

parameter values estimated from the shorter run with the highest likelihood. We calculated

demographic parameter values from the estimated value of theta (4NeμL; L is sequence length)

based on a 1 year generation time for Savannah Sparrows (Wheelwright & Rising 2008) and the

average mutation rate for Passeriformes: 3.3×10^{-9} substitutions/site/year (Zhang et al. 2014).

We calculated uncertainty for parameter estimates using a non-parametric bootstrapping

approach: sampling with replacement over the 8,614 loci, generating frequency spectra from 100

resampled SNP datasets, and using these spectra to calculate parameter uncertainties using the

Godambe information matrix (GIM) in ∂a∂i (Coffman et al. 2016). We used an Akaike

information theoretic approach to identify the top demographic models. ∂a∂i uses composite

likelihoods to estimate model parameters, which assumes independence among SNPs in the SFS.

Given the presence of linked sites in our dataset (i.e. mean of 2.8 and median 2 SNPs per 89 bp

locus), AIC analyses could be associated with increased error and bias toward more complex

models and this analysis should be interpreted with caution (Coffman et al. 2016). However,

other studies apply AIC methods to composite likelihoods as a first approximation in ranking

models (e.g. Meier et al. 2017; Oswald et al. 2017). In cases where the model with the highest

likelihood included more parameters than hierarchically nested models with lower likelihood

values, we performed a likelihood ratio test with an adjustment based on the GIM to account for

the use of composite likelihoods (Coffmann et al. 2016).

Linking demographic parameters from nuclear genome to patterns of mtDNA diversity:

      Assuming that the mitochondrial genome experienced population demographic history

similarly to the nuclear genome, we assessed whether the demographic histories estimated using

∂a∂i analyses could result in the observed patterns of mtDNA diversity. To do this, we used point

estimates from all single-population ∂a∂i models to parameterize coalescent simulations of

mtDNA diversity in the program *ms* (Hudson 2002). The empirical mtDNA data (see *mtDNA sequencing methods*) were used to calculate nucleotide diversity, average number of pairwise differences (π), and the total number of segregating sites (*S*) for nominate populations in the program Arlequin 3.5 (Excoffier & Lischer 2010). A mtDNA mutation rate (μ) of 1.1×10^{-8}/site/generation (Weir & Schluter 2008) was used for calculation of effective population size (Ne) of *ND2* and theta values (Ne*μ*locus length). mtDNA Ne is predicted to be ¼ nuclear Ne, however, selection and other processes can lead to significant deviations from this prediction (Hudson & Turelli 2003; Lynch 2007). Rather than assume that mtDNA Ne was equal to 1/4 nuclear Ne, we directly estimated a range of Ne for *ND2* based on upper and lower bounds ($\pm$ 1 sd of the mean) of nucleotide diversity (0.011 ± 0.006) divided by μ (1.1×10^{-8}/site/generation). This gave bounds on Ne from 500,000 to 1,650,000. The $\partial a \partial i$ estimates of nuclear Ne for most demographic models also fall within the estimated range of mtDNA Ne when divided by four, further suggesting that our results are not biased by how we parameterized mtDNA Ne. We ran a model for each increment of 50,000 between these Ne bounds for a total of 24 different Ne models. For all models, π and *S* were calculated using the sample_stats function within *ms* across 100,000 simulations and the 99th, 95th, 75th, 25th, 5th, and 1st percentiles for the distribution of π and *S* were determined in R. We considered a given model to be likely to explain patterns of mitochondrial diversity if observed values of π and *S* fell between the 99th and 1st percentiles of the simulated distribution.

The influence of demographic parameter variation on panmixia versus admixture models*:*

Finally, we wanted to assess whether observed mtDNA patterns may be more likely to arise under a history of panmixia or admixture given different demographic conditions (e.g. varying population size and divergence time parameters). Specifically, are there areas of

18

parameter space where divergent, sympatric mtDNA haplogroups are more likely to have arisen under a history of isolation followed by admixture as opposed to within a panmictic population? To address this question we performed a series of simulations within *ms* where we modeled: (1) a panmictic population with constant Ne; (2) a panmictic population that experiences a bottleneck; (3) two populations that evolved in isolation then merged via admixture; and (4) an admixture model with a bottleneck occurring during isolation. In each of these models we varied the ancestral Ne, bottleneck Ne, Ne in isolation, and the timing of these events (see Table 1 for parameter values). We ran simulations for each combination of parameter values across a range of Ne from 100,000 to 2,000,000 by increments of 50,000. The number of individuals was set to 163 for all simulations (the same as 163 haploid mitochondrial chromosomes), the number of individuals for which observed mtDNA diversity statistics were calculated in the nominate clade. We ran 780 different parameter combinations for the constant population size model; 9,844 different parameter combinations for both the bottleneck and admixture models; and 7,488 combinations for the admixture with bottleneck model. For all of these different models we ran 25,000 simulations and calculated π, S, and their percentiles as above. Based on these simulations we calculated the 99th percentile Ne, which is the lowest simulated Ne where the observed value of π or S falls within the 99th and 1st percentiles of the 25,000 simulations. We plotted variation in this measure to assess the influence of the various time and Ne parameters on mtDNA diversity.

RESULTS:

mtDNA variation:

The time-calibrated mtDNA phylogeny estimated in BEAST showed the nominate subspecies group was represented by two clades A & B with clade B sister to the northwest

Mexican clade, C (Fig. 2a). All nodes were well supported with high posterior probabilities >0.9. Estimated mean divergence times between clade A and clades B & C was estimated to be 1.3 Ma (95% HPD: 0.4-2.7); and the divergence between clades B and C at 0.8 Ma (95% HPD: 0.2-1.6). We found that clades A & B were broadly sympatric across the breeding range of the nominate subspecies group with the A haplogroup occurring at a higher frequency through much of the range (Fig. 2b). The population sampled at Morro Bay, CA mostly consisted of individuals with the clade C haplotype with a single individual from clade A.

Population structure in the nuclear genome:

The first principal component (19.7% of variance) of the full dataset revealed three clusters: (1) the nominate Savannah Sparrows found across much of North America; (2) populations from northwest Mexico; and (3) an intermediate population from Morro Bay, CA near the distribution limits of the first two populations. A fourth cluster, corresponding to the subspecies *P.s. sanctorum* restricted to Isla San Benito, separated along the second component axis (1.7% of variance) (Fig. 3a). Performing PCA on only individuals from the Mexican clade also distinguished the Isla San Benito population from others along the first principal component axis (10.2% of variance), while along the second axis (6.9% of variance), four clusters were separated, corresponding to subspecies distributed along the coast of Baja California and Sonora (Fig. 3b). Finally, the focused analysis on the nominate group again identified a split between individuals sampled in Morro Bay, CA from all others along the first axis (3.4% of variance), and while there was some evidence of a split between birds sampled along the Pacific coast in California from those sampled throughout the rest of North America along the second axis (2.0% of variance), individuals of the subspecies *P. s. brooksi* from coastal Washington state were found in both of these clusters (Fig. 3c), suggesting that this subtle genetic variation is not

strongly geographically structured. Varying the amount of missing data included in these analyses had no effect on overall patterns of population structure (Appendix 3: Fig. 3.7).

Analyses in fastSTRUCTURE employing the simple prior found K=2 to maximize the marginal likelihood. Similar to PCA analysis, these clusters reflect the divergence between nominate and Mexican Savannah Sparrows (Fig. 4). These analyses provide additional evidence for admixture between the nominate and Mexican populations at Morro Bay, CA, where individuals are assigned to either group with roughly equal probabilities. Analysis with a logistic prior revealed similar patterns, however, the best supported model was K=3 where the third cluster represented the two individuals of *P.s. beldingi* from southern California and some of the genetic variation in Morro Bay birds (Fig. 4). Independent analyses of the nominate and Mexican datasets found K=1 to be the best supported model for each, suggesting that the larger genetic divide between these populations was not impeding the identification of more subtle structure within the full dataset. Moreover, plotting K=2-4 for the nominate group did not recover any additional structure (Appendix 3: Fig. 3.8). .

Phylogenetic analysis in RAxML found *Passerculus sandwichensis* to be a well-supported monophyletic group, Bootstrap (BS): 100 (Fig. 5). Individuals from northwest Mexico and southern California formed a distinct clade with strong bootstrap support (BS 100), interestingly, individuals from Morro Bay were found to be sister to this entire group, again with strong support (BS 100). Within the Mexican clade (excluding birds from Morro Bay), patterns of genetic structure were similar to the PCA results. Members of the *P. s. beldingi* subspecies were found to be sister to the rest of the members of the Mexican clade with strong support. Finally, the Mexican subspecies *P. s. anulus, P. s. sanctorum, P. s. guttatus, P. s. magdalanae, P. s. atratus,* and *P. s. rostratus* each formed well-supported monophyletic clades (Fig. 5). Again

we found little evidence for structure in the nominate group, corroborating results from fastSTRUCTURE and PCA analysis of the full dataset (Fig. 3a). In sum, the bulk of our population structure results do not support our first hypothesis that mitochondrial introgression has exceeded nuclear introgression upon contact of historically isolated lineages.

Demographic analyses:

Nominate population SFS analysis:

A single panmictic population that experienced a bottleneck was found to be the best-supported model (Table 2). Four other models also had high AIC scores, including: a bottleneck-population growth model, and three models involving admixture from a "ghost" population. Adjusted likelihood ratio tests confirm that the bottleneck model was the best fit model (likelihood: -44.3) compared to the bottleneck-population growth model (likelihood: -46.0; adjusted D statistic: 137.43; p-value: 0) and the admixture with growth model (likelihood: -44.2; adjusted D statistic: 0.17; p-value: 0.34). In contrast, simulations based on parameter estimates from single-population $\partial a \partial i$ analyses (Appendix 3: Fig. 3.9-3.10) indicate that a constant Ne was the only history that could result in observed levels of mtDNA diversity. Indeed, for a constant Ne, the observed levels of π (11.42) fell within the 99th and 95th percentiles for the entire range of potential mtDNA Ne (500,000 to 1,650,000) tested in the simulations (Appendix 3: Fig. 3.9) and for segregating sites (*S*), the observed *S* (76) fell within the 99th percentile at Ne greater than 650,000 and the 95th percentile above an Ne of 800,000 (Appendix 3: Fig. 3.10). Despite conflicting results between the best-supported model from $\partial a \partial i$ (bottleneck) and the *ms* simulations (constant Ne), they both are consistent with our second hypothesis that divergent mtDNA clades within the nominate population arose within a panmictic population.

Analysis of Mexican and nominate joint SFS:

By far the best-fit model to the joint SFS (ΔAIC for next best model: ~24) was an

isolation-with-migration (IM) model where low levels of gene flow continued following

divergence between the Mexican and nominate clades with the nominate clade maintaining a

constant population size and the Mexican population experiencing a bottleneck (Fig. 6; Table 4).

In general, IM models showed much greater likelihoods, and all top models involved a

bottleneck or exponential growth within the Mexican population (Table 4). Parameter estimates

from the best-fit model suggest a population split occurring ~480,000 generations ago (95% CI:

240,829-2,066,377), following this split, the nominate population maintained a large Ne of

~1,950,000 (95% CI: 758,589-3,684,813). The Mexican population experienced a bottleneck

roughly ~380,000 generations ago (95% CI: 240,829-541,737) during which the Ne was reduced

to ~7,400 (95% CI: 0-22,132). This bottleneck ended ~100,000 generations ago (95% CI:

59,429-147,642) and the current Mexican Ne was estimated to be ~150,000 (95% CI: 51,276-

303,320). Migration rates between the two populations were roughly symmetric though slightly

greater from the Mexican into the nominate population (Table 4). Simulations of the best-fit two-

population model (Fig. 6) also matched observed π (13.48) and S (86) for both populations (Fig.

7). The observed levels of π fell within the 99th percentile at Ne greater than 1,050,000 and the

95th percentile above 1,550,000; and the observed levels of S fell into the 99th and 95th percentiles

at population sizes of 1,100,000 and 1,250,000, respectively. We also ran simulations based on

the upper and lower bounds for parameter estimates. Observed levels of π and S again fell within

the 99th and 95th percentiles for a similar range of mtDNA effective population sizes for

simulations based on parameter estimates from both the upper and lower bounds (Appendix 3:

Fig. 3.11-3.12). Results from demographic analysis of the joint SFS and *ms* simulations strongly

support a demographic history where divergent mtDNA clades within the nominate clade arose within a panmictic population of Savannah Sparrows further supporting our second hypothesis.

The influence of panmixia versus admixture histories on mtDNA diversity:

The simulations described above allowed us to identify the most likely demographic history for Savannah Sparrows based on the nuclear dataset. We complimented these analyses with a series of additional simulations to determine: (1) the range of demographic histories that could produce divergent but sympatric haplotype clades; and (2) whether this evolutionary outcome was more likely under a history of isolation followed by secondary contact compared to a history of lineage sorting within a panmictic population. Population size proved to be the key parameter contributing to patterns of mtDNA diversity across all simulations. In the absence of a bottleneck, both model classes (panmixia and admixture) required a population size of over 350,000 to generate observed levels of mtDNA diversity with little differences existing between the two sets of models (Appendix 3: Fig. 3.13, 3.15). Fluctuations in population size due to bottlenecks or increases from a small ancestral population proved to have the greatest influence on mtDNA diversity across all simulated models. Lower population sizes in the ancestral population or during bottlenecks required a much greater contemporary effective population size to generate observed levels of mtDNA diversity (Appendix 3: Fig. 3.13-3.16). Variation in parameters related to the duration of bottlenecks or isolation and time since admixture had comparatively little influence on the effective population size required to generate observed patterns (Appendix 3: Fig. 3.14-3.16). In cases where time parameters did influence 99th percentile Ne, it was usually dependent on population size parameters. For example, longer bottlenecks led to decreases in the 99th percentile Ne in instances where the bottleneck was less severe (i.e. 25-50% reduction in Ne; Appendix 3: Fig. 3.14, 3.16). In summary, these simulations

show that there is little reason to assume *a priori* that divergent, sympatric mtDNA haplogroups are more likely to arise when historically isolated populations come into secondary contact than within a single large and panmictic population. Rather, we show that if populations remain relatively large and constant through time both scenarios can produce the occurrence of divergent but sympatric haplotype clades across a wide range of parameter space.

DISCUSSION:

Phylogeographic analysis of the Savannah Sparrow based on mitochondrial DNA found two divergent (~2%) mtDNA clades to be broadly sympatric across much of the breeding range (Fig. 2; Zink et al. 2005). Here, we revisited this phylogeographic pattern with a genomic SNP dataset consisting of 191 individuals sampled from across the species' distribution. Although analysis of this SNP dataset found divergent Mexican and nominate clades within Savannah Sparrows, there was little evidence for population genetic structure within the nominate clade (Fig. 3-5). This pattern of divergent and sympatric mtDNA haplogroups in the absence of nuclear population structure could result from either divergent mtDNA haplotypes that arose and were maintained within a large, panmictic population or the complete merger of two historically isolated clades. To discern between these alternative hypotheses, we first fit a series of demographic models to both the SFS of the nominate group and the joint-SFS of the Mexican and nominate groups; and second, used the parameter estimates from the best-fitting models to run coalescent simulations to assess the likelihood that various demographic scenarios could generate the observed patterns of mtDNA diversity. Based on the best-fit models from $\partial a \partial i$ analyses (Table 2,4; Fig. 6) and the corresponding simulations (Fig. 7) we only find support for the hypothesis that the two divergent mtDNA lineages within the nominate clade arose in a large,

panmictic population. Divergent and sympatric mtDNA lineages have been frequently

interpreted as evidence for admixture of historically isolated lineages (Quinn et al. 1992; Avise

2000; Hogner et al. 2012); however, our analyses indicate that this mtDNA pattern should not

necessarily be interpreted as evidence for secondary contact and admixture. Rather our results

highlight the need for large, multi-locus datasets for discerning demographic history and for

resolving the processes underlying anomalous mtDNA patterns.

Patterns of genetic structure:

Across all analyses, we found little evidence for genetic structure within the nominate

subspecies group (Fig. 3-5). While the results of the PCA analysis of the nominate group may be

interpreted as suggesting the existence of some subtle population structure along the Pacific

coast of California (Fig. 3c), we consider this potential structure to be weak. First, populations

from coastal Washington state include individuals spanning both of these clusters. Secondly, this

cluster was not recovered in any other analyses of population structure. Finally, it is likely that

this evidence for subtle structure reflects some degree of isolation-by-distance and/or greater

gene flow with Mexican populations in coastal California, which is supported by the $\partial a \partial i$ results

(Table 5). Regardless, Savannah Sparrows exhibit a surprising lack of structure within the

nominate clade given that samples spanned most of the breeding distribution from Alaska to

Virginia and included eight described subspecies. In many cases, studies of similar data sets have

been successful in resolving subtle patterns of genetic structure in recently diverged populations

(e.g., Emerson et al. 2010; Friis et al. 2016; Walsh et al. 2017; but see Mason & Taylor 2015).

The lack of structure within the nominate *P. sandwichensis* group may reflect an association with

open habitats. Across much of the Holarctic, open habitat species tend to exhibit less genetic

structure than forest-dwelling taxa (e.g., Drovetski et al. 2010). This includes some species, such

as the Song Sparrow (*Melospiza melodia*) and Red-winged Blackbird (*Agelaius phoeniceus*), which like Savannah Sparrows, exhibit high levels of phenotypic diversity across their broad distributions with little to no mtDNA structure (Ball et al. 1988; Fry & Zink 1998). Analysis of a RADseq dataset in redpoll finches (*Acanthis spp.*), another open-country taxon, also found complete lack of population structure across their circumpolar distribution (Mason & Taylor 2015). Redpolls exhibit a large level of phenotypic diversity with many described taxa and high levels of polymorphism even within a population. An interesting yet unresolved question is the degree to which these high levels of phenotypic diversity reflect an increased capacity for polymorphisms to arise and be maintained in large populations.

We did find salt marsh populations from southern California and northwest Mexico to form a distinct clade across all population structure analyses (Fig. 3-5), consistent with mtDNA patterns (Fig. 2). Within this Mexican clade, the SNP dataset also uncovered more subtle patterns of structure that largely corresponds to recognized subspecies (Fig. 5; van Rossem 1947). Structure among these different subspecies appears to be maintained despite high post-breeding dispersal to other salt marshes and coastal areas in southern California and northwest Mexico (van Rossem 1947; Garrett 2008). This pattern likely reflects a high degree of breeding-site fidelity to relatively small islands of estuarine habitat isolated by large swaths of desert.

Finally, given our increased sampling along the Pacific coast relative to previous studies we were able to show: (1) that birds from Morro Bay primarily have mitochondrial haplotypes from the Mexican clade (Fig. 2); (2) cluster between individuals of nominate and Mexican clades in principal components analysis (Fig. 3); (3) are assigned with equal probability to either nominate or Mexican groups in fastStructure analysis (Fig. 4); and (4) fall out as sister to all Mexican populations in the maximum likelihood phylogeny (Fig. 5). These analyses strongly

suggest that the Morro Bay population is derived from a history of admixture between nominate and Mexican populations of the Savannah Sparrows; however, the precise nature of this history and the extent of introgression between Savannah Sparrow populations will require further sampling and analyses.

Divergent mtDNA haplogroups arose within a panmictic nominate clade:

The best-fit models across all ∂a∂i analyses were consistent with the nominate population maintaining a single panmictic population, while models of secondary contact and admixture among populations received little support (Table 2, 4). Although we found no support for a hypothesis of secondary contact and admixture, the exact demographic history experienced by a panmictic nominate group was not fully resolved. ∂a∂i analyses of only the nominate group SFS identified a suite of models with a bottleneck or population expansion to be a well-supported fit (Table 2). However, in our *ms* simulations based on parameter estimates for each of the models compared within ∂a∂i, only a model of constant population size was able to generate observed levels of mtDNA π and S (Appendix 3: Fig. 3.9-3.10). It is possible that these conflicts reflect the different demographic information contained within the SFS versus the summary statistics π and S, but a more likely explanation for the discordant results is that individuals from the Mexican clade were not included in the analysis of the nominate SFS. Migration from unsampled populations can lead to high support for a bottleneck model (Nielsen & Beaumont 2009). When the Mexican population is included, analysis of the joint SFS strongly supported a model with migration between the nominate and Mexican clades with the nominate population maintaining a constant population size following the initial divergence (Table 3; Fig. 6). Coalescent simulations performed on parameter estimates from this best-fit model reproduced observed levels of mtDNA variation (Fig. 7). Simulations also showed that this model was robust to

parameter estimate error with simulations parameterized on upper and lower confidence intervals also reproducing observed mtDNA diversity (Appendix 3: Fig. 3.11-3.12). Despite some of these inconsistencies all contrasting results are consistent with sympatric mitochondrial clades arising within a panmictic population.

Mexican and nominate Savannah Sparrows diverged nearly 500,000 years ago according to the best-fit model (Table 5). Although there was a fair range of error around this estimate (Table 4), the upper and lower bounds of divergence between these clades falls entirely within the Pleistocene. These estimates also overlap broadly with divergence time estimates (0.8 Ma) based on mtDNA (Fig. 2). Despite some discrepancies (see preceding paragraph), the bulk of our results point to the nominate Savannah Sparrow clade maintaining a large and constant population size throughout much of the Pleistocene, a period characterized by regular glacial cycles (Clark et al. 1999). This inference contrasts with many other North American taxa, which show profound population responses to the glaciation cycles of the last 2.4 million years that include divergence in glacial refugia (e.g., Weir & Schluter 2004; Shafer et al. 2010) or population contraction followed by expansion to re-occupy habitats made available by retreating glaciers (e.g., Ball et al. 1988; Milá et al. 2000). Current populations of Savannah Sparrows span a large geographic distribution (Fig. 1) and occupy a broad range of open habitats that include: tundra, meadows, arid grasslands, salt marshes, pastures, cultivated fields, sedge bogs, coastal grasslands, and a range of forest edges (Wheelwright & Rising 2008). If Savannah Sparrows occupied a similarly broad niche over the past 500,000 years it could explain how this species maintained a large and contiguous population through several glacial cycles. Palynological, fossil, and other climatic evidence suggests that contiguous tundra, grassland, and steppe habitats existed across the southern edge of advancing glaciers and further south in the United States

during the last glacial maxima (Williams et al. 2004; Dyke 2005; Williams et al. 2009). This record supports the inference that Savannah Sparrows could have maintained a geographically widespread population through glacial and inter-glacial cycles without being compressed into disjunct refugia as occurred with many forest taxa (e.g. Weir & Schluter 2004).

Sympatry of divergent mtDNA lineages can arise under a range of demographic scenarios:

We designed a final set of simulations to characterize the range of demographic conditions in which a history of secondary contact and admixture would be more likely to produce observed mtDNA patterns than linage processes in a panmictic population. Based on these simulations we found that either history could produce observed mtDNA diversity present in Savannah Sparrows over a broad range of population genetic parameter values. However, a key result from this analysis was that the observed mtDNA diversity in Savannah Sparrows could only arise in large populations (Ne > 350,000). Parameters related to historical fluctuations in Ne also played a critical role in shaping patterns of genetic diversity with small ancestral Ne or bottlenecks significantly eroding mtDNA diversity. The simulations performed here do not represent the entire range of parameters that could lead to divergent and sympatric mtDNA lineages. However, even in a model of recent contact and admixture, populations would need to maintain a large Ne throughout their history to produce observed patterns of mtDNA diversity. Our simulations do suggest that lower values of Ne could result in the observed patterns of mtDNA diversity via admixture, but this scenario would require an extended period of isolation. In the latter case our simulation results find that even at relatively large and constant population sizes, isolation for 200,000 generations prior to admixture did not lead to measurable increases in mtDNA diversity. Based on mtDNA data alone, these simulations demonstrate that it is

impossible to discern among different demographic scenarios across a wide range of parameter space, necessitating demographic analyses based on genomic datasets.

The results from these simulations also help to elucidate some of the conflicting or surprising results from other analyses. First, the close relationship of Mexican mtDNA haplotypes to only one of the two mtDNA haplogroups is likely due to the smaller population size and evidence for bottlenecks experienced by the Mexican population. Even if the founding Mexican population contained both haplogroups it is likely that the much smaller population size of the Mexican population (Table 5) led to the erosion of mtDNA diversity and the fixation of only a single mtDNA haplotype. Secondly, the high sensitivity to historical fluctuations in population size suggests that to generate observed levels of mtDNA diversity nominate Savannah Sparrows likely maintained a large and stable population size throughout the Pleistocene, despite glaciers expanding and retreating across much of their contemporary breeding range.

Conclusions:

Using a large genomic SNP dataset, we revisited a previous phylogeography of the Savannah Sparrow where two mtDNA haplogroups were found to be sympatric across much of the species' distribution (Zink et al. 2005). Our reanalysis revealed that these two mitochondrial clades were not associated with significant population structure in the nuclear genome. Instead, a series of demographic analyses using the SFS coupled with coalescent simulations suggest that the divergent mtDNA lineages arose within a single large and panmictic population. Coalescent theory suggests that divergent haplotypes of a non-recombining locus can arise within a large, panmictic population (Slatkin & Hudson 1991). This process underlies the generation of multi-modal mismatch distributions in stable populations (Slatkin & Hudson 1991) and the strong influence of ancestral population size on patterns of incomplete lineage sorting (e.g. Edwards &

Beerli 2001). Here we show that these same processes can also result in sympatry of divergent mtDNA clades. These results contrast with the most frequent interpretation of this pattern, which is often assumed to reflect a history of isolation, secondary contact, and admixture. In general, revisiting mtDNA phylogeographic studies with demographic analyses of genomic datasets provides a promising approach for understanding the processes that give rise to peculiar mtDNA-based phylogeographic patterns.

REFERENCES:

Andersson, M. 1999. Hybridization and skua phylogeny. Proc. R. Soc. B. 266: 1579.

Avise, J.C. 2000. *Phylogeography: the history and formation of species.* Harvard University Press, Cambridge, Massachussetts.

Bachtrog, D., K. Thornton, A. Clark, and P. Andolfatto. 2006. Extensive introgression of mitochondrial DNA relative to nuclear genes in the *Drosophila yakuba* species group. Evolution 60: 292-302.

Ball, R. M., S. Freeman, F. C. James, E. Bermingham, and J. C. Avise. 1988. Phylogeographic population structure of Red-winged Blackbirds assessed by mitochondrial DNA. Proc. Nat. Acad. Sci. USA 85: 1558-1562.

Ballard, J. W. O., and M. C. Whitlock. 2004. The incomplete natural history of mitochondria. Mol. Ecol. 13: 729-744.

Beckman, E. J., and C. C. Witt. 2015. Phylogeny and biogeography of the New World siskins and goldfinches: Rapid, recent diversification in the Central Andes. Mol. Phylogenet. Evol. 87: 28-45.

Block, N. L., S. M. Goodman, S. J. Hackett, J. M. Bates, and M. J. Raherilalao. 2015. Potential merger of ancient lineages in a passerine bird discovered based on evidence from host-specific ectoparasites. Ecology and Evolution 5: 3743-3755.

Catchen, J. M., A. Amores, P. Hohenlohe, W. Cresko, J. H. Postlethwait, and D. J. De Koning. 2011. Stacks: building and genotyping loci de novo from short-read sequences. G3: Genes, Genomes, Genetics 1: 171-182.

Catchen, J. M., P. A. Hohenlohe, S. Bassham, A. Amores, and W. A. Cresko. 2013. Stacks: An analysis tool set for population genomics. Mol. Ecol. 22: 3124-3140.

Clark, P. U. 1999. Northern Hemisphere Ice-Sheet Influences on Global Climate Change. Science 286:1104-1111.

Coffman, A. J., P. H. Hsieh, S. Gravel, and R. N. Gutenkunst. 2016. Computationally efficient composite likelihood statistics for demographic inference. Mol. Biol. Evol. 33: 591-593.

Currat, M., M. Ruedi, R. J. Petit, and L. Excoffier. 2008. The hidden side of invasions: massive introgression by local genes. Evolution 62: 1908-1920.

Dickinson, E.C. and L. Christidis (eds.). 2014. *The Howard & Moore complete checklist of the birds of the world, 4th edition, volume 2 Passerines.* Aves Press, East Sussex, UK.

Drovetski, S. V., R. M. Zink, P. G. P. Ericson, and I. V. Fadeev. 2010. A multilocus study of pine grosbeak phylogeography supports the pattern of greater intercontinental divergence in Holarctic boreal forest birds than in birds inhabiting other high-latitude habitats. J. Biogeog. 37: 696-706.

Drummond, A.J., S.Y.W. Ho, M.J. Phillips, and A. Rambaut. 2006. Relaxed phylogenetics and dating with confidence. PLoS Biology 4: 699-710.

Drummond, A. J., M. A. Suchard, D. Xie, and A. Rambaut. 2012. Bayesian phylogenetics with BEAUti and the BEAST 1.7. Mol. Biol. Evol. 29: 1969-1973.

Dyke, A. S. 2005. Late quaternary vegetation history of northern North America based on pollen, macrofossil and faunal remains. Geographie Physique et Quaternaire 59: 211-262.

Edgar, R. C. (2004). MUSCLE: a multiple sequence alignment method with reduced time and space complexity. BMC Bioinformatics 5: 113.

Edwards, S. V, and P. Beerli. 2000. Perspective: gene divergence, population divergence, and the variance in coalescence time in phylogeographic studies. Evolution 54: 1839-1854.

Emerson, K. J., C. R. Merz, J. M. Catchen, P. A. Hohenlohe, W. A. Cresko, W. E. Bradshaw, and C. M. Holzapfel. 2010. Resolving postglacial phylogeography using high-throughput sequencing. Proc. Nat. Acad. Sci. USA 107: 16196-16200.

Excoffier, L., and H. E. L. Lischer. 2010. Arlequin suite ver 3.5: A new series of programs to perform population genetics analyses under Linux and Windows. Mol. Ecol. Res. 10: 564-567.

Francis, R. M. 2016. pophelper: An r package and web app to analyse and visualize population structure. Mol. Ecol. Res. 17: 27-32.

Friis, G., P. Aleixandre, R. Rodriguez-Estrella, A. Navarro-Sigüenza, and B. Milá. 2016. Rapid postglacial diversification and long-term stasis within the songbird genus Junco: phylogeographic and phylogenomic evidence. Mol. Ecol. 25: 6175-6195.

Fry, A. J., and R. M. Zink. 1998. Geographic analysis of nucleotide diversity and song sparrow (Aves: Emberizidae) population history. Mol. Ecol. 7: 1303-1313.

Garrett, K. L. 2008. Large-billed savannah sparrow (*Passerculus sandwichensis rostratus*). *In:* California bird species of special concern: a ranked assessment of species, subspecies, and distinct populations of birds of immediate conservation concern in California (W. D. Shuford and T. Gardali, eds.). Studies of Western Birds 1. pgs. 388-392.

Giska, I., P. Sechi, and W. Babik. 2015. Deeply divergent sympatric mitochondrial lineages of the earthworm *Lumbricus rubellus* are not reproductively isolated. BMC Evol. Biol. 15: 217.

Good, J. M., D. Vanderpool, S. Keeble, and K. Bi. 2015. Negligible nuclear introgression despite complete mitochondrial capture between two species of chipmunks. Evolution 69: 1961-1972.

Gosselin, T. and L. Bernatchez. 2016. stackr: GBS/RAD data exploration, manipulation and visualization using R. R package version 0.4.6 https://github.com/thierrygosselin/stackr. doi: 10.5281/zenodo.154432.

Gutenkunst, R. N., R. D. Hernandez, S. H. Williamson, and C. D. Bustamante. 2009. Inferring the joint demographic history of multiple populations from multidimensional SNP frequency data. PLoS Genetics 5: e1000695.

Hoelzer, G. A., W. P. Dittus, M. V. Ashley, and D. J. Melnick. 1994. The local distribution of highly divergent mitochondrial DNA haplotypes in toque macaques *Macaca sinica* at Polonnaruwa, Sri Lanka. Mol. Ecol. 3: 451-458.

Hogner, S., T. Laskemoen, J. T. Lifjeld, J. Porkert, O. Kleven, T. Albayrak, B. Kabasakal, and A. Johnsen. 2012. Deep sympatric mitochondrial divergence without reproductive isolation in the common redstart *Phoenicurus phoenicurus*. Ecology and Evolution 2: 2974-2988.

Hudson, R. R., and M. Turelli. 2003. Stochasticity overrules the "three-times rule": genetic drift, genetic draft, and coalescence times for nuclear loci versus mitochondrial DNA. Evolution 57: 182-190.

Hudson, R. 2002. Ms a program for generating samples under neutral models. Bioinformatics 18: 337-338.

Irwin, D.E., 2002. Phylogeographic breaks without geographic barriers to gene flow. Evolution, 56: 2383-2394.

Jombart, T., and I. Ahmed. 2011. Adegenet 1.3-1: New tools for the analysis of genome-wide SNP data. Bioinformatics 27: 3070-3071.

Kazancioğlu, E., and G. Arnqvist. 2014. The maintenance of mitochondrial genetic variation by negative frequency-dependent selection. Ecol. Lett. 17: 22-27.

Klicka, J., K. F. Barker, K. J. Burns, S. M. Lanyon, I. J. Lovette, J. A. Chaves, and R. W. Bryson. 2014. A comprehensive multilocus assessment of sparrow (Aves: Passerellidae) relationships. Mol. Phylogenet. Evol. 77: 177-182.

Lanfear, R., P. B. Frandsen, A. M. Wright, T. Senfeld, and B. Calcott. 2016. PartitionFinder 2: new methods for selecting partitioned models of evolution for molecular and morphological phylogenetic analyses. Mol. Biol. Evol. 34: 772-773.

Leaché, A. D., B. L. Banbury, J. Felsenstein, A. N. M. De Oca, and A. Stamatakis. 2015. Short tree, long tree, right tree, wrong tree: new acquisition bias corrections for inferring SNP phylogenies. Syst. Biol. 64: 1032-1047.

Mason, N. A., and S. A. Taylor. 2015. Differentially expressed genes match bill morphology and plumage despite largely undifferentiated genomes in a Holarctic songbird. Mol. Ecol. 24: 3009-3025.

Mastretta-Yanes, A., N. Arrigo, N. Alvarez, T. H. Jorgensen, D. Piñero, and B. C. Emerson. 2015. Restriction site-associated DNA sequencing, genotyping error estimation and de novo assembly optimization for population genetic inference. Mol. Ecol. Res. 15: 28-41.

Meier, J. I., V. C. Sousa, D. A. Marques, O. M. Selz, C. E. Wagner, L. Excoffier, and O. Seehausen 2016. Demographic modeling with whole-genome data reveals parallel origin of similar *Pundamilia* cichlid species after hybridization. Mol. Ecol. 26: 123-141.

Milá, B., D. J. Girman, M Kimura, and T. B. Smith. 2000. Genetic evidence for the effect of a postglacial population expansion on the phylogeography of a North American songbird. Proc. R. Soc. B. 267: 1033-1040.

Miller, M.A., W. Pfeiffer, and T. Schwartz. 2010. Creating the CIPRES science gateway for inference of large phylogenetic trees. 2010 Gateway Computing Environments Workshop (GCE 2010), pp. 45–52. Institute of Electrical and Elec- tronics Engineers, Piscataway, NJ.

Mims, M. C., C. D. Hulsey, B. M. Fitzpatrick, and J. T. Streelman. 2010. Geography disentangles introgression from ancestral polymorphism in Lake Malawi cichlids. Mol. Ecol. 19: 940-951.

Nielsen, R., and M. A. Beaumont. 2009. Statistical inferences in phylogeography. Mol. Ecol. 18: 1034-1047.

Oswald, J. A., I. Overcast, W. M. Mauck, M. J. Andersen, and B. T. Smith. 2017. Isolation with asymmetric gene flow during the nonsynchronous divergence of dry forest birds. Mol. Ecol. 26: 1386-1400.

Parchman, T. L., Z. Gompert, J. Mudge, F. D. Schilkey, C. W. Benkman, and C. A. Buerkle. 2012. Genome-wide association genetics of an adaptive trait in lodgepole pine. Mol. Ecol. 21: 2991-3005.

Paris, J. R., J.R. Stevens, and J.M. Catchen. 2017. Lost in parameter space: A road map for Stacks. Methods in Ecology and Evolution. 8: 1360-1373.

Quinn, T. W. 1992. The genetic legacy of Mother Goose—phylogeographic patterns of lesser snow goose *Chen caerulescens caerulescens* maternal lineages. Mol. Ecol. 1: 105-117.

Raj, A., M. Stephens, and J. K. Pritchard. 2014. FastSTRUCTURE: variational inference of population structure in large SNP data sets. Genetics 197: 573-589.

Rambaut A., M. A. Suchard, D. Xie, and A. J. Drummond. 2014. Tracer v1.6, Available from http://beast.bio.ed.ac.uk/Tracer

Rising, J. 2017. Belding's Sparrow (*Passerculus guttatus*). In: del Hoyo, J., Elliott, A., Sargatal, J., Christie, D.A. & de Juana, E. (eds.). *Handbook of the Birds of the World Alive*. Lynx Edicions, Barcelona. (retrieved from http://www.hbw.com/node/61919 on 5 April 2017).

Shafer, A. B. A., C. I. Cullingham, S. D. Côté, and D. W. Coltman, D. W. 2010. Of glaciers and refugia: A decade of study sheds new light on the phylogeography of northwestern North America. Mol. Ecol. 19: 4589-4621.

Slatkin, M., and R. R. Hudson. 1991. Pairwise comparisons of mitochondrial DNA sequences in stable and exponentially growing populations. Genetics 129: 555-562.

Sloan, D. B., J. C. Havird, and J. Sharbrough. 2016. The on-again-off-again relationship between mitochondrial genomes and species boundaries. Mol. Ecol. 26: 2212-2236.

Smith, B. T., and J. Klicka. 2010. The profound influence of the late Pliocene Panamanian uplift on the exchange, diversification, and distribution of new world birds. Ecography 33: 333-342.

Spottiswoode, C. N., K. F. Stryjewski, S. Quader, J. F. R. Colebrook-Robjent, and M. D. Sorenson. 2011. Ancient host specificity within a single species of brood parasitic bird. Proc. Nat. Acad. Sci. USA 108: 17738-17742.

Stamatakis, A. 2014. RaxML version 8: A tool for phylogenetic analysis and post-analysis of large phylogenies. Bioinformatics 30: 1312-1313.

van Rossem, J. 1947. A synopsis of the savannah sparrows of northwestern Mexico. Condor 49: 97-107.

Walsh, J., I. J. Lovette, V. Winder, C. S. Elphick, B. J. Olsen, W. G. Shriver, and A. I. Kovach. 2017. Subspecies delineation amid phenotypic, geographic, and genetic discordance in a songbird. Mol. Ecol. 26: 1242-1255.

Walstrom, V. W., J. Klicka, and G. M. Spellman. 2012. Speciation in the white-breasted nuthatch (*Sitta carolinensis*): A multilocus perspective. Mol. Ecol. 21: 907-920.

Weckstein, J., R.M. Zink, R.C. Blackwell-Rago, and D.A. Nelson. 2001. Anomalous variation in mitochondrial genomes of white-crowned (*Zonotrichia leucophrys*) and golden-crowned (*Z. atricapilla*) sparrows: pseudogenes, hybridization, or incomplete lineage sorting? The Auk 118: 231-236.

Weir, J. T., and D. Schluter. 2004. Ice sheets promote speciation in boreal birds. Proc. R. Soc. B. 271: 1881-1887.

Weir, J. T., and D. Schluter. 2008. Calibrating the avian molecular clock. Mol. Ecol. 17: 2321-2328.

Wheelwright, N. T and J. D. Rising. 2008. Savannah Sparrow (*Passerculus sandwichensis*). *in* Birds of North American Online (A. Poole, Ed.). Cornell Lab of Ornithology, Ithaca, NY.

Williams, J. W., B. N. Shuman, T. Webb, P. J. Bartlein, and P. L. Leduc. 2004. Late-Quaternary vegetation dynamics in North America: scaling from taxa to biomes. Ecological Monographs 74: 309-334.

Williams, J. W., B. N. Shuman, and P. J. Bartlein. 2009. Rapid responses of the prairie-forest ecotone to early Holocene aridity in mid-continental North America. Global and Planetary Change 66: 195-207.

Xiao, J. H., N. X. Wang, R. W. Murphy, J. Cook, L. Y. Jia, and D. W. Huang. 2012. Wolbachia infection and dramatic intraspecific mitochondrial DNA divergence in a fig wasp. Evolution 66: 1907-1916.

Zhang, G., C. Li, Q. Li, B. Li, D. M. Larkin, C. Lee, J. F. Storz, A. Antunes, M. J. Greenwold, R. W. Meredith, A. Odeen, J. Cui, Q. Zhou, L. Xu, H. Pan, Z. Wang, L. Jin, P. Zhang, H. Hu, W. Yang, J. Hu, J. Xiao, Z. Yang, Y. Liu, Q. Xie, H. Yu, j. Lian, P. Wen, F. Zhang, H. Li, Y. Zeng, Z. Xiong, S. Liu, L. Zhou, Z. Huang, N. An, J. Wang, Y. Fan, R. R. da Fonesca, A. Alfaro-Núñez, M. Schubert, L. Orlando, T. Mourier, J. T. Howard, G. Ganapathy, A. Pfenning, O. Whitney, M. V. Rivas, E. Hara, J. Smith, M. Farré, J. Narayan, G. Slavov, M. N. Romanov, R. Borges, J. P. Machado, I. Khan, M. S. Springer, J. Gatesy, F. G. Hoffmann, J. C. Opazo, O. Hastad, R. H. Sawyer, H. Kim, K. W. Kim, H. J. Kim, S. Cho, N. Li, Y. Huang, M. W. Bruford, X. Zhan, A. Dixon, M. F. Bertelsen, E. Derryberry, W. Warren, R.

K. Wilson, S. Li, D. A. Ray, R. E. Green, S. J. O'Brien, D. Griffen, W. E. Johnson, D. Haussler, O. A. Ryder, E. Willerslev, G. R. Graves, P. Alstrom, J. Fjeldsa.. D. P. Mindell, S. V. Edwards, E. L. Braun, C. Rahbek, D. W. Burt, P. Houde, Y. Zhang, H. Yang, J. Wang, Avian Genome Consortium, E. D. Jarvis, M. T. P Gilbert, and J. Wang. 2014. Comparative genomics reveals insights into avian genome evolution and adaptation. Science 346: 1311-1320.

Zink, R. M., J. D. Rising, S. Mockford, A. G. Horn, J. M. Wright, M. Leonard, and M. C. Westberg (2005). Mitochondrial DNA Variation, Species Limits, and Rapid Evolution of Plumage Coloration and Size in the Savannah Sparrow. The Condor 107: 21-28.
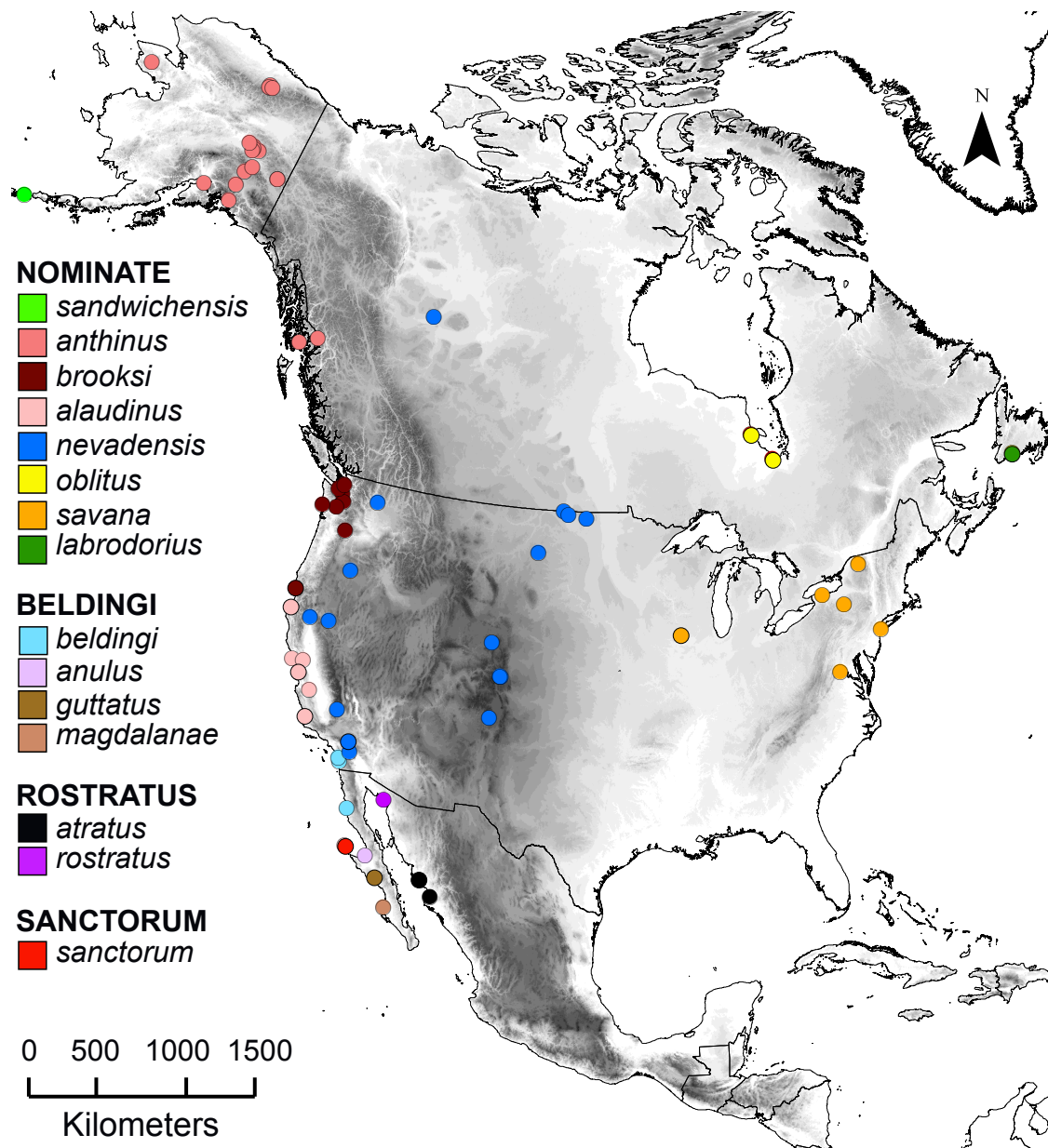
Figure 1: Savannah Sparrow sampling map for this study. Each circle represents the geographic locality for all samples colored by putative subspecies. The subspecies are clustered into five frequently recognized subspecies groups (Wheelwright & Rising 2008).
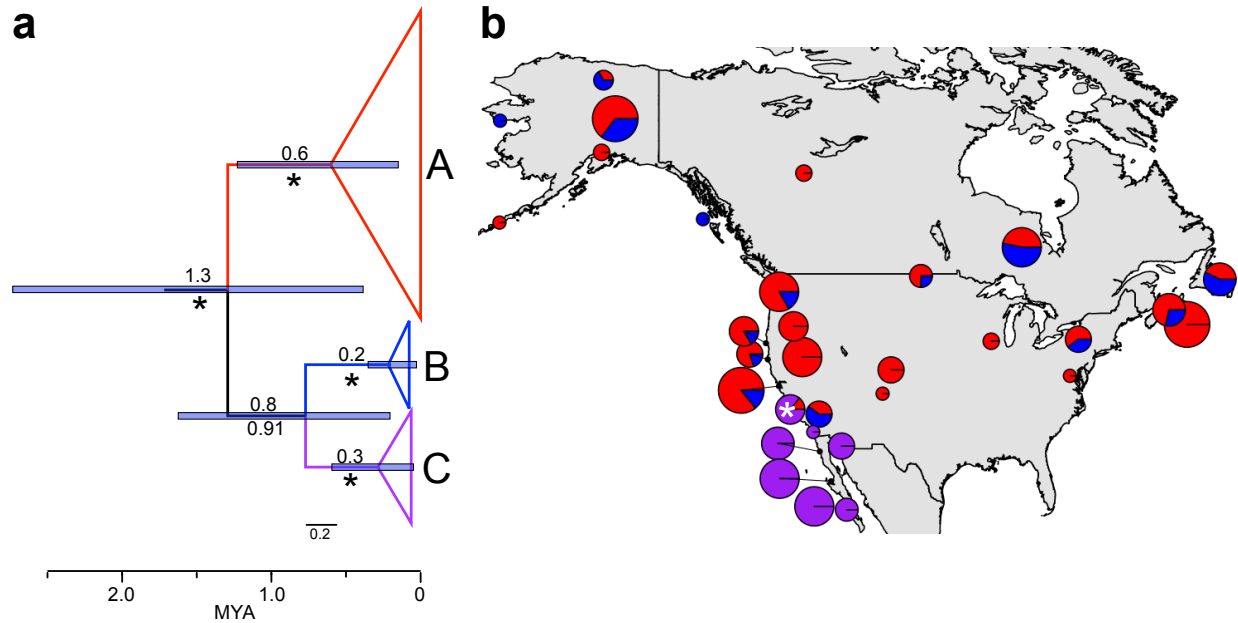
Figure 2: Genetic structure within Savannah Sparrows based on the mitochondrial locus ND2 across 212 individuals. (a) Bayesian, time-calibrated phylogeny estimated within the program BEAST. The outgroup has been removed for visualization. Mean divergence time estimates for each node are denoted above branches with purple error bars representing 95% HPD. Posterior probabilities (PP) for each node are below branches, asterisk signifying PP>0.95. (b) Mapped distribution of the three ND2 clades recovered by phylogenetic analyses. Red and Blue clades correspond to the Nominate subspecies group (Fig. 1) and are broadly sympatric across the breeding range of the Nominate group despite being ~1.3 ma divergent. The purple clade corresponds to salt marsh resident populations in southern California and northwest Mexico. Morro Bay population (subspecies *P. s. alaudinus*) is marked with an asterisk and includes individuals with Mexican and nominate haplotypes.
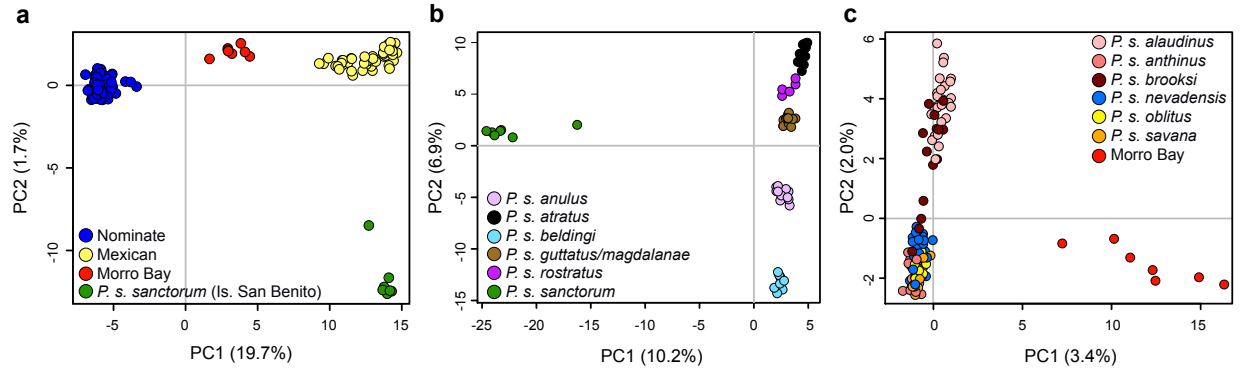
Figure 3: Principal components analysis for: a) full dataset (n=191); b) Mexican dataset (n=56); and c) nominate dataset (n=135). Analysis on dataset with 10% missing data is shown.
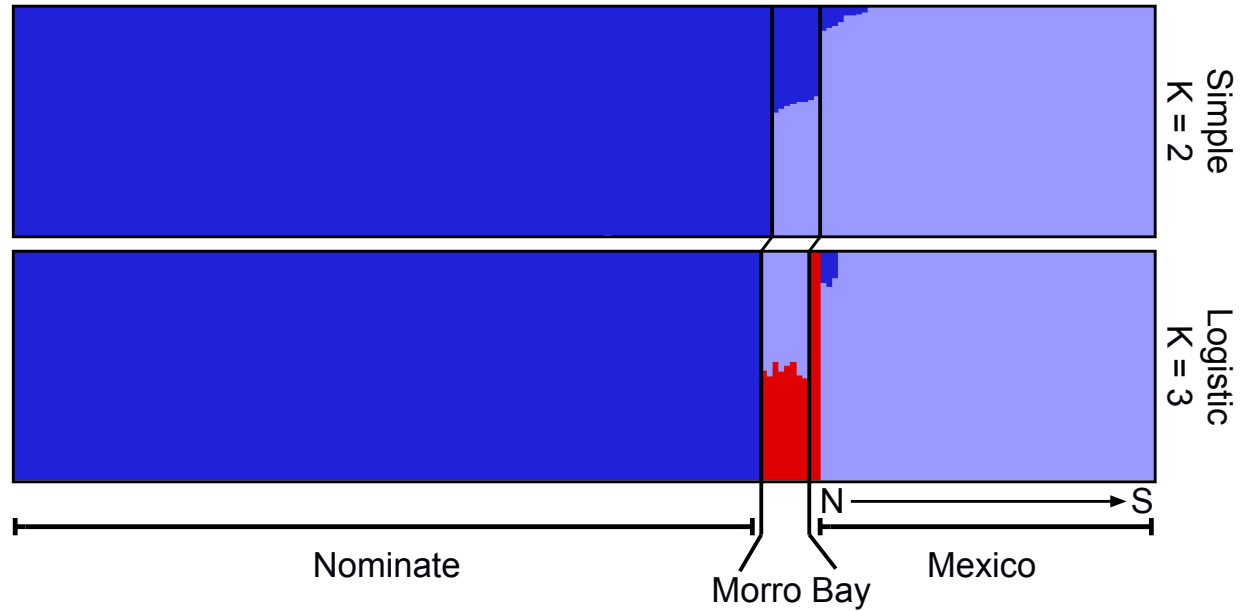
Figure 4: Population structure in Savannah Sparrows determined in fastSTRUCTURE. Plots show variation in output when simple prior (upper panel) versus logistic prior for allele frequencies was set. For analyses using simple prior K=2 was found to optimize the marginal likelihood of the clusters, whereas K=3 was found under a logistic prior. Structure existed between Mexican and nominate Savannah Sparrows in both analyses. Both also identified an apparent zone of secondary contact at Morro Bay along the California coast. Barplots were generate in the r-package pophelper v. 1.1.6 (Francis 2016).
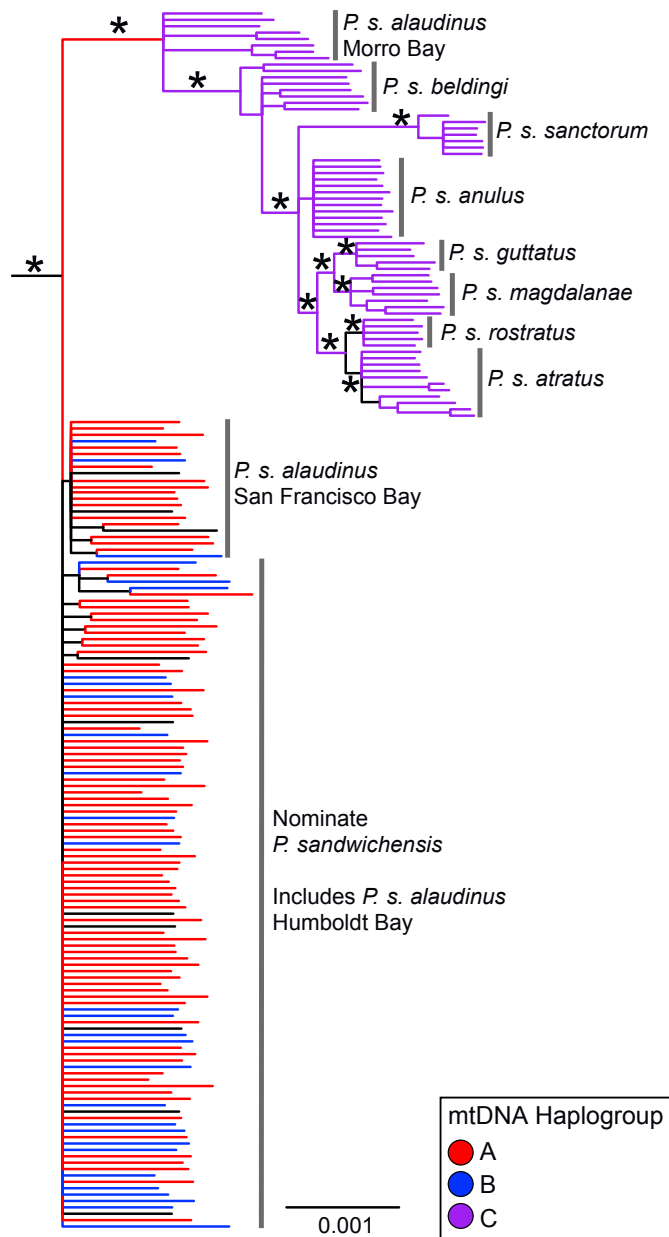
Figure 5: Maximum likelihood phylogeny of *Passerculus sandwichensis* generated in RAxML 8.2.4. Phylogeny constructed with 25% missing data dataset and using the Felsenstein correction for ascertainment bias. Asterisks denote nodes with >95 Bootstrap support. Nodes with bootstrap support <50 have been collapsed. Outgroups not shown. Individuals on the phylogeny are colored by mtDNA haplogroup (Fig. 2). Black branches signify individuals for which we lack mtDNA.
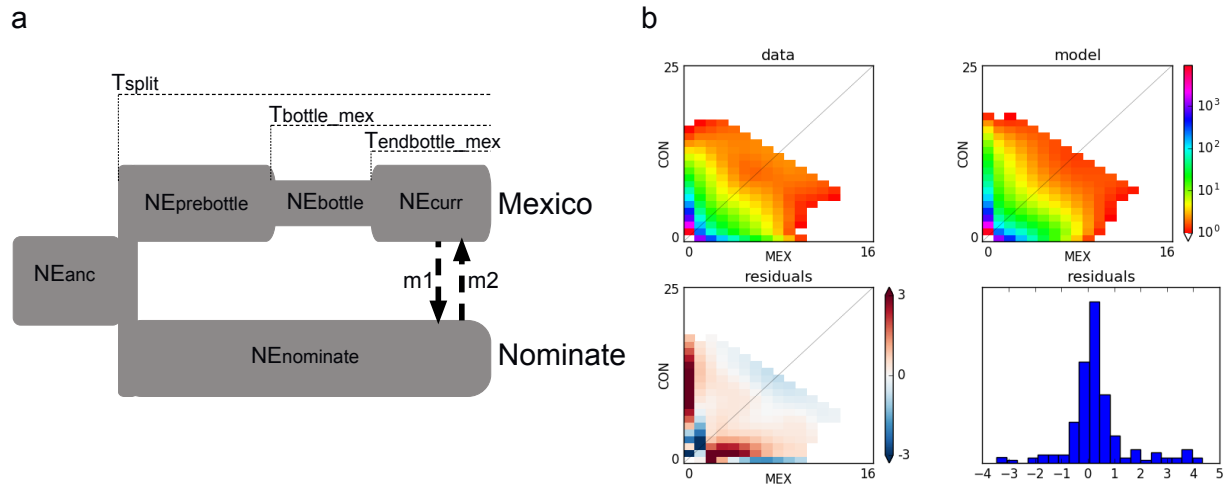
Figure 6: a) Schematic of best supported model, where Mexican and nominate populations diverged at Tsplit followed by a bottleneck in the Mexican population size from Tbottle_mex to Tendbottle_mex, whereas the nominate population maintained a constant population size following the split. Labeled parameters correspond to point estimates and uncertainties listed in table 4. **b)** Comparison of observed site frequency spectrum to simulated spectra given parameter values from model in Fig. 6a. Lower panels represent residuals between fit of model and data.
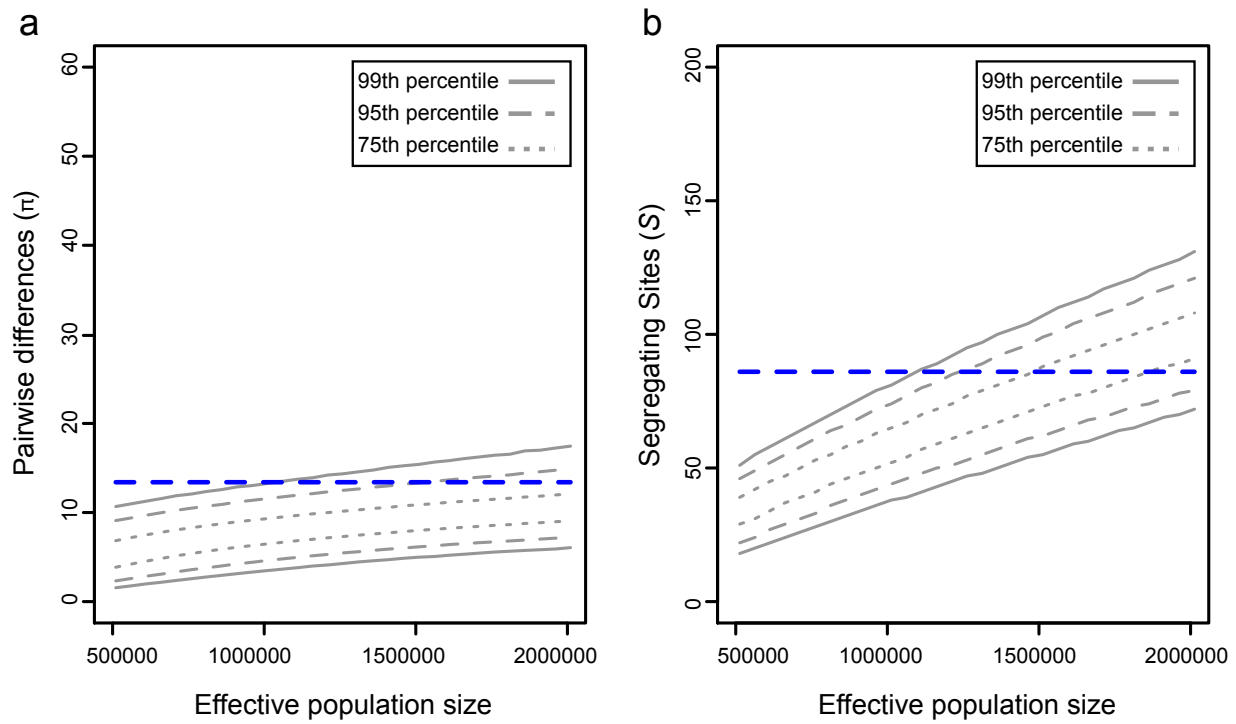
Figure 7: Results from *ms* simulations where parameter estimates from the best-supported demographic model from dadi analyses (Fig. 6) were used to assess whether this demographic model could result in observed mtDNA diversity within Savannah Sparrows. Simulations are based on 204 individuals across a range of effective population sizes relevant to empirical estimates of mtDNA Ne with the range of Ne based on variance in nucleotide diversity. For average pairwise differences (a) and number of segregating sites (b) solid, dashed, and dotted gray lines represent 99%, 95%, and 75% quantiles, respectively, of these summary statistics calculated from across 100,000 simulations for each effective population size. Blue line represents empirical estimate of mtDNA average pairwise differences (13.48) and number of segregating sites (86).

TABLES:

Table 1: The four demographic models and parameters evaluated in the coalescent simulator *ms*. Ne is effective population size and Ne for the ancestor, bottleneck population, or during isolation prior to admixture is listed as a proportion of contemporary Ne. f is the admixture proportion.

| Models | Ne (x10³) | Ne | | | Time (Kya) | | | | |
		Ancestor	Bottle	Isolation	Bottle	Bottle Length	Isolation	Admix	f
Panmixia Constant Ne	100–2,000 (by 50)	0.1, 0.25, 0.5, 0.75, 1	NA	NA	NA	NA	NA	NA	NA
Panmixia Bottleneck	100–2,000 (by 50)	0.1, 0.25, 0.5, 0.75	0.1, 0.25, 0.5, 0.75	NA	1, 10, 50, 100	10, 50, 100, 200	NA	NA	NA
Admixture Stable Ne	100–2,000 (by 50)	0.1, 0.25, 0.5, 0.75	NA	0.1, 0.25, 0.5, 0.75	NA	NA	10, 50, 100, 200	1, 10, 50, 100	0.5
Admixture Bottleneck	100–2,000 (by 50)	0.1, 0.25, 0.5, 0.75	0.1, 0.25, 0.5	0.75	11, 20, 60, 110	50	70, 110, 160, 260	1, 10, 50, 100	0.5

Table 2: Comparisons of results from analysis of nominate population SFS in $\partial a \partial i$ (22,066 SNPs; Appendix 3: Fig. 4). Models in bold are consistent with the second hypothesis that divergent mtDNA clades arose within a panmictic population, and non-bolded models are consistent with the third hypothesis of historical isolation followed by admixture. Values included are likelihoods (LL), number of parameters (K), AIC, ΔAIC, and Akaike weights (the relative likelihood of each model).

Models	LL	K	AIC	ΔAIC	weights
Bottleneck	-44.3	4	96.5	0	0.608
Bottleneck-exponential growth	-46.0	3	98.0	1.5	0.290
Admix "ghost", constant	-44.4	6	100.9	4.3	0.069
Admix "ghost", exponential growth	-44.2	7	102.5	5.9	0.031
Admix "ghost", bottleneck	-44.3	10	108.5	12.0	0.001
Exponential growth	-141.6	2	287.3	190.8	0
Admix mtDNA, exponential growth	-183.7	5	377.5	281.0	0
Admix mtDNA, constant	-183.9	5	377.9	281.3	0
Admix mtDNA, bottleneck	-182.0	8	379.9	283.3	0
Constant	-6501	1	13004	12908	0

Table 3: Point estimates for best-supported models in Table 2. Listed are estimates for ancestral population size (Ne_{anc}), current population size (Ne_{curr}), bottleneck population size (Ne_{bot}), start time of the bottleneck (T_{bot}), end of the bottleneck (T_{rec}), population divergence time (T_{split}), and population admixture (T_{merge}). All times are listed in years before present (assuming a 1 year generation time). Entries of NA denote parameters not estimated for certain models. Parentheticals indicate ± 95% confidence intervals.

Models	Ne_{anc}	$Ne_{current}$	Ne_{bot}	T_{bot}	T_{rec}	T_{split}	T_{merge}
bottleneck	29,708	6,984,899	998,553	336,790	59,709	NA	NA
	(±3,844)	(±2,946,755)	(±247,023)	(±75,930)	(±20,692)		
bottleneck then exp grow	23,281	3,180,248	265,640	NA	356,946	NA	NA
	(±1,047)	(±404,446)	(±39,030)		(±38,647)		
Admix "ghost", constant size	29,801	4,785,697	NA	NA	NA	349,647	77,819
	(±4,128)	(±1,661,912)				(±109,076)	(±18,951)
Admix "ghost", exp grow	29,736	5,055,069	NA	NA	NA	338,522	80,626
	(±5,068)	(±1,834,546)				(±73,556)	(±32,467)
Admix "ghost", bottle	29,847	10,318,680	1,202,173	142,858	84,139	336,822	32,303
	(±5,335)	(±2,988,222)	(±2,220,346)	(±154,195)	(±47,710)	(±293,864)	(±31,597)

Table 4: Comparisons of results from analysis of joint SFS of the Mexican and Nominate population in $\partial a \partial i$. Models in bold are consistent with the second hypothesis that divergent mtDNA clades arose within a panmictic population, and non-bolded models are consistent with the third hypothesis of historical isolation followed by admixture. Values included are likelihoods (LL), number of parameters (K), AIC, ΔAIC, and Akaike weights (the relative likelihood of each model).

MODELS	LL	K	AIC	ΔAIC	weights
IM, constant size Nom, bottle Mex	-473.08	9	964.16	0	1.000
IM, bottle both	-481.06	13	988.12	23.96	0.000
IM, Admix "ghost", bottle both	-503.88	16	1039.76	75.6	0.000
IM, Admix "ghost", constant size Nom., bottle Mex	-600.3	12	1224.6	260.44	0.000
IM, constant size Nom, exp grow Mex	-610.97	6	1233.94	269.78	0.000
IM, exp grow both	-611.92	7	1237.84	273.68	0.000
IM Admix "ghost", exp grow Nom, bottle Mex	-668.01	14	1364.02	399.86	0.000
IM, exp grow Nom, constant size Mex	-1074.29	6	2160.58	1196.42	0.000
IM, Admix "ghost", constant size both	-1083.26	8	2182.52	1218.36	0.000
IM, constant size both	-1086.71	5	2183.42	1219.26	0.000
IM, bottle Nom, constant size Mex	-1085.14	9	2188.28	1224.12	0.000
IM, Admix mtDNA, constant size both	-1651.71	8	3319.42	2355.26	0.000
IM Admix mtDNA, constant size Nom, bottle Mex	-1806.19	12	3636.38	2672.22	0.000
No mig., constant size Nom, bottle Mex	-2142.44	7	4298.88	3334.72	0.000
No mig., bottle both	-2154	11	4330	3365.84	0.000
No mig., exp grow both	-2199.18	5	4408.36	3444.2	0.000
No mig., constant size Nom, exp grow Mex	-2211.58	4	4431.16	3467	0.000
No mig., exp grow Nom, constant size Mex	-2322.55	4	4653.1	3688.94	0.000
No mig., bottle Nom, constant size Mex	-2319.7	7	4653.4	3689.24	0.000
IM, Admix mtDNA, bottle both	-2331.49	16	4694.98	3730.82	0.000
No mig., constant size both	-2383.22	3	4772.44	3808.28	0.000
Mig., Admix mtDNA, exp grow Nom, bottle Mex	-3023.11	14	6074.22	5110.06	0.000

Table 5: parameter estimates from best model (Fig. 6)

with 95% CI calculated based on GIM uncertainties.

Parameter	ML estimate	95% CI low	95% CI High
Theta (4NeµL)	2646.28	1771.31	3520.69
$NE_{ancestor}$	261,497	175,035	347,904
$NE_{nominate}$	1,951,471	758,589	3,684,813
$NE_{prebottle\ mex}$	14,878,428	0	111,940,918
$NE_{bottle\ mex}$	7,408	0	22,132
$NE_{curr\ mex}$	152,296	51,276	303,320
T_{split}	481,386	240,829	2,066,377
$T_{bottle\ mex}$	383,490	240,829	541,737
$T_{endbottle\ mex}$	99,879	59,429	147,642
m1 (mex-->nom)	6.31E-06	5.83E-06	6.56E-06
m2 (nom-->mex)	1.37E-06	8.75E-07	1.63E-06

CHAPTER 2:

The influence of demographic history and ecological variation on functional divergence in tidal marsh Savannah Sparrows (*Passerculus sandwichensis*).

Phred M. Benham & Zachary A. Cheviron

Division of Biological Sciences, University of Montana, 32 Campus Dr. HS104, Missoula, MT 59812

ABSTRACT: Linking spatial patterns of phenotypic variation with environmental variation has long been a cornerstone of research on adaptation. However, a persistent challenge in making these phenotype-environment associations is understanding how ecological and demographic factors interact to shape adaptive outcomes. To address this issue, we took advantage of multiple populations of Savannah Sparrows found in tidal marshes along the Pacific coast of North America. The high salinities characterizing tidal marsh environments poses severe osmoregulatory challenges for terrestrial vertebrates. We collected data on physiological traits associated with osmoregulatory performance from 10 tidal marshes and 3 interior populations of the Savannah Sparrow to compare patterns of trait divergence between interior and tidal marsh populations within the context of ecological and demographic variation among sites. Based on these analyses, we found that divergence in kidney mass, medulla volume, plasma osmolality, and total evaporative water loss (TEWL) among the 10 tidal marsh populations was best explained by variation in genetic divergence (measured by Fst) from the interior. In contrast, urine osmolality and urine:plasma osmolality ratio (measures of salt excretion ability) were best explained by environmental variation among sites with May-June maximum temperature being the best predictor. These results underscore the importance of simultaneously quantifying

ecological and population genetic parameters to understand the drivers of phneotypic variation in widespread taxa.

INTRODUCTION:

Analyzing patterns of geographic variation in widespread taxa has always played a central role in the development of evolutionary thought (Bergmann 1847; Darwin 1859; Allen 1877; Jordan 1905; Dobzhansky 1937; Mayr 1963; Avise 2000). This phenotypic variation is often thought to arise via local adaptation to spatial environmental heterogeneity (Mayr 1963; James 1970; Kawecki & Ebert 2004; Savolainen et al. 2013). Although ultimately driven by spatially-varying selection, the outcome of local adaptation can be strongly influenced by demographic processes (Kawecki & Ebert 2004; Stone et al. 2011; Savolainen et al. 2013; Roseman & Auerbach 2015). For example, reductions in effective population size can reduce the efficacy of natural selection to drive populations toward local adaptive optima and reduce the amount of standing genetic variation available for selection to act upon (Wright 1982; Weber & Diggins 1990; Leimu & Fischer 2008; Agashe et al. 2012; Leinonen et al. 2012). Similarly, high rates of gene flow between populations in different habitats may impede local adaptation by swamping genetic divergence through an influx of maladapted immigrants (Slatkin 1987; Lenormand 2002; Nosil & Crespi 2004; Garant et al. 2007; Räsänen & Hendry 2008). Alternatively, in small, peripheral populations gene flow can be an important source of genetic variation that promotes adaptation and 'rescues' populations from inbreeding depression (Lenormand 2002; Whiteley et al 2015; Fitzpatrick et al. 2016). Finally, although early responses

to a novel selective pressure may initially facilitate population persistence in new environments, some studies suggest that these early solutions may represent stop-gap measures, and that longer-term exposure may result in more optimal adaptive solutions that move populations closer to adaptive peaks (Mopper 2000; Beall 2006, 2007; Storz et al. 2010). Evaluating the influence of these different processes on adaptive outcomes is challenging in natural systems, but is critical for advancing our understanding of adaptation dynamics.

Comparing multiple populations of the same species occupying similar environments is one common approach to assess the degree to which adaptation proceeds in parallel across populations with patterns of non-parallel divergence potentially due to non-ecological factors (e.g. Oke et al. 2017; Leinonen et al. 2012; Langerhans 2018). This approach assumes that qualitatively similar habitats do not vary in the nature or magnitude of relevant selection pressures, yet this is often not the case (e.g., Kaeuffer et al. 2012). Thus, a full accounting of variation in patterns of adaptive divergence, requires the quantification of ecological variation among populations in addition to characterization of key demographic parameters (Stuart et al. 2017). Despite the need to examine different ecological and demographic drivers of spatial variation in adaptive traits, few studies simultaneously examine these factors across replicate populations (Berner et al. 2009; Kaeuffer et al. 2012; Raeymaekers et al. 2014; Theis et al. 2014; Stuart et al. 2017). Among the studies that do account for both ecological and demographic variation, results are mixed with ecological differences underlying non-parallel trait divergence in some cases (e.g. Kaeuffer et al. 2012; Theis et al. 2014) and demographic factors in others (e.g. Raeymaekers et al. 2012). In many cases, it is also likely that variation in ecological and demographic factors shapes patterns of trait divergence in different ways. For instance, Stuart et al. (2017) showed that across 16 pairs of lake-stream three-spined sticklebacks ecological

differences primarily influenced the direction of morphological divergence while variation in gene flow negatively influenced the magnitude of divergence among population pairs. Moreover, interpretation of divergence patterns could depend on the phenotypic traits investigated as genetic architecture (Yeaman & Whitlock 2011; Savolainen et al. 2013; Pfeifer et al. 2018), functional context (Arnold 1983; Alfaro et al. 2005; Kaeuffer et al. 2012), and plasticity (Wund et al. 2008; Dalziel et al. 2015; Oke et al. 2016) could all impact the relative influence of ecological and demographic factors on trait divergence.

The range of factors that can influence patterns of population divergence underscores the difficulty in developing a predictive framework for the relative roles demographic and historical processes play in shaping geographic patterns of local adaptation. Nonetheless, case studies that parse the influence of ecological and demographic variation on divergence in functionally relevant traits can provide key empirical data to guide theoretical efforts. Analyzing patterns of divergence in adaptive traits within the context of ecological and phylogeographic data can provide information on colonization history, the degree of connectivity among populations, and the nature of spatial variation in selection pressures. Thus providing an essential framework for evaluating the influence of demographic history on local adaptation. Here we take this approach to address the relative roles of demographic and ecological variation in shaping variation in a suite of traits associated with functional performance in replicate populations of tidal marsh Savannah Sparrows (*Passerculus sandwichensis*).

Savannah Sparrows are one of the most widespread songbird species in North America, breeding across a diverse array of environments from northern Alaska to Guatemala, including multiple resident populations in tidal marsh habitats along the Pacific coast (Wheelwright & Rising 2008). Daily inundations of seawater into tidal marsh environments impose significant

selective pressures on terrestrial organisms (Greenberg et al. 2006). Specifically, increased salt ingestion and limited access to freshwater challenges the abilities of organisms to maintain internal salt-water balance and selects for physiological mechanisms that increase salt excretion and water conservation. Early experiments demonstrated that tidal marsh Savannah Sparrows have evolved greater salinity tolerance compared to interior populations. Although interior birds were unable to maintain body weight and experienced substantial mortality (up to 60% of experimental individuals) when exposed to salinities half that of seawater (0.3 M NaCl), individuals sampled from tidal marshes maintained normal body weight with no mortality when exposed to water that exceeded the normal salinity of seawater (0.6 M NaCl; Cade & Bartholomew 1959; Poulson & Bartholomew 1962; Johnson & Ohmart 1973). Tidal marsh Savannah Sparrows exhibit greater blood plasma osmolality levels, which may be indicative of increased salinity tolerance (Cade & Bartholomew 1959; Poulson & Bartholomew 1962; Goldstein et al. 1990), but they also exhibit an increased ability to excrete salts in their urine (Poulson & Bartholomew 1962; Goldstein et al. 1990). This increased ability to excrete salts likely contributes to their ability to maintain internally stable osmolality in the face of increased salt loads (i.e. osmoregulatory capacity). Underpinning divergence in osmoregulatory capacity between tidal marsh and interior populations are a number of alterations in kidney morphology that include overall increases in kidney size (Goldstein et al. 1990), increased medullary tissue (Poulson 1965; Johnson & Mugaas 1970; Johnson & Ohmart 1973), and greater area of the proximal and distal tubules of the loop of Henle (Casotti & Braun 2000). These latter traits play a critical role in building up a steep osmotic gradient within the renal medulla via the countercurrent multiplier mechanism of the loop of Henle that enables increased salt excretion and enhanced osmoregulatory capacity (Hill et al. 2012).

The maintenance of internal salt-water balance in tidal marsh environments may also be accomplished through mechanisms that reduce water loss. Adaptations increasing water conservation could involve the renal mechanisms outlined above, but increases in water conservation can also be achieved via alteration of mechanisms that maintain heat balance. Evaporative cooling is one of the primary mechanisms that birds use to maintain body temperature during heat exposure, however, this strategy imposes water balance costs in freshwater-limited environments, such as tidal marshes. As a result, several avian species that are native to water limited environments exhibit reduced rates of evaporative loss under heat stress (Dawson 1982; Tieleman & Williams 2002; Williams & Tieleman 2002; McKechnie & Wolf 2004; Williams & Tieleman 2005; Williams et al. 2012). Although patterns of evaporative water loss have not been measured in any tidal marsh bird species, some evidence suggests that tidal marsh taxa likely evolved adaptations to reduce reliance on evaporative cooling. First, an increase in bill size compared to interior relatives is repeatedly associated with colonization of tidal marshes in sparrows, including Savannah Sparrows (Grenier & Greenberg 2005). Dietary differences may contribute to this divergence in bill size, however, within tidal marsh populations, variation in bill size is tightly correlated to summer maximum temperatures (Greenberg et al. 2012a). Indeed, thermal imaging studies confirm that increased bill size in Atlantic coast Song Sparrows (*Melospiza melodia atlantica*) allows them to dissipate 33% more heat from their bills than smaller billed interior birds, which allows them to reduce their reliance on evaporative water loss to maintain heat balance (Greenberg et al. 2012b). Finally, microCT scans of Atlantic Song Sparrow bills show greater surface area of the nasal conchae, which should enable increased recapture of water from exhaled air (Danner et al. 2017).

This body of research provides a detailed understanding of the traits underlying

enhanced osmoregulatory capacity in tidal marsh sparrows and provides expectations on how selection and demography might interact to shape patterns of variation in these osmoregulatory traits. Eight Savannah Sparrow subspecies occupy tidal marsh habitats from northern California south to Baja California and Sonora, Mexico (Fig. 1), yet the bulk of the physiological research performed thus far focuses on just a single subspecies, *P. s. beldingi.* Substantial variation in ecological variables and demographic histories likely exists across different tidal marsh populations of the Savannah Sparrow, which may drive variation in adaptive divergence among the different tidal marsh subspecies. First, across the distribution of tidal marsh Savannah Sparrows precipitation, temperature, and salinity varies extensively with southern populations experiencing hotter and drier conditions, and generally higher salinities, all of which might exacerbate osmoregulatory stress and could result in greater divergence in traits associated with osmoregulatory performance. Secondly, demographic history also varies among tidal marsh populations with previous phylogeographic work (Zink et al. 2005; Chapter 1) indicating that tidal marshes were colonized at least twice by freshwater-adapted interior birds: (1) an older colonization of marshes in southern California and northwest Mexico; and (2) a more recent colonization of the central California coast, which exhibits little genetic divergence from freshwater-adapted populations. As a result, tidal marsh Savannah Sparrows provide an excellent opportunity to assess the ecological and demographic contributions to variation in osmoregulatory traits, and how complex interactions among these forces shape patterns of adaptive divergence.

Here, we measure a suite of traits associated with osmoregulatory performance, including salt excretion, kidney morphology, and evaporative water loss in Savannah Sparrows sampled from 10 tidal marsh and three interior populations. This physiological dataset is coupled with

population genetic and environmental data to address the following hypotheses: **(1)** demographic processes drive variation in adaptive responses to tidal marshes; and **(2)** differences in the severity of selective pressures underlie variation in physiological adaptation among different tidal marsh populations. If demographic forces constrain adaptation then we expect the oldest, most isolated, and largest of the tidal marsh populations to show the greatest physiological divergence from interior relatives; whereas, if environmental differences drive patterns of geographic variation, then we will expect a tight correlation between environmental and physiological trait variation regardless of demographic parameters. These hypotheses are not mutually exclusive. We may expect ecology or demography to better explain divergence in different traits. Additionally, interactions between demographic history and ecological variation may shape observed patterns with greatest trait divergence occurring in the largest, most isolated populations that also occupy the hottest and driest localities. Parsing these different possibilities will require analyses that simultaneously quantify correlations between ecological and demographic factors on trait divergence while accounting for covariance between ecological and demographic variation.

METHODS:

Field Sampling: We visited five separate tidal marsh localities in Mexico from May-June 2014 and we sampled five tidal marsh and three interior localities in California in May-June 2015 (Fig. 1). Each of the five Mexican localities were occupied by a distinct subspecies of Savannah Sparrow: *P. s. beldingi, P. s. anulus, P. s. guttatus, P. s. magdalanae, & P. s. atratus* (van Rossem 1947). Four of the California tidal marsh localities were occupied by the subspecies *P. s. alaudinus* while the fifth -- Morro Bay-- represents a contact zone between *P. s. alaudinus* and *P.*

s. beldingi (Chapter 1). Interior localities correspond to *P. s. brooksi* (Lake Earl) and *P. s. nevadensis* (Grinnell & Miller 1944).

Physiological data: From each locality 4-11 birds were captured using mist nets. Immediately after capture, a urine sample was taken using a closed end cannula, with a small window cut in the side, inserted briefly into the cloaca (Goldstein & Braun 1989), and a blood sample was taken from the brachial vein. Blood and urine samples were frozen in liquid nitrogen to measure osmolality later (see below). Birds were held overnight to measure total evaporative water loss (TEWL) using flow-through respirometry. The respirometry experiments involved placing birds in dark, 1-liter open-circuit metabolic chambers with wire mesh above a thin layer of mineral oil to capture feces. Chambers were placed in a thermal cabinet to maintain birds at a constant 28ºC, which is within the thermal neutral zone of the species (Yarbrough 1971). Incurrent air was dried, using drierite (W.A. Hammond Drierite Co., Xenia, OH) before being pumped through animal chambers and a control chamber at constant rates (~500 ml/min). Upon exiting animal chambers air first passed through an RH-300 water vapor analyzer (Sable Systems, Inc., North Las Vegas, NV), air was then dried using drierite prior to entering a Foxbox gas analyzer (Sable Systems, Inc., North Las Vegas, NV) where we first measured carbon dioxide, followed by scrubbing CO_2 with ascarite and scrubbing additional water produced from the reaction of ascarite and CO_2 with drierite before measuring O_2 levels. Water vapor and gas measurements from the RH-300 and Foxbox were recorded continuously and differences in gas traces between the animal and control chambers were used to assess water loss for each bird. Birds were allowed to adjust to chambers for an hour and then data were collected for two hours with 15 minutes of sampling air from the bird chamber and 5 minutes from the control chamber. Following the

respirometry measurements, birds were euthanized to collect muscle tissue, extract and weigh whole kidneys (0.002 g precision balance) with the left kidney preserved in paraformaldehyde-glutaraldehyde solution for histological analyses (Karnovsky's Fixative; Electron Microscopy Sciences, Hatfield, PA). Data on kidney morphology were not collected from two sites in California (Morro Bay and Grizzly Island) as permit restrictions did not allow the sacrifice of birds from these sites.

We measured osmolality (mOsmol/kg) for each urine and blood plasma sample using a Wescor[®] osmometer. The amount of salt birds were able to excrete was calculated as the ratio of urine: plasma osmolality (U:P ratio) where greater values of U:P ratio are associated with a greater capacity to excrete salt and maintain salt-water balance (Bartholomew & Poulson 1963). This can also reflect an individual's current salt-water balance, which depends on recent dietary inputs. Water vapor traces recorded from respirometry experiments were analyzed using the program Expedata by Sable Systems, inc. (North Las Vegas, NV) to estimate total evaporative water loss (TEWL; mg H_2O/g bird/hour). In this analysis, we converted data from relative humidity to mg/ml H_2O, corrected for flow rate (~500 ml/min.), and measured TEWL as the average value of a 5 min. nadir from the lowest and most stable 15 min. sampling period. Measurements of kidney length and width were taken before and after embedding tissue in paraffin to account for shrinkage. All kidneys were embedded in paraffin wax using routine procedures (e.g. Casotti 2001). Using a microtome, 6-8 transverse sections, 5 μm thick and ~1.5 mm apart, were taken from each kidney sample. Sections were stained with haemotoxylin and eosin for routine light microscopy. Images of the sections were digitized and volume estimates of the medulla and cortex were made using the Cavalieri point-counting method (Gundersen et al. 1988) in imageJ (Schneider et al. 2012).

Environmental data: We obtained bioclimatic data at 30-arc second resolution from the WorldClim dataset (Hijmans et al. 2005) to assess environmental differences among all specimen localities. We used coordinates for each sampling locality to extract data from gridfiles of the BioClim variables within the program DIVA-GIS (http://www.diva-gis.org/). The climatic data includes 19 variables related to measures of temperature, precipitation and seasonality as well as monthly means for minimum/maximum temperature and precipitation (see Table 1). These data were derived from interpolated climate surfaces available for the entire globe at 30-arc second spatial resolution and were gathered from several independent sources between 1950-2000. To control for covariance of correlated environmental metrics in these data, we performed a principal components analysis on all 19 BioClim variables. Principal component 1 (PC1) explained 93.8% variance with annual precipitation loading most heavily on this axis. PC2 explained 5.2% of variance, and temperature seasonality exhibited the highest loading (Table 1). We also extracted data on monthly minimum temperature (Tmin), maximum temperature (Tmax), and precipitation (Prec). These monthly estimates were used to calculate average Tmin, Tmax, and Prec for the months of May and June when birds were sampled (Table 2). Finally, from each sampling locality we took 1-5 water samples randomly from different potential water sources (e.g. standing water, open estuary) and quantified osmolality (mOsmol/kg) for these samples using a Wescor® osmometer to estimate salinity for each locality (Table 2).

Genetic data: To infer population structure, migration rate, and effective population size for all populations we extracted genomic DNA from 112 individuals (see Appendix 1) from muscle tissue or whole blood using a Qiagen DNeasy Blood & Tissue extraction kit following the

manufacturer's protocols (Valencia, CA). These individuals include the 86 sampled during our

fieldwork plus an additional 26 specimens from museum collections. Samples were sequenced

using a double-digest, genotyping-by-sequencing (GBS) like approach (Parchman et al. 2012) to

generate a large SNP dataset. See Chapter 1 for library preparation details. Libraries were

submitted to the W. M. Keck Sequencing Center at the University of Illinois, Urbana-Champaign

for sequencing on an Illumina HiSeq 2500 platform. Individuals were sequenced on three

separate flow-cell lanes, each resulting in over 200 million, 100-nt single-end reads with quality

scores greater than 30, and a mean of 1,794,006 reads per individual. Reads were demultiplexed,

barcodes removed, and reads assembled into 89 bp 'stacks' using the STACKS *de novo* pipeline

(Catchen et al. 2011; Catchen et al. 2013). Briefly, this pipeline involves assembling reads from

each individual into stacks (hereafter referred to as RADloci), then matching RADloci across all

individuals to generate a catalog of shared RADloci, and, finally, RADloci from all individuals

were matched against the catalog and genotyped at this panel of loci. See Chapter 1 and

Appendix 2 for further details on RADloci assembly and selection of parameters. Following

assembly of reads into RADloci we used the 'populations' module (Catchen et al. 2013) within

STACKS to calculate the summary statistics nucleotide diversity (based on formulae presented

in Hohenlohe et al. 2010) and Fst (based on Weir & Cockerham 1984) among all 13 populations.

Larger populations are expected to exhibit greater nucleotide diversity, making it a useful proxy

for effective population size (Frankham 2012). Fst is a common measure of genetic divergence

influenced by time since divergence, gene flow between populations, and nucleotide diversity

(Holsinger & Weir 2009).

Data analysis:

Phylogeographic studies of the Savannah Sparrow indicated that two colonization events gave rise to two independent tidal marsh populations of the Savannah Sparrow. These independent tidal marsh lineages consisted of individuals sampled from 1.) Southern California and Mexico (hereafter termed Mexico tidal marsh), and 2.) those sampled from the central California coast (hereafter termed California tidal marsh) (Chapter 1). The Mexico tidal marsh populations were estimated to have diverged from their interior ancestors approximately 480,000 ybp (95% CI: 240,829 - 2,066,377 ybp), while the central California populations were not genetically differentiated from interior populations, indicating a relatively recent colonization of tidal marshes and/or greater levels of gene flow with interior birds. Based on these different colonization histories, we predicted that Mexican populations would exhibit greater magnitude of divergence in osmoregulatory traits compared to the California populations. To test this prediction, we analyzed sampling localities as three groups: 1) Mexico tidal marsh; 2) California tidal marsh; and 3) interior California. We calculated effect size (Cohen's D) for each trait based on t-tests between California tidal marsh and the interior and between Mexico tidal marsh and interior. We further evaluated statistical differences among the three groups using one-way ANOVA and TukeyHSD post-hoc tests. All statistical analyses were performed in the open source program R (https://www.r-project.org/).

We took two complementary approaches to assess the relative importance of demographic and environmental factors in shaping divergence in osmoregulatory traits. First, we performed a series of regression analyses to test for correlations between variation in demographic parameters [effective population size (as indicated by nucleotide diversity-π), genetic divergence (as indicated by Fst)] or ecological factors (osmolality, tmax, tmin, precipitation, bioclim PC1, bioclim PC2) on variation in divergence in each of the six

osmoregulatory traits across the 10 sampled tidal marsh populations. See Table 3 for a list of all 21 models compared for each of the six traits. Divergence for each osmoregulatory trait is measured as the difference between the trait mean for each tidal marsh population and the mean for each trait of the three interior populations. All variables were z-transformed prior to regression analyses. We compared likelihoods of all models using the Akaike Information Criterion corrected for sample size (AICc). Each model was ranked using ΔAICc and Akaike weights to determine which variables best predicted divergence in osmoregulatory traits.

Second, we used a structural equation modelling (SEM) approach to determine whether differences in abiotic environmental conditions or population genetic differentiation better predicted osmoregulatory trait variation among different tidal marsh populations. For each SEM model, we measured the influence of genetic divergence and a latent variable 'ecological differences' on the response variable, osmoregulatory trait divergence [see above for calculation of trait divergence (Fig. 2)]. Genetic divergence was measured as mean Fst between each tidal marsh locality and the three interior populations, i.e. the mean of three different Fst values. The latent variable ecological differences was inferred in the model from four observed ecological variables: minimum salinity, May-June Tmax, May-June Tmin, and May-June Prec. The estimated beta coefficients for genetic divergence and ecological differences were used to estimate the relative contributions of these two components on variation in trait divergence, while controlling for covariance between the genetic divergence and ecological differences. Analysis of the model was performed using maximum-likelihood estimation in the 'lavaan' R package (Rosseel 2012). We also corrected for spatial autocorrelation among the predictor variables using Moran's I implemented in the function 'lavSpatialCorrect' (https://github.com/jebyrnes/spatial_correction_lavaan).

RESULTS:

Among tidal marsh variation in physiological traits:

Across the different populations most trait values were larger in the two tidal marsh populations with a trend toward larger values in Mexico tidal marsh than California (Table 4). We first tested whether the different levels of genetic divergence observed between Mexico and California tidal marsh populations influenced patterns of physiological divergence from the three freshwater-adapted, interior populations. For most traits, the effect sizes calculated from comparisons between tidal marsh and interior populations were in the expected direction of divergence for both tidal marsh groups (California and Mexico), however, Mexico tidal marsh birds consistently exhibited greater divergence from interior birds in kidney mass, medulla volume, plasma osmolality, urine osmolality, and only Mexico tidal marsh birds exhibited significant increases in the Urine:Plasma osmolality ratio (Fig. 3). Total evaporative water loss (TEWL) was not significantly different between the interior and Mexican tidal marsh populations. Counterintuitively, rates of TEWL were greater in California tidal marshes than interior birds, opposite of the prediction that TEWL should be reduced in freshwater-limited tidal marsh habitats. These patterns were corroborated by the ANOVA and post hoc analyses, which showed that both Mexico and California tidal marsh birds were significantly different from interior populations in mean kidney mass (cal: $p=0.02$; mex: $p<0.0001$) and plasma osmolality (cal: $p=0.0001$; mex: $p<0.0001$); however, only the Mexican tidal marsh populations were significantly divergent from interior birds in medulla volume ($p<0.0001$) and urine osmolality (cal: $p=0.897$; mex: $p=0.011$; Fig. 3). Moreover, Mexican populations had significantly larger kidney mass ($p<0.0001$), medulla volume ($p<0.0001$), and plasma osmolality than the California tidal marsh birds ($p<0.0001$). Neither California nor Mexico statistically differed from the

interior in the U:P ratio, though Mexican birds did exhibit greater divergence in this metric (cal: p=0.972; mex: p=0.09; Fig. 3).

Patterns of genetic diversity:

Across the 10 tidal marsh populations, nucleotide diversity (π) increased from south-to-north with populations from Sonora, Mex. and southern Baja California exhibiting the lowest π (0.0012-0.0013) and populations from northern California exhibiting levels of π comparable to interior populations (0.0028-0.0029; Fig. 4a). Genetic divergence as measured by mean Fst between the three interior and each coastal population showed the opposite trend; southern tidal marsh populations exhibited the greatest Fst (0.12), while the northern populations exhibited the lowest (0.041-0.059; Fig. 4b).

The role of demographic versus ecological factors shaping physiological variation:

AIC analyses generally found demographic parameters (π & Fst) to be the best predictors of variation in divergence for kidney mass, medulla volume, plasma osmolality, and TEWL (Table 5; Figs. 5-6). For kidney mass, medulla volume, and TEWL, π and Fst both exhibited comparable support (ΔAICc<2), whereas π was the strongest predictor of plasma osmolality. However, environmental variables were also among the best predictors of divergence for some traits. Tmax was included among the top models predicting divergence in kidney mass, urine osmolality and urine:plasma osmolality ratio. Bioclim PC2 and Tmin also exhibiting strong support (ΔAICc<2) for urine:plasma osmolality (Table 5; Figure 7). Despite AIC analyses finding equally strong support for both π and Fst in shaping trait divergence, these two parameters exhibit opposing trends with Fst increasing from north-to-south, but π decreasing (Fig. 4). Both π and Fst were predicted to positively correlate with trait divergence; however,

plotting trait divergence and Fst (Fig. 5) or π (Fig. 6) indicates that only Fst exhibits the predicted pattern.

SEM analyses provided comparable results (Table 6). Fst explained a greater amount of variation in divergence in medulla volume (0.973 ± 0.279), plasma osmolality (0.687 ± 0.186), and TEWL (-1.0 ± 0.162) and was the only significant predictor of variance in these traits. Similar to regression analyses, ecological differences explained a greater amount of variance in urine osmolality (0.636 ± 0.228) and urine:plasma osmolality ratio (0.558 ± 0.227). Neither Fst nor ecological differences significantly explained divergence in kidney mass. Performing a correction for spatial autocorrelation using Moran's I did not influence results (Table 6).

DISCUSSION:

We took advantage of the multiple populations of Savannah Sparrows found in tidal marshes along the Pacific coast of North America to analyze how different demographic and ecological parameters may influence patterns of divergence in a suite of traits associated with functional performance. We collected population genetic, ecological, and physiological data from 10 tidal marsh and 3 interior populations to analyze patterns of physiological variation within a population genetic context. Based on these analyses, we found that variation in kidney mass, medulla volume, plasma osmolality, and TEWL divergence among the 10 tidal marsh populations was best explained by variation in genetic divergence (Fst) from the interior (Table 5-6; Fig. 5). In contrast, urine osmolality and urine:plasma osmolality ratio (measures of salt excretion ability) were best explained by variation in May-June maximum temperature among the different sampling sites (Table 5; Fig. 7). These results underscore the importance of

simultaneously quantifying ecological and population genetic parameters to understand the drivers of geographic variation in widespread taxa.

Patterns of geographic variation in traits associated with osmoregulatory performance:

Past physiological work in Savannah Sparrows identified a suite of traits associated with observed differences in salinity tolerance between interior and tidal marsh Savannah Sparrows, including: increases in kidney size (Johnson & Mugaas 1970; Goldstein et al. 1990; Casotti & Braun 2000); medullary volume (Johnson & Mugaas 1970; Casotti & Braun 2000); number of medullary cones (Poulson 1965); area of proximal and distal tubules of the loop of Henle, collecting duct, and kidney capillaries (Poulson 1965; Casotti & Braun 2000); and plasma osmolality and urine osmolality (Cade & Bartholomew 1959; Poulson & Bartholomew 1962; Goldstein et al. 1990). However, all of this work was focused on a single tidal marsh subspecies, *P. s. beldingi,* which is found from Santa Barbara, CA to Rosario, Baja California (van Rossem 1947). A single study (Johnson & Ohmart 1973) also looked at the subspecies *P. s. rostratus* from the northern Gulf of California and found similar tolerance of drinking seawater, similar kidney mass, but larger percent medulla (38.8 vs. 22.2%). The present study is the first to expand on this previous work and document patterns of variation in functional trait divergence among multiple tidal marsh populations (Table 4). Our measurements in *P. s. beldingi* were comparable to measurements reported by Goldstein et al. (1990) for kidney mass (us: 0.36 ± 0.06; them: 0.34 ± 0.04), plasma osmolality (us: 346 ± 9.9 them: 349.9 ± 6.6), and urine osmolality (us: 654.3 ± 81.7; them: 577 ± 163.6). However, across other tidal marsh subspecies, we found a general pattern of smaller kidney size, medulla volume, plasma osmolality and urine osmolality in central California coast populations relative to Mexican subspecies (Figure 3; Table 4).

Total evaporative water loss (TEWL) comprises both respiratory and cutaneous sources of evaporative water loss and together these represent important sources of water in birds (Bartholomew & Cade 1963; Dawson 1982; Williams et al. 2012). In addition to selection for mechanisms that increase salt excretion, adaptations increasing water conservation in tidal marsh birds may also be favored in high salinity environments with little access to freshwater. We found that in Mexican tidal marsh populations TEWL was significantly reduced relative to interior birds (apart from the San Bernardino Mountains population; Table 4); however, tidal marsh populations from the central California coast generally exhibited greater TEWL than the three interior populations (Table 4; Fig. 3). These results suggest that water conservation via reduced water loss may be important for adaptation to tidal marshes under some ecological and/or demographic conditions (see below), but is either not a universal response to high salinity or evolutionary divergence in this trait may be constrained in northern California. A growing body of work has pointed to the potential importance of increased bill size in tidal marsh sparrows as a key adaptation for dissipating heat at high temperatures without relying on increased evaporative water loss to guard against hyperthermia (e.g. Grenier & Greenberg 2005; Greenberg et al. 2012a; Greenberg et al. 2012b; Danner et al. 2017). Bill size in Savannah Sparrows decreases from north-to-south along the Pacific coast (Rising 2001) with the largest billed populations also exhibiting the lowest levels of TEWL. This qualitative association between bill size and TEWL is consistent with the hypothesized function of larger bills in tidal marshes for allowing increased dissipation of excess body heat while conserving water in freshwater-limited environments. However, more comprehensive work that exposes birds to thermal challenges while simultaneously measuring heat dissipation and evaporative water loss

will be required to fully understand the importance of these characters as adaptations to tidal marshes.

Demographic versus ecological drivers of variation in osmoregulatory trait divergence:

A persistent challenge for interpreting patterns of geographic variation is discerning among the different demographic or ecological factors that may be shaping patterns of variation (Stone et al. 2011; Roseman & Auerbach 2015; Stuart et al. 2017). Based on our analyses, we find that the relative influence of demographic versus ecological factors on adaptive divergence in different tidal marsh populations depended on the different traits measured. For kidney mass, medulla volume, plasma osmolality, and TEWL we found a significant relationship between genetic divergence (Fst) and the magnitude of trait divergence from interior populations (Fig. 3; Fig. 5; Tables 5-6). Genetic divergence as measured by Fst is influenced by divergence time and gene flow, with older, more isolated populations exhibiting larger values of Fst. Reductions in gene flow rate and increased divergence time would be expected to shape adaptive outcomes in similar ways. To the extent that Fst variation is driven by differences in migration rate, we find a strong negative influence of gene flow on the magnitude of trait divergence in tidal marshes, consistent with several other empirical studies documenting a constraining influence of gene flow on trait divergence (e.g. Nosil & Crespi 2004; Postma & Noordwijk 2005; Räsänen & Hendry 2008; Raeymaekers 2014; Benham & Witt 2016; Stuart et al. 2017). Greater genetic divergence also corresponds to the greater divergence times observed in Mexican tidal marsh populations (Chapter 1). Our results suggest that longer term divergence between populations occupying different environments leads to greater adaptive divergence. This result is consistent with other studies comparing adaptive divergence across multiple populations in the context of

divergence time (e.g. Mopper et al. 2000; Beall 2007). This pattern also suggests limits to selection on standing variation that may allow for rapid phenotypic responses in the short-term, but longer time scales are likely necessary for the appearance of beneficial *de novo* mutations (Barrett & Schluter 2008). Moreover, while short-term responses based on selection on standing variation may enable initial persistence, these initial responses may come with additional costs that require novel compensatory mutations. For instance, many younger high elevation populations exhibit elevated hemoglobin concentration relative to lowlanders to cope with the low partial pressures of oxygen at high elevation, however, this initial response is associated with a number of negative side-effects associated with increased blood viscosity (Villafuerte et al. 2004). As a consequence, populations occupying high elevation for longer periods have evolved other mechanisms [e.g. increased hemoglobin O2 affinity (Chappell and Snyder 1984: Storz et al. 2009), increased levels of circulating vasodilators (Beall et al. 2001)]to more efficiently deliver O_2 to the tissues without increases in red blood cell concentration and blood viscosity (Beall 2007; Storz et al. 2010). These results highlight the importance of contrasting short- and long-term responses to ecological pressures, particularly in the light of rapidly changing environments.

We also explored whether variation in nucleotide diversity, a proxy for effective population size (Ne), influences patterns of trait divergence with the prediction that larger populations would exhibit greater magnitude of divergence in osmoregulatory traits than smaller populations. This prediction stems from the expectation that larger populations would harbor greater levels of standing genetic variation, and that selection operates more efficiently in larger populations (Weber 1990; Weber & Diggins 1990; Willi et al. 2006; Leimu & Fischer 2008). Although we did find genome-wide nucleotide diversity (π), to be strongly correlated with

kidney mass, medulla volume, plasma osmolality, and TEWL (Table 5; Fig. 6), in each case the trends were in the opposite direction expected with the greatest levels of trait divergence corresponding to the populations with the smallest π (Fig. 6). The pattern of decreasing nucleotide diversity from north-to-south along the Baja peninsula (Fig. 4) is consistent with a serial founder effect (e.g. Henn et al. 2012) and stepwise colonization of Mexican tidal marshes from north-to-south. Given reduced π will be associated with greater Fst, declining π from north-to-south along the Pacific coast may also be contribute to patterns of Fst. Nevertheless, negative correlations between trait divergence and π run counter to expectations and differences in divergence time and/or gene flow were likely more important drivers of spatial variation in Fst and trait divergence.

Unlike other osmoregulatory traits, ecological factors (i.e. maximum temperature) shaped two measures of salt excretion ability: urine osmolality and the urine:plasma osmolality ratio (Table 5; Fig. 7). It is unclear why maximum temperature was found to be positively correlated with urine concentrating ability. One possibility is that it could reflect selection for reduced water losses from excreta in thermally challenging conditions as opposed to selection for increased salt excretion, which might be associated more strongly with variation in salinity among tidal marshes. Secondly, it was surprising that these two measures of salt excretion ability did not correlate with genetic divergence like other osmoregulatory traits given that variation in kidney morphology and plasma osmolality should be linked to variation in urine concentration. Past research on salt concentrating abilities in birds has focused on making links between kidney morphology and urine concentrations (e.g. Poulson 1965; Johnson & Mugaas 1970; Goldstein & Braun 1989; Casotti & Braun 2000); however, these studies do not report consistent findings. Earlier work suggested that the number of medullary cones (i.e. number of looped nephrons) and

medullary volume strongly predicted the ability to concentrate salts in the urine (Poulson 1965; Johnson & Mugaas 1970), whereas, more recent studies found little correlation between kidney morphology and urine concentrating ability (Goldstein & Braun 1989; Casotti & Braun 2000). Part of the discordance could be due to changes in techniques associated with collecting urine samples from birds. Goldstein & Braun (1989) developed a method of collecting urine from birds using a closed-end cannula that prevents contamination of the sample from intestinal fluids and using this method in species including Savannah Sparrows found significantly lower urine:plasma osmolality ratios (e.g. Goldstein et al. 1990) compared with earlier studies (e.g. Cade & Bartholomew 1959; Poulson & Bartholomew 1962). A second challenge related to accurately measuring urine osmolality is that it is a highly flexible trait influenced by fluctuations in plasma osmolality that are in turn associated with salt levels of recently consumed food and drink (Hill et al. 2012), consequently field measures of this trait are associated with high levels of variance (Table 4). A more accurate way to link kidney morphology with urine concentrating ability would be to expose birds to a known quantity and concentration of salt and measure the time course required to clear the salt. Taking this approach Sabat et al. (2004) found a qualitative association between urine concentrating ability and kidney morphology in *Cinclodes* songbirds (i.e. number of medullary cones, medullary tissue). A similar approach should be used to compare variation in urine osmolality and urine:plasma osmolality ratio across the different tidal marsh populations of the Savannah Sparrow to better understand how ecological and demographic parameters shape variation in this key functional trait.

Conclusions:

Replicate populations occupying qualitatively similar habitats provides a natural experiment for evaluating how various demographic parameters and/or ecological variation might shape adaptive outcomes. We took this approach to understand how spatially varying demography and selection pressures shapes variation in functionally relevant traits across multiple tidal marsh populations of the Savannah Sparrow. For the majority of traits measured we find a strong influence of genetic divergence on variation in trait divergence among the different tidal marshes. This indicates that gene flow and/or time since divergence plays a significant role in shaping patterns of adaptive divergence within this system. However, this result was not consistent across all measured traits as urine concentrating ability was shaped more by environmental variation among sites. These contrasting results suggest that demographic and ecological parameters can differentially influence interacting traits that contribute to increased performance (i.e. osmoregulatory capacity). Understanding adaptive dynamics to spatially varying environments thus requires careful consideration of different aspects of environmental variation, spatial variation in demography, and the functional significance of traits being investigated.

REFERENCES:

Agashe, D., Falk, J. J., & Bolnick, D. I. 2011. Effects of founding genetic variation on adaptation to a novel resource. *Evolution*, 65: 2481-2491.

Alfaro, M. E., Bolnick, D. I., & Wainwright, P. C. 2005. Evolutionary consequences of many-to-one mapping of jaw morphology to mechanics in labrid fishes. *The American Naturalist*, 165: E140-E154.

Allen, J. A. 1877. The influence of physical conditions in the genesis of species. *Radical Review*, 1, 108-140.

Arnold, S. J. 1983. Morphology, performance and fitness. *American Zoologist*, 23: 347-361.

Avise, J. C. 2000. *Phylogeography: the history and formation of species*. Harvard University Press, Cambridge, MA.

Barrett, R. D. H., & Schluter, D. 2008. Adaptation from standing genetic variation. *Trends in Ecology and Evolution*, 23: 38-44.

Bartholomew, G. A., & Cade, T. J. 1963. The water economy of land birds. *The Auk*, 80: 504-539.

Beall, C. M. 2006. Andean, Tibetan, and Ethiopian patterns of adaptation to high-altitude hypoxia. *Integrative and Comparative Biology*, 46: 18-24.

Beall, C. M. 2007. Two routes to functional adaptation: Tibetan and Andean high-altitude natives. *Proceedings of the National Academy of Sciences of the United States of America*, 104: 8655-8660.

Beall, C., Laskowski, D., Strohl, K. P., Soria R., Villena, M., Vargas, E., Alarcon, A. M., Gonzales, C. and Erzurum, S. C. 2001. Pulmonary nitric oxide in mountain dwellers. *Nature,* 414: 411-412

Benham, P. M., & Witt, C. C. 2016. The dual role of Andean topography in primary divergence: functional and neutral variation among populations of the hummingbird, *Metallura tyrianthina*. *BMC Evolutionary Biology*, 16: 22.

Bergmann, C. 1847. Über die Verhältnisse der Wärmeökonomie der Thiere zu ihrer Grösse. *Göttinger Studien,* 3: 595-708.

Berner, D., Grandchamp, A. C., & Hendry, A. P. (2009). Variable progress toward ecological speciation in parapatry: Stickleback across eight lake-stream transitions. *Evolution*, *63*(7), 1740-1753.

Cade, T., & Bartholomew, G. A. 1959. Sea-water and salt utilization by Savannah sparrows. *Physiological Zoology*, 32: 230-238.

Casotti, G., & Braun, E. J. 2000. Renal anatomy in sparrows from different environments. *Journal of Morphology*, 243: 283-291

Casotti, G. 2001. Effects of season on kidney morphology in house sparrows. *The Journal of Experimental Biology*, 204: 1201-1206.

Catchen, J. M., Amores, A., Hohenlohe, P., Cresko, W., Postlethwait, J. H., & De Koning, D.-J. 2011. Stacks: building and genotyping loci de novo from short-read sequences. *G3: Genes|Genomes|Genetics*, 1: 171-182.

Catchen, J., Hohenlohe, P. A., Bassham, S., Amores, A., & Cresko, W. A. 2013. Stacks: An analysis tool set for population genomics. *Molecular Ecology*, 22: 3124-3140.

Chappell, M.A., & Snyder, L. R. G. 1984 Biochemical and physiological correlates of deer mouse chain hemoglobin polymorphisms. *Proc Natl Acad Sci USA,* 81: 5484-5488.

Dalziel, A. C., Martin, N., Laporte, M., Guderley, H., & Bernatchez, L. 2015. Adaptation and acclimation of aerobic exercise physiology in Lake Whitefish ecotypes (Coregonus clupeaformis). *Evolution*, 69: 2167-2186.

Danner, R. M., Gulson-castillo, E. R., James, H. F., Dzielski, S. A., Iii, D. C. F., Sibbald, E. T., & Winkler, D. W. 2017. Habitat-specific divergence of air conditioning structures in bird bills. *The Auk*, 134: 65-75.

Darwin, C. 1859. *On the origin of species.* John Murray, London, UK.

Dawson, W. R. (1982). Evaporative losses of water by birds. *Comparative Biochemistry and Physiology - Part A: Physiology*, 71: 495-509.

Dobzhansky, T. 1937. *Genetics and the origin of species.* Columbia University Press, New York, NY.

Fitzpatrick, S. W., Gerberich, J. C., Angeloni, L. M., Bailey, L. L., Broder, E. D., Torres-Dowdall, J., … Chris Funk, W. 2016. Gene flow from an adaptively divergent source causes rescue through genetic and demographic factors in two wild populations of Trinidadian guppies. *Evolutionary Applications*, 9: 879-891.

Frankham, R. 2012. How closely does genetic diversity in finite populations conform to predictions of neutral theory Large deficits in regions of low recombination. *Heredity*, 108: 167-178.

Garant, D., Forde, S. E., & Hendry, A. P. 2007. The multifarious effects of dispersal and gene flow on contemporary adaptation. *Functional Ecology*, 21: 434-443.

Goldstein, D. L., & Braun, E. J. 1989. Structure and concentrating ability in the avian kidney. *The American Journal of Physiology*, 256: 501-509.

Goldstein, D. L., Williams, J. B., & Braun, E. J. 1990. Osmoregulation in the field by salt-marsh savannah sparrows Passerculus sandwichensis beldingi. *Physiological Zoology*, 63: 669-682.

Greenberg, R., Maldonado, J. E., Droege, S., & McDonald, M. V. 2006. Tidal Marshes: A Global Perspective on the Evolution and Conservation of Their Terrestrial Vertebrates. *BioScience*, 56: 675-685.

Greenberg, R., Danner, R., Olsen, B., & Luther, D. 2012a. High summer temperature explains bill size variation in salt marsh sparrows. *Ecography*, 35: 146-152.

Greenberg, R., Cadena, V., Danner, R. M., & Tattersall, G. 2012b. Heat loss may explain bill size differences between birds occupying different habitats. *PLoS ONE*, 7: 1-9.

Grenier, J. L., & Greenberg, R. 2005. A biogeographic pattern in sparrow bill morphology: parallel adaptation to tidal marshes. *Evolution*, 59: 1588-1595.

Grinnell, J. & Miller, A. H. 1944. The distribution of the birds of California. *Pacific Coast Avifauna,* 27, 1-608.

Gundersen, H. J. G., Bendtsen, T. F., Korbo, L., Marcussen, N., Møller, A., Nielsen, K., … West, M. J. 1988. Some new, simple and efficient stereological methods and their use in pathological research and diagnosis. *Apmis*, 96: 379-394.

Henn, B. M., Cavalli-Sforza, L. L., & Feldman, M. W. 2012. The great human expansion. *Proceedings of the National Academy of Sciences*, 109: 17758-17764.

Hijmans, R. J., Cameron, S. E., Parra, J. L., Jones, P. G., & Jarvis, A. 2005. Very high resolution interpolated climate surfaces for global land areas. *International Journal of Climatology*, 25: 1965-1978.

Hill, R. W., Wyse, G. A. & M. Anderson. 2012. *Animal physiology, 3rd ed.* Sinauer Associates, Inc., Sunderland, MA.

Hohenlohe, P. A., Bassham, S., Etter, P. D., Stiffler, N., Johnson, E. A., & Cresko, W. A. 2010. Population genomics of parallel adaptation in threespine stickleback using sequenced RAD tags. *PLoS Genetics*, 6.

Holsinger, K. E., & Weir, B. S. 2009. Genetics in geographically structured populations: defining, estimating and interpreting Fst. *Nature Reviews Genetics*, 10: 639-650.

James, F. C. 1970. Geographic Size Variation in Birds and Its Relationship to Climate. *Ecology*, 51: 365-390.

Johnson, O. W., & Mugaas, J. N. 1970. Quantitative and Organizational Features of the Avian Renal Medulla. *The Condor*, 72: 288-292.

Johnson, O. W., & Ohmart, R. D. 1973. Some features of water economy and kidney microstructure in the large-billed savannah sparrow (*Passerculus sandwichensis rostratus*). *Physiological Zoology*, 46: 276-284.

Jordan, D. S. 1905. The origin of species through isolation. *Science,* 22: 545-562.

Kaeuffer, R., Peichel, C. L., Bolnick, D. I., & Hendry, A. P. 2012. Parallel and nonparallel aspects of ecological, phenotypic, and genetic divergence across replicate population pairs of lake and stream stickleback. *Evolution*, 66: 402-418.

Kawecki, T. J., & Ebert, D. 2004. Conceptual issues in local adaptation. *Ecology Letters*, 7: 1225-1241.

Langerhans, R. B. 2018. Predictability and parallelism of multitrait adaptation. *Journal of Heredity*, 109: 59-70.

Leimu, R., & Fischer, M. 2008. A meta-analysis of local adaptation in plants. *PLoS ONE*, 3: 1-8.

Leinonen, T., McCairns, R. J. S., Herczeg, G., & Merilä, J. 2012. Multiple evolutionary pathways to decreased lateral plate coverage in freshwater threespine sticklebacks. *Evolution*, 66: 3866-3875.

Lenormand, T. 2002. Gene flow and the limits to natural selection. *Trends in Ecology and Evolution*, 17: 183-189.

Mayr, E. 1963. *Animal species and evolution.* Harvard University: Belknap Press, Cambridge, MA.

McKechnie, A. E., & Wolf, B. O. 2004. Partitioning of evaporative water loss in white-winged doves: plasticity in response to short-term thermal acclimation. *The Journal of Experimental Biology*, *207*, 203-210.

Mopper, S., Stiling, P., Landau, K., Simberloff, D., & Van Zandt, P. 2000. Spatiotemporal variation in leafminer population structure and adaptation to individual oak trees. *Ecology*, 1577-1587.

Nosil, P., & Crespi, B. J. 2004. Does gene flow constrain adaptive divergence or vice versa? A test using ecomorphology and sexual isolation in *Timena cristinae* walking-sticks. *Evolution*, 58*:* 102-112.

Oke, K. B., Bukhari, M., Kaeuffer, R., Rolshausen, G., Räsänen, K., Bolnick, D. I., … Hendry, A. P. 2016. Does plasticity enhance or dampen phenotypic parallelism? A test with three lake-stream stickleback pairs. *Journal of Evolutionary Biology*, 29: 126-143.

Oke, K. B., Rolshausen, G., LeBlond, C., & Hendry, A. P. 2017. How Parallel Is Parallel Evolution? A Comparative Analysis in Fishes. *The American Naturalist*, 190: 1-16.

Parchman, T. L., Gompert, Z., Mudge, J., Schilkey, F. D., Benkman, C. W., & Buerkle, C. A. 2012. Genome-wide association genetics of an adaptive trait in lodgepole pine. *Molecular Ecology*, 21: 2991-3005.

Pfeifer, S. P., Laurent, S., Sousa, V. C., Linnen, C. R., Foll, M., Excoffier, L., … Jensen, J. D. 2018. The Evolutionary History of Nebraska Deer Mice: Local Adaptation in the Face of Strong Gene Flow. *Molecular Biology and Evolution*, 1-40.

Postma, E., & van Noordwijk, A. J. 2005. Gene flow maintains a large genetic difference in clutch size at a small spatial scale. *Nature*, 433: 65-68.

Poulson, T. L., & Bartholomew, G. A. 1962. Salt balance in the Savannah Sparrow. *Physiological Zoology*, 35: 109-119.

Poulson, T. L. 1965. Countercurrent Multipliers in Avian Kidneys. *Science*, 14*:* 389-391.

Räsänen, K., & Hendry, A. P. 2008. Disentangling interactions between adaptive divergence and gene flow when ecology drives diversification. *Ecology Letters*, 11: 624-636.

Raeymaekers, J. A. M., Konijnendijk, N., Larmuseau, M. H. D., Hellemans, B., De Meester, L., & Volckaert, F. A. M. 2014. A gene with major phenotypic effects as a target for selection vs. homogenizing gene flow. *Molecular Ecology*, 23: 162-181.

Rising, J. D. 2001. Geographic Variation in Size and Shape of Savannah Sparrows (*Passerculus Sandwichensis*) Geographic Variation in Size and Shape of. *Studies in Avian Biology*, 23: 1-65.

Rosseel, Y. 2012. lavaan: An R Package for Structural Equation Modeling. *Journal of Statistical Software*, 48: 1-36.

Roseman, C. C., & Auerbach, B. M. 2015. Ecogeography, genetics, and the evolution of human body form. *Journal of Human Evolution*, 78: 80-90.

Sabat, P., Maldonado, K., Rivera-Hutinel, A., & Farfan, G. 2004. Coping with salt without salt glands: osmoregulatory plasticity in three species of coastal songbirds (ovenbirds) of the genus Cinclodes (Passeriformes: Furnariidae). *Journal of Comparative Physiology. B, Biochemical, Systemic, and Environmental Physiology*, 174: 415-420.

Savolainen, O., Lascoux, M., & Merilä, J. 2013. Ecological genomics of local adaptation. *Nature Reviews. Genetics*, 14: 807-20.

Schneider, C. A., Rasband, W. S., & Eliceiri, K. W. 2012. NIH Image to ImageJ: 25 years of image analysis. *Nature Methods*, 9: 671-675.

Slatkin, M. 1987. Gene flow and the geographic structure of natural populations. *Science*, 236: 787-792.

Stone, G. N., Nee, S., & Felsenstein, J. 2011. Controlling for non-independence in comparative analysis of patterns across populations within species. *Philosophical Transactions of the Royal Society of London. Series B, Biological Sciences*, 366: 1410-1424.

Storz, J. F., Scott, G. R., & Cheviron, Z. A. 2010. Phenotypic plasticity and genetic adaptation to high-altitude hypoxia in vertebrates. *The Journal of Experimental Biology*, 213: 4125-36.

Storz, J. F., A. M. Runck, S. J. Sabatino, J. K. Kelly, N. Ferrand, H. Moriyama, R. E. Weber, and A. Fago. 2009. Evolutionary and functional insights into the mechanism underlying high altitude adaptation of deer mouse hemoglobin. *Proceedings of the National Academy of Sciences USA*, 106: 14450-14455

Stuart, Y. E., Veen, T., Thompson, C., Tasneem, T., Ahmed, N., Izen, R., … Bolnick, D. I. 2017. Contrasting effects of environment and genetics generate a predictable continuum of parallel evolution. *Nature Ecology and Evolution*, 1: 1-7.

Theis, A., Ronco, F., Indermaur, A., Salzburger, W., & Egger, B. 2014. Adaptive divergence between lake and stream populations of an East African cichlid fish. *Molecular Ecology*, 23: 5304-5322.

Tieleman,B. Irene & Williams, J. B. 2002. Cutaneous and Respiratory Water Loss in Larks from Arid and Mesic Environments. *Physiological and Biochemical Zoology: Ecological and Evolutionary Approaches*, 75: 590-599.

van Rossem, A. J. 1947. A Synopsis of the Savannah Sparrows of Northwestern Mexico. *The Condor*, 49: 97-107.

Villafuerte, F. C. 2004. Optimal hemoglobin concentration and high altitude: a theoretical approach for Andean men at rest. *Journal of Applied Physiology*, 96: 1581-1588.

Weber, K. E. 1990. Increased selection response in larger populations. I. Selection for wing-tip height in Drosophila melanogaster at three population sizes. *Genetics*, 125: 579-584.

Weber, K. E., & Diggins, L. T. 1990. Increased selection response in larger populations. II. Selection for ethanol vapor resistance in Drosophila melanogaster at two population sizes. *Genetics*, 125: 585-597.

Weir, B.S. & Cockerham, C. C. 1984. Estimating F-statistics for the analysis of population structure. *Evolution*, 38: 1358-1370.

Wheelwright, N.T., and J.D. Rising. 2008. Savannah Sparrow (*Passerculus sandwichensis*). *in* Birds of North American Online (A. Poole, Ed.). Cornell Lab of Ornithology, Ithaca, NY.

Whiteley, A. R., Fitzpatrick, S. W., Funk, W. C., & Tallmon, D. A. 2015. Genetic rescue to the rescue. *Trends in Ecology and Evolution*, 30: 42-49.

Willi, Y., Van Buskirk, J., & Hoffmann, A. A. 2006. Limits to the adaptive potential of small populations. *Annual Review of Ecology, Evolution, and Systematics*, 37: 433-458.

Williams, J. B., & Tieleman, B. I. 2002. Ecological and evolutionary physiology of desert birds: a progress report. *Integrative and Comparative Biology*, 42: 68-75.

Williams, J. B., & Tieleman, B. I. 2005. Physiological Adaptation in Desert Birds. *BioScience*, 55: 416-425.

Williams, J. B., Munoz-Garcia, A., & Champagne, A. 2012. Climate change and cutaneous water loss of birds. *Journal of Experimental Biology*, 215: 1053-1060.

Wright, S. 1982. Character change, speciation, and the higher taxa. *Evolution*, 36: 427-443.

Wund, M. A., Baker, J. A., Clancy, B., Golub, J. L., & Foster, S. A. 2008. A Test of the "Flexible Stem" model of evolution: ancestral plasticity, genetic accommodation, and morphological divergence in the threespine stickleback radiation. *The American Naturalist*, 172: 449-462.

Yarbrough, C. G. 1971. The influence of distribution and ecology on the thermoregulation of small birds. *Comparative Biochemistry and Physiology - Part A: Physiology*, 39: 235-266.

Yeaman, S., & Whitlock, M. C. 2011. The genetic architecture of adaptation under migration-selection balance. *Evolution*, 65: 1897-1911.

Zink, R. M., Rising, J. D., Mockford, S., Horn, A. G., Wright, J. M., Leonard, M., & Westberg, M. C. 2005. Mitochondrial DNA variation, species limits, and rapid evolution of plumage coloration and size in the Savannah Sparrow. *The Condor*, 107: 21-28.
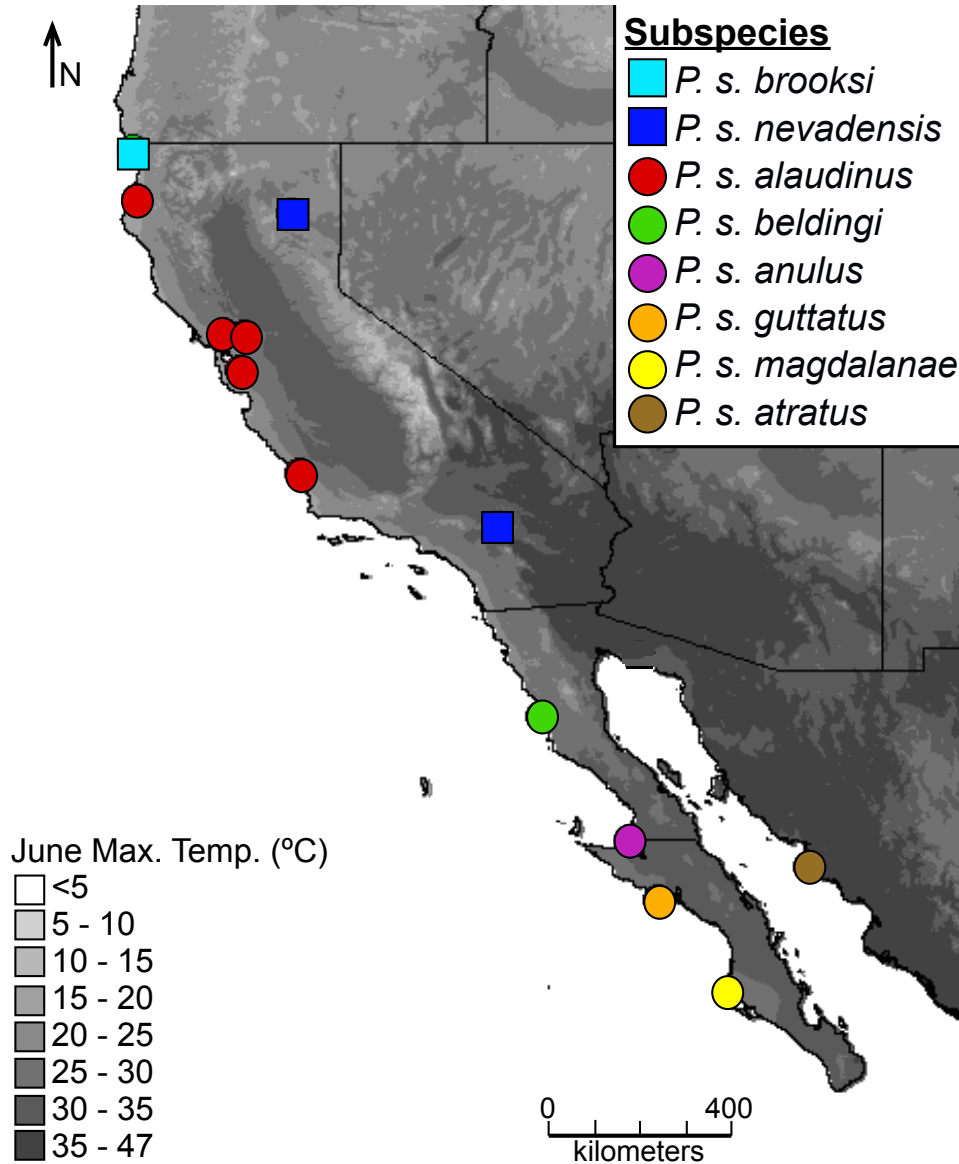
Figure 1: Map of California and northwest Mexico showing sampling localities for the study. Each point colored by subspecies distinction. Squares denote interior populations and circles tidal marsh populations. Grayscale of map reflects the maximum June temperature (ºC) from the WorldClim dataset.
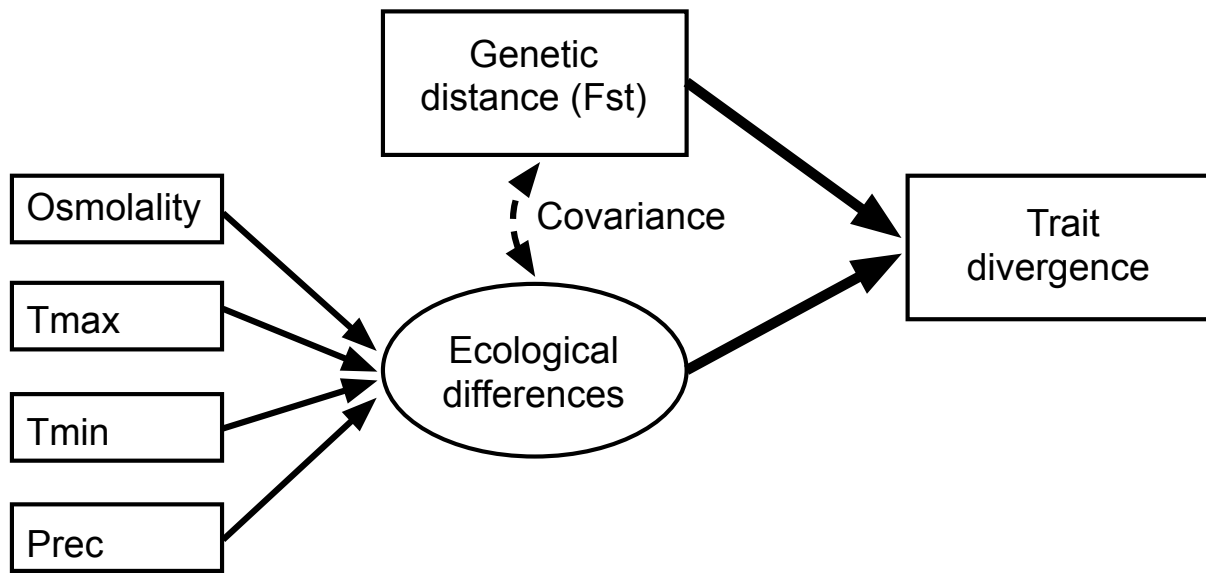
Figure 2: Model tested using structural equation modeling to dissect the relative influence of ecological variation and genetic distance on variation in divergence in the six measured traits associated with osmoregulatory performance.
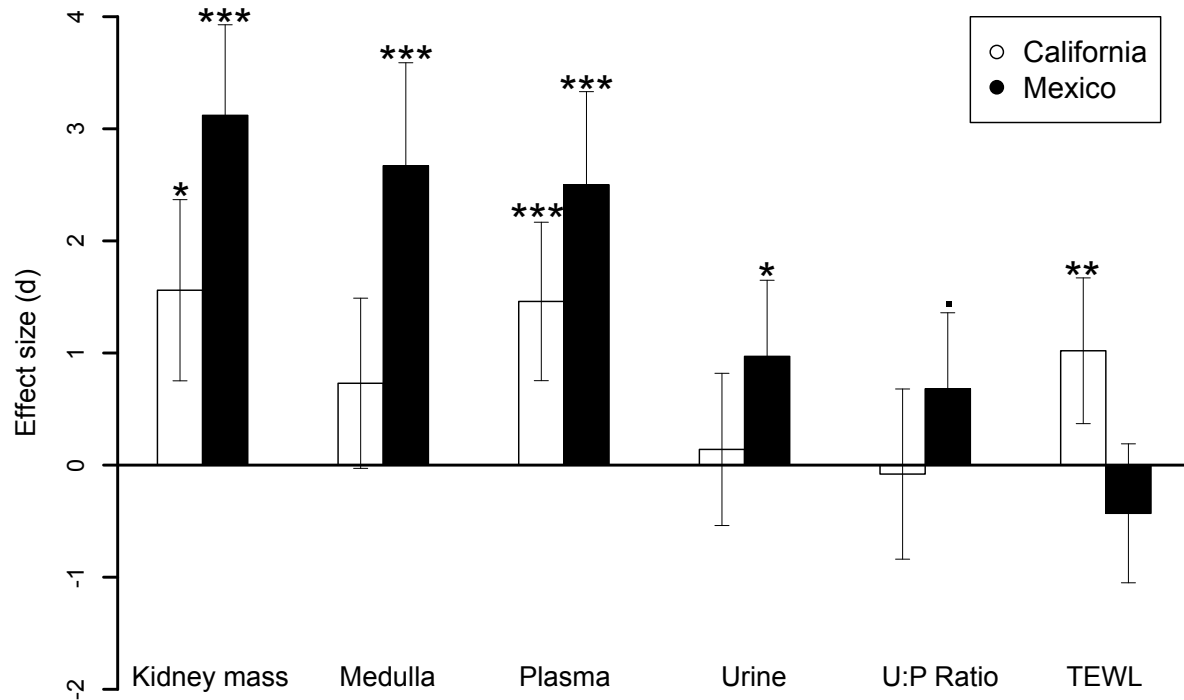
Figure 3: Plot of effect sizes for each trait. Zero line represents mean trait value from the three interior populations. Effect size was calculated using Cohen's D based on t-tests from between California tidal marsh and interior or Mexico tidal marsh and interior. Traits are kidney mass corrected for variaton in body size, volume of medulla tissue in the kidneys (mm^3), plasma osmolality (mOsmol/kg), urine osmolality (mOsmol/kg), ratio between urine and plasma osmolality, and total evaporative water loss- TEWL (mg/g/hr). Asterisks denote results from ANOVA and TukeyHSD posthoc analyses of the three groups (interior, Mexico tidal marsh, California tidal marsh). *** <0.001; **<0.01; *<0.05; . <0.1.
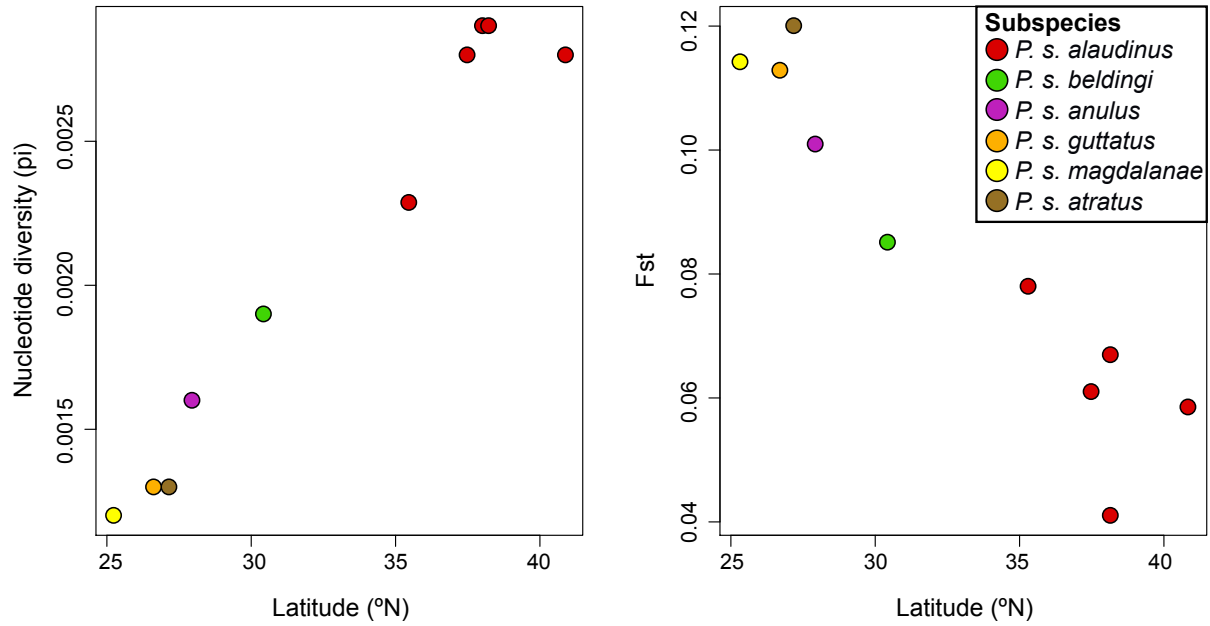
Figure 4: Latitudinal variation in nucleotide diversity (left panel) and Fst between inland populations and each tidal marsh population (right panel) across the 10 tidal marsh populations of Savannah Sparrow sampled. Circles are colored by subspecies classifications for each of the sampled populations.

Figure 5: Linear regression results showing the relationship between genetic divergence and each of the measured osmoregulatory traits. Genetic divergence is measured as mean Fst between the three inland populations and each tidal marsh population. All values are z-transformed.
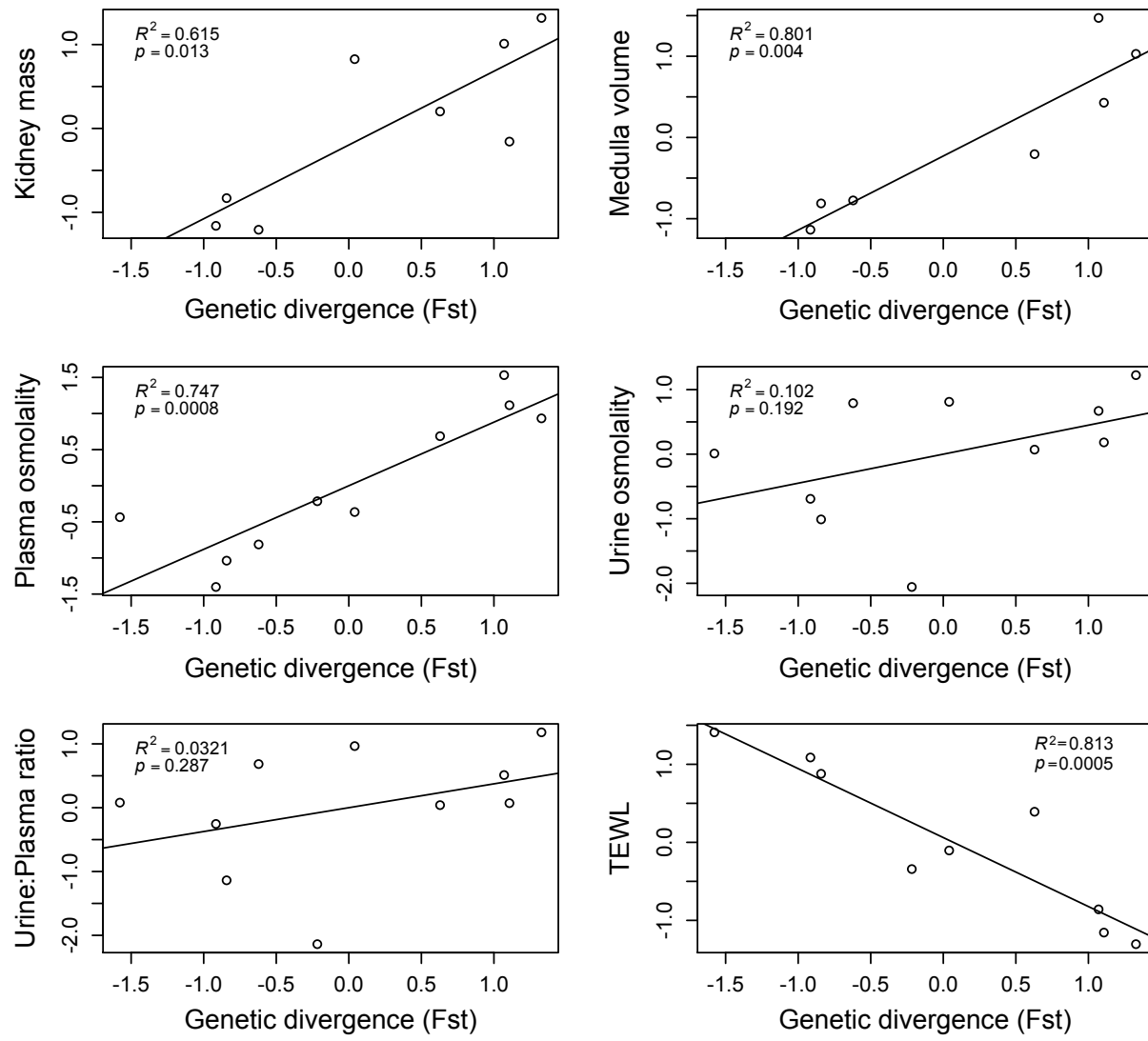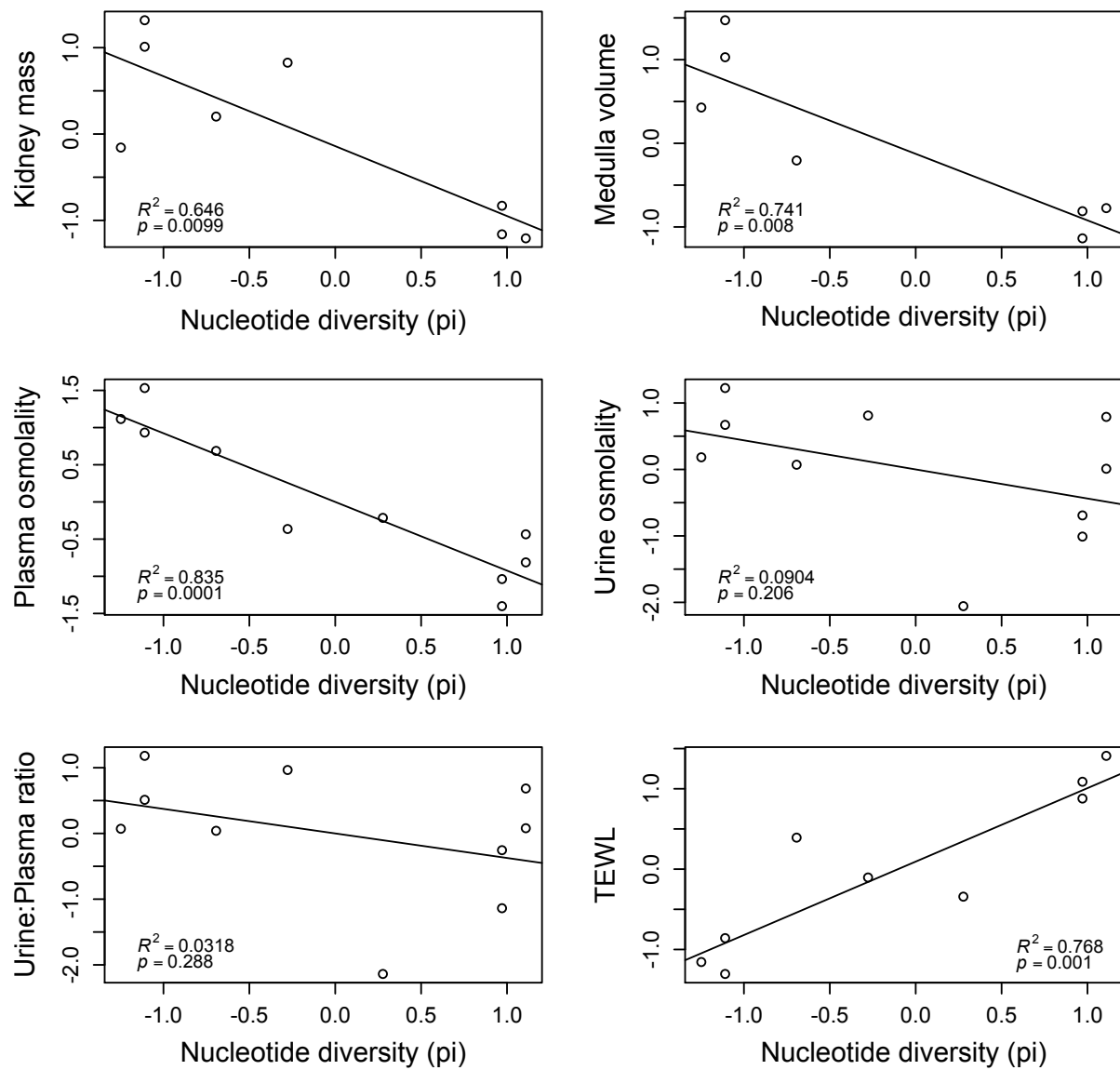
Figure 6: Linear regression results showing the relationship between nucleotide diversity and each of the measured osmoregulatory traits. All values are z-transformed.
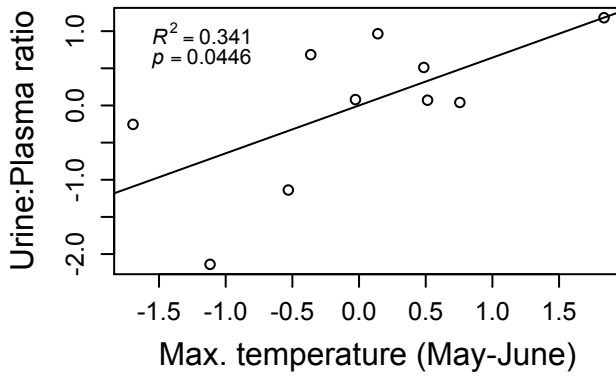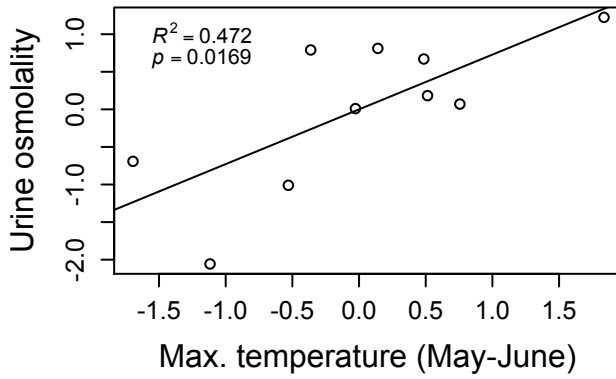
Figure 7: Linear regression results showing the relationship between the maximum average temperature (ºC) for the months of May-June and urine osmolality and urine:plasma osmolality ratio. All values z-transformed.

Table 1: Loadings from principal component analysis of all 19 Bioclim variables for the first

four principal components (PCs), which cumulatively explain 99.97% of the variance.

Bioclim Variables	PC1	PC2	PC3	PC4
Annual mean temperature	0.0086	0.0113	0.0441	-0.0035
Mean diurnal range	0.0055	0.0041	-0.0063	-0.0157
Isothermality	0.0048	-0.0409	0.0119	-0.0757
Temperature seasonality	0.0942	0.9723	-0.1473	0.1330
Max. temp warmest month	0.0125	0.0214	0.0214	0.0050
Min. temp coldest month	0.0047	-0.0032	0.0389	0.0138
Temp annual range	0.0078	0.0246	-0.0175	-0.0088
Mean temp wettest quarter	0.0109	0.0218	0.1239	-0.0570
Mean temp driest quarter	0.0049	0.0153	-0.0030	0.0037
Mean temp warmest quarter	0.0103	0.0215	0.0448	0.0073
Mean temp coldest quarter	0.0078	-0.0022	0.0483	0.0001
Annual precipitation	-0.7968	0.0633	0.3245	0.4138
Precip. wettest month	-0.1477	0.0634	-0.1474	-0.2389
Precip. driest month	-0.0028	-0.0014	0.0058	0.0151
Precip seasonality	0.0032	0.0331	-0.0450	-0.4539
Precip wettest quarter	-0.4035	0.1122	-0.0424	-0.5939
Precip driest quarter	-0.0205	-0.0035	0.0824	0.1672
Precip warmest quarter	0.0061	0.1677	0.7150	-0.3776
Precip coldest quarter	-0.4130	-0.0276	-0.5525	-0.1222
Proportion of variance	0.9379	0.0521	0.0081	0.0016
Cumulative proportion	0.9379	0.9900	0.9981	0.9997

Table 2: Environmental data from each sampling locality. Includes mean salinity measured from each site of capture, as well as average May-June maximum temperature, minimum temperature and precipitation from the WorldClim dataset (Hijmans et al. 2005).

Location	Subspecies	Group	Min. Salinity (mOsmol/kg)	Tmax(ºC)	Tmin(ºC)	Prec (mm)
Humboldt Bay	*alaudinus*	Cal salt	166	17.05	9.25	31.5
San Pablo Bay	*alaudinus*	Cal salt	589.67	24.2	10.25	7.5
Suisun Bay	*alaudinus*	Cal salt	171.67	26	11.35	6
San Francisco Bay	*alaudinus*	Cal salt	608	23.3	11.5	4
Morro Bay	*alaudinus*	Cal salt	989	20.15	9.05	4
Bahía San Quintin	*beldingi*	Mex salt	1095	26.9	12.15	0.5
Guerrero Negro	*anulus*	Mex salt	1049	30.2	13.3	0.5
Punta Abreojos	*guttatus*	Mex salt	1172.7	28.75	12.65	0
Lopez Mateos	*magdalanae*	Mex salt	2322.7	28.9	14.6	0
La Atanasia	*atratus*	Mex salt	1164.3	36	19.65	1
Lake Earl	*brooksi*	interior	0	17.8	8.5	65
Lassen NF	*nevadensis*	interior	0	19.8	1.85	33.5
San Bernardino NF	*nevadensis*	interior	no water	21.3	3.45	10.5

Table 3: List of models compared using AIC analyses. Osmolality refers to minimum salinity (mOsmol/kg) at each site, Tmax and Tmin are maximum and minimum average temperature(ºC) for May-June, Precipitation is average precipitation (mm) for May-June. See Table X for specific values at each site.

Model
Fst
Nucleotide diversity (π)
Osmolality
Bioclim PC1
Bioclim PC2
Precipitation
Tmax
Tmin
Osmolality + Bioclim PC1
Osmolality + Bioclim PC2
Osmolality + Precipitation
Osmolality + Tmax
Osmolality + Tmin
Precipitation + Bioclim PC1
Precipitation + Bioclim PC2
Tmax + Bioclim PC1
Tmax + Bioclim PC2
Tmax + Precipitation
Tmin + Bioclim PC1
Tmin + Bioclim PC2
Tmin + Precipitation
Tmin + Tmax

Table 4: Mean trait values for each sampled population with standard deviation in parentheses.

Population	Subspecies	Group	Kidney mass (g)	Medulla volume (mm^3)	Plasma osmolality (mOsmol/kg)	Urine osmolality (mOsmol/kg)	Urine:Plasma	TEWL (mg/g/h)
Humboldt Bay	*alaudinus*	Cal tidal	0.13 (0.01)	14.26 (3.55)	335.6 (25.2)	491.67 (200.9)	1.53 (0.66)	7.22 (0.75)
San Pablo Bay	*alaudinus*	Cal tidal	0.13 (0.01)	24.62 (4.71)	341.5	652.0 (42.8)	1.81	NA
Suisun Bay	*alaudinus*	Cal tidal	NA	NA	345.3 (9.0)	567.6 (214.9)	1.63 (0.73)	7.95 (1.30)
San Francisco Bay	*alaudinus*	Cal tidal	0.13 (0.01)	23.56 (7.88)	339.3 (4.4)	457.2 (221.9)	1.26 (0.71)	6.75 (1.27)
Morro Bay	*alaudinus*	Cal tidal	NA	NA	346.5 (11.0)	344.0 (148.1)	0.96 (0.46)	3.99 (0.79)
Bahía San Quintin	*beldingi*	Mex tidal	0.18 (0.03)	NA	346.0 (9.9)	654.3 (81.7)	1.9 (0.29)	4.53 (0.89)
Guerrero Negro	*anulus*	Mex tidal	0.17 (0.02)	40.94 (13.44)	356.5 (9.6)	574.1 (157.1)	1.62 (0.46)	5.65 (1.02)
Punta Abreojos	*guttatus*	Mex tidal	0.19 (0.03)	89 (42.59)	365.0 (20.9)	639.0 (75.8)	1.76 (0.25)	2.82 (0.62)
Lopez Mateos	*magdalanae*	Mex tidal	0.14 (0.02)	59.09 (11.34)	360.8 (16.9)	586.0 (203.0)	1.63 (0.57)	2.14 (0.35)
La Atanasia	*atratus*	Mex tidal	0.2 (0.01)	76.32 (14.86)	359.0 (16.3)	698.9 (154.7)	1.96 (0.5)	1.81 (0.13)
Lake Earl	*brooksi*	interior	0.11 (0.01)	14.33 (4.69)	317.6 (9.5)	324.2 (130.8)	1.03 (0.42)	5.81 (1.56)
Lassen NF	*nevadensis*	interior	0.11 (0.01)	13.75 (3.63)	328.8 (19.1)	484.5 (201.6)	1.37 (0.64)	4.7 (0.84)
San Bernardino NF	*nevadensis*	interior	0.09 (0.01)	22.5 (6.99)	318.6 (11.7)	664.0 (71.4)	2.11 (0.21)	2.09 (0.08)

Table 5: Top regression models explaining variance in trait divergence based on AIC analysis. Values included are number of parameters (K), AICc, ΔAICc, Akaike weights (the relative likelihood of each model; AICc.Wt), cumulative weight (Cum.Wt), and model likelihoods (LL). Table only shows models up to a cumulative weight of 0.95.

Kidney mass						Medulla volume					
Model	K	AICc	ΔAICc	AICc Wt	Cum. Wt	LL	Model	K	AICc	ΔAICc	AICc Wt	Cum. Wt	LL
Pi	3	24.09	0.00	0.33	0.33	-6.04	Fst	3	20.20	0.00	0.65	0.65	-3.10
Fst	3	24.77	0.69	0.24	0.57	-6.39	Pi	3	22.05	1.85	0.26	0.91	-4.03
Tmax	3	24.87	0.79	0.22	0.79	-6.44	Tmax	3	26.04	5.84	0.04	0.95	-6.02
PC1	3	26.70	2.61	0.09	0.88	-7.35							
Tmin	3	27.43	3.35	0.06	0.94	-7.72							
Prec	3	29.68	5.59	0.02	0.97	-8.84							

Plasma osmolality							TEWL						
Model	K	AICc	ΔAICc	AICc Wt	Cum. Wt	LL	Model	K	AICc	ΔAICc	AICc Wt	Cum. Wt	LL
Pi	3	18.15	0.00	0.82	0.82	-4.07	Fst	3	18.98	0.00	0.67	0.67	-4.09
Fst	3	22.40	4.25	0.10	0.92	-6.20	Pi	3	20.91	1.94	0.25	0.93	-5.06
Tmax+PC2	4	23.96	5.81	0.05	0.97	-3.98	Osmo	3	24.74	5.76	0.04	0.96	-6.97

Urine osmolality							Urine:Plasma ratio						
Model	K	AICc	ΔAICc	AICc Wt	Cum. Wt	LL	Model	K	AICc	ΔAICc	AICc Wt	Cum. Wt	LL
Tmax	3	29.76	0.00	0.40	0.40	-9.88	Tmax	3	31.97	0.00	0.26	0.26	-10.99
Tmin	3	32.23	2.47	0.12	0.52	-11.12	PC2	3	32.86	0.88	0.17	0.42	-11.43
Tmax+PC1	4	32.75	2.99	0.09	0.61	-8.38	Tmin	3	33.26	1.29	0.14	0.56	-11.63
PC2	3	33.04	3.28	0.08	0.69	-11.52	Tmax+PC2	4	34.18	2.21	0.09	0.65	-9.09
Tmax+Prec	4	33.75	3.99	0.06	0.75	-8.87	Tmax+Prec	4	34.48	2.51	0.07	0.72	-9.24
Tmax+PC2	4	34.16	4.40	0.04	0.79	-9.08	Fst	3	35.82	3.85	0.04	0.76	-12.91
Fst	3	35.07	5.31	0.03	0.82	-12.53	Pi	3	35.82	3.85	0.04	0.79	-12.91
Osmo+Tmax	4	35.10	5.34	0.03	0.85	-9.55	Tmax+PC2	4	36.01	4.03	0.03	0.83	-10.00
pi	3	35.20	5.44	0.03	0.88	-12.60	PC1	3	36.67	4.70	0.02	0.85	-13.33
Tmin+Tmax	4	35.56	5.80	0.02	0.90	-9.78	Prec	3	37.06	5.09	0.02	0.87	-13.53
PC1	3	35.87	6.11	0.02	0.92	-12.93	Osm+Tmax	4	37.07	5.09	0.02	0.89	-10.53
Prec	3	36.33	6.56	0.02	0.93	-13.16	Osmo	3	37.12	5.14	0.02	0.91	-13.56
Osmo+PC2	4	36.40	6.63	0.01	0.95	-10.20	Tmin+PC2	4	37.28	5.30	0.02	0.93	-10.64
							Osmo+PC2	4	37.34	5.37	0.02	0.95	-10.67

Table 6: Structural equation modeling results examining relative influence of ecology and genetic divergence on trait divergence across the 10 sampled tidal marsh populations (see Fig. 2). For each trait the estimated coefficients for genetic divergence (Fst) and the latent variable ecology plus or minus the standard errors are presented as well as the covariance between Fst and ecology (cov). Asterisks following each value denote the significance of each model: *** <0.001; **<0.01; *<0.05; ns >0.05. Salinity, Tmax, Tmin, and Prec were the four variables used to generate the latent variable ecology, presented are factor loading coefficients for each variable. Also shown are coefficients and significance for Fst and ecology following correction for spatial autocorrelation.

Trait	no correction			ecological variables				spatial correction	
	Fst ± se	ecology ± se	cov	salinity	tmax	tmin	prec	Fst	ecology
Kidney mass	0.518 ± 0.336 ns	0.348 ± 0.321 ns	0.754	0.513	1	0.877	-0.79	0.518 ns	0.348 ns
Medulla volume	0.973 ± 0.279***	-0.06 ± 0.267 ns	0.747	0.53	1	0.89	-0.81	0.972***	-0.068 ns
Plasma osmolality	0.687 ± 0.186***	0.278 ± 0.183 ns	0.628	0.462	1	0.898	-0.7	0.687*	0.278 ns
Urine osmolality	0.087 ± 0.241 ns	0.636 ± 0.228 **	0.513	0.223	1	0.814	-0.69	0.086 ns	0.636**
Urine:Plasma ratio	0.091 ± 0.252 ns	0.558 ± 0.227 *	0.456	0.105	1	0.769	-0.67	0.091 ns	0.558*
TEWL	-1.0 ± 0.162***	0.141 ± 0.151 ns	0.579	0.378	1	0.871	-0.70	-1.0***	0.141 ns

CHAPTER 3:

Genetic accommodation of ancestral plasticity aided the colonization of tidal marshes in Savannah Sparrows (*Passerculus sandwichensis*).

Phred M. Benham, Zachary A. Cheviron

Division of Biological Sciences, University of Montana, 32 Campus Dr. HS104, Missoula, MT 59812

ABSTRACT: A central question in evolutionary biology is how do individuals within a population produce phenotypes approaching or matching the adaptive peak in a novel environment and evade extinction? Although ancestrally plastic responses have long been invoked as a potentially important mechanism for adapting to new environments, whether plasticity plays a positive, negative, or no role in adaptation remains a heavily debated question. We assessed support for a series of predictions consistent with the hypothesis that genetic accommodation of ancestral plasticity facilitated colonization of new environments, including: (1) the ancestral population will exhibit acclimation responses in the adaptive direction; (2) there will be evidence for evolutionary divergence in reaction norms in the derived population; and (3) selection has canalized acclimation responses resulting in reduced variance around environmentally induced phenotypic means. We evaluated each of these predictions across an integrated suite of behavioral and physiological traits that contribute to osmoregulatory performance in tidal marsh environments. We found support for all three predictions in some traits (e.g. plasma volume, drinking responses), some traits provided mixed support (e.g. medulla volume), and in other traits plasticity played no apparent role in divergence between environments (e.g. maximal urine concentration). Variable responses across these different

physiological and behavioral traits that contribute to osmoregulatory performance suggest different evolutionary mechanisms can shape divergence in different components within the same integrated system. To understand how organisms colonize and adapt to different environments thus requires consideration of multiple potential mechanisms operating across hierarchically integrated phenotypes that relate to organismal performance.

KEYWORDS: Genetic accommodation, osmoregulation, *Passerculus,* plasticity, tidal marshes.

INTRODUCTION:

Colonization of novel environments that impose severe selective pressures is often thought to be constrained by physiological limitations (e.g. Wiens & Graham 2005; Wiens 2011; Louthan et al. 2015; Srinivasan et al. 2018). Yet organisms have routinely overcome these limitations to establish populations in novel environments, and this process of colonization has important consequences for phenotypic evolution (Endler 1980; Colosimo et al. 2005; Langerhans 2018) and lineage diversification (Pigot et al. 2010; Kozak & Wiens 2010). Thus, a central question in evolutionary biology is how do individuals within a population produce phenotypes approaching or matching the adaptive peak in the novel environment and evade extinction (Mayr 1947; Gomulkiewicz & Holt 1995; Price et al. 2003; Orr & Unckless 2008; Badyaev 2009)? Selection on standing genotypic variation and/or *de novo* mutations is one possibility allowing populations to escape extinction (Gomulkiewicz & Holt 1995; Barrett & Schluter 2008; Orr & Unckless 2008). A second possibility is the production of phenotypes from plastic responses to the novel environmental stimuli (Ghalambor et al. 2007; Lande 2009; Badyaev 2009). It is likely that both processes contribute to adaptation to different environments either over time or in different traits underlying increased functional performance in the novel environment (Storz et al. 2010; Cheviron et al. 2013; Dalziel et al. 2015; Laporte et al. 2016).

However, despite the long-recognized potential of plastic responses to assist with colonization and adaptation to novel environments (Baldwin 1896; Agrawal et al. 2001; Price et al. 2003; West-Eberhard 2005; Wund 2012; Levis & Pfennig 2016), the frequency and context in which adaptive plastic responses contribute to the successful colonization of new environments remains poorly understood.

A range of plastic responses to novel environmental stimuli are possible, and a strong body of theory provides explicit predictions for how different plastic responses may influence adaptation to novel environments (Price et al. 2003; Pigliucci et al. 2006; Ghalambor et al. 2007; Lande 2009; Fischer et al 2016). Theoretical studies typically focus on the evolution of reaction norms, which represent the range of phenotypes produced by an individual genotype in different environments. Selection can operate on inter-individual variation in either the slope (the level of plasticity) and/or elevation (the trait values) of these reaction norms to drive adaptation to novel environments (Via et al. 1995; Ghalambor et al. 2007; Aubin-Horth & Renn 2009). Initial population-level responses to novel environmental stimuli could range from maladaptive phenotypic responses (phenotypic change away from the local adaptive peak) to the production of phenotypes that place the individuals at or near local adaptive optima. In the former case selection should favor the attenuation of maladaptive plasticity (Grether 2005; Ghalambor et al. 2015; Fischer et al. 2016). In the latter case, reaction norm evolution will be unlikely and will only occur if the novel environment remains constant and (1) there is some associated cost with maintaining plasticity (DeWitt et al. 1998; Price et al. 2003; Murren et al. 2015) or (2) through degradation of the plastic response via relaxed selection and drift (Masel et al. 2007; Masel & Maughan 2007). Exposure to novel stimuli could also induce intermediate responses that are in an adaptive direction, but are associated with large levels of inter-individual variation in reaction

97

norms (Ghalambor et al. 2007). In this case, the most optimal variants will be favored by selection, which will reduce inter-individual variation of reaction norms yielding a population that consistently produces adaptive phenotypes in response to a given stimulus, a process known as genetic accommodation (Pigliucci & Murren 2003; West-Eberhard 2005; Suzuki & Nijhout 2006; Ghalambor et al. 2007; Scoville & Pfrender 2010). Selection on variable reaction norms could also lead to constitutive expression of an initially plastic phenotype. This process, referred to as genetic assimilation, is a specific case of genetic accommodation that may be favored in populations that are continuously exposed to the stimulus that initially induced variable plastic responses in the ancestral population (Waddington 1953; Lande 2009; Aubret & Shine 2009). The genetic accommodation of ancestral plasticity is thought to be one of primary ways in which plasticity can contribute to adaptation to new environments, yet few compelling empirical examples from natural systems exist.

Determining whether accommodation of ancestral plasticity contributed to adaptive divergence in a novel environment first requires comparative analysis of acclimation responses to similar environmental pressures in both ancestral and derived populations (e.g. Dalziel et al. 2015). Assuming that ancestral and derived populations can be successfully identified, a number of predictions must be tested to determine whether patterns of reaction norm divergence between ancestral and derived populations are consistent with a history of accommodation of ancestral plasticity. First, plastic responses in an ancestral population should be in the same direction, but not necessarily the same magnitude, as trait divergence in the derived population (Ghalambor et al. 2007; Levis & Pfennig 2016). Second, selection on plastic responses in the derived population will lead to evolution of the reaction norm to produce trait values with higher fitness in the new environment (Levis & Pfennig 2016). Similarly, selection operating on variable reaction norms

in the ancestral population will have reduced reaction norm variation in the derived population to more consistently produce adaptive phenotypes (Lande 2009; Shaw et al. 2014; Levis & Pfennig 2016). Although demographic effects (e.g. bottlenecks) could also explain reduced variance, this can be accounted for by comparing patterns of variance in reference traits that are not expected to be under divergent selection. Here, we compare plastic responses to salinity challenges in both ancestral and derived populations of tidal marsh Savannah Sparrows (*Passerculus sandwichensis*) to test whether selection on ancestral plasticity may have facilitated colonization of these extreme environments.

The Savannah Sparrow is one of the most widespread North American bird species with populations distributed across a range of open habitats, including several subspecies that occupy tidal marsh environments along the Pacific coast of California and northern Mexico (Wheelwright & Rising 2008). Daily inundations of seawater into tidal marshes impose severe osmoregulatory challenges for terrestrial vertebrates. To cope with these pressures, the few species that have successfully colonized salt marshes exhibit rapid divergence from interior relatives in behavioral, physiological, and morphological traits (Greenberg et al. 2006). Early experiments comparing salinity tolerance and drinking behavior in interior versus salt marsh Savannah Sparrows observed stark differences in response to drinking salt water between these populations. Interior birds were unable to maintain body weight and experienced substantial mortality (up to 60% of experimental individuals) when exposed to salinities of 0.3 M NaCl (roughly half-strength seawater), whereas tidal marsh subspecies were able to maintain normal body weight with no mortality when exposed to water exceeding the normal salinity of seawater (0.6 M NaCl; Cade & Bartholomew 1959; Poulson & Bartholomew 1962). Despite the severe consequences of consuming salt water on survival for freshwater-adapted populations of the

Savannah Sparrow, phylogeographic analyses indicate two independent colonizations of tidal

marshes by a freshwater-adapted ancestor (Chapter 1). The role plasticity played in the

successful colonization of tidal marshes in this species remains unknown. However, evolution of

increased salinity tolerance in tidal marshes is associated with an inherently flexible

osmoregulatory system that responds to environmental fluctuations in salinity or water

availability to maintain homeostasis of internal plasma osmolality. Consequently, this

physiological system is a prime candidate for testing the influence of accommodation in adaptive

divergence.

Within this system, increased plasma osmolality from salt ingestion causes shrinkage in

osmoreceptor cells in the brain that trigger both a thirst response (McKinley & Johnson 2004)

and release of the antidiuretic hormone, arginine vasotocin (AVT), which targets kidney

components (e.g. glomerular filtration rate and movement of aquaporins to cell wall) to increase

water retention (Stallone & Braun 1986; Goldstein 2006a). These two immediate responses serve

to increase free water and return plasma osmolality to normal levels (~300 mosm/kg). This also

causes volume increases of the extra-cellular fluid, which triggers increased Na^+ excretion

(Giebisch & Windhager 2012). This regulation of water retention and Na^+ excretion maintains

salt-water balance in the face of environmental inputs and is defined as an organism's

osmoregulatory capacity. Chronic salt exposure presents a severe osmoregulatory challenge, and

survival under increased salt loads would require concomitant increases in osmoregulatory

capacity (Skadhauge 1981; Braun 2015). An increase in osmoregulatory capacity can be

achieved by morphological change of several key renal components. These include increases in

total kidney size, increases in the number of nephrons, and/or elongation of the loop of Henle,

which would also require coordinated changes in the amount of medullary tissue to build a

steeper osmotic gradient. These morphological modifications would increase the ability to retain water, increase salt secretion to maintain homeostatic plasma osmolality, and ultimately blunt the thirst response. Indeed, differences in salinity tolerance and drinking rate are linked to an increased ability to concentrate salts in the urine of tidal marsh sparrows (Poulson & Bartholomew 1962; Goldstein et al. 1990; Chapter 2), which are in turn associated with a variety of renal modifications in salt marsh populations [e.g. larger kidney mass; increased medulla size, and number of medullary cones in the kidneys of tidal marsh birds (Johnson & Mugaas 1970; Johnson & Ohmart 1973; Chapter 2)]. Flexibility in some of these renal traits (e.g. medullary tissue, kidney size, urine concentration) has been documented in freshwater-adapted bird species in response to osmoregulatory stress (Goldstein & Ellis 1991; Goldstein 1995; Sabat et al. 2004; Peña-Villalobos et al. 2013) and high-protein diets (Goldstein et al. 2001). This suggests that ancestral plasticity in at least some traits associated with osmoregulatory capacity may have played an important role in facilitating colonization of tidal marshes, yet this remains to be tested.

To test whether ancestral phenotypic plasticity in traits contributing to osmoregulatory capacity may have contributed to tidal marsh adaptation, we performed replicate acclimation experiments to salinity in both a freshwater-adapted and tidal marsh population of the Savannah Sparrow. In both acclimation experiments we assayed acclimation responses in drinking behavior, renal traits, and urine excretion capability to test the following predictions: **(1)** the freshwater-adapted population exhibits acclimation responses in the adaptive direction (i.e. toward trait values that would increase osmoregulatory capacity); **(2)** evolutionary divergence in reaction norms of the derived tidal marsh population has occurred; and **(3)** selection has canalized acclimation responses to salinity resulting in reduced variance around phenotypic

means induced by salinity exposure. Evaluating each of these predictions across a suite of physiological and behavioral traits will contribute a nuanced perspective on how selection may have targeted different elements within an ancestrally flexible osmoregulatory system to facilitate colonization of an extreme environment.

METHODS:

Sampling and experimental design: In June 2016, we captured 43 male Savannah Sparrows from western Wyoming, a population resembling the ancestral, freshwater-adapted condition (Chapter 1). All birds were brought into captivity at the University of Montana and maintained under constant conditions (mean temp- 21.8ºC; mean humidity- 43.5%; light:dark cycle- 12:12hrs) with food and fresh drinking water provided *ad libitum* for 36 days. Following this preliminary acclimation to captivity, we randomly assigned birds to two groups: a control group maintained on fresh drinking water (n=19), and a treatment group (n=25) given salt drinking water (0.2 M concentration- less than half strength seawater). Although the salinity given to the birds was less than experienced by individuals that inhabit salt marshes (see Chapter 2), molarities greater than 0.3 M NaCl may result in death of interior birds (Cade & Bartholomew 1959). No birds died in response to the 0.2 M NaCl solution provided, and 0.2 M was previously found to induce plastic responses in other sparrow species (Peña-Villalobos et al. 2013).

Following the start of salinity treatment, we serially sampled birds at 24 hrs, 7 days (salt-treatment only), 15 days, and 30 days (Fig. 1). During the entire acclimation experiment, we monitored daily water consumption (to the nearest 0.5 mL) by training birds to drink from graduated drinking tubes. Two control tubes were placed in the room to account for evaporation and the daily amount of water that was lost from these tubes was subtracted from measures of

daily drinking rate for each bird (Bartholomew & Dawson 1954). At each sampling point, we took a blood sample from the brachial vein, centrifuged the sample, and measured percent hematocrit and plasma using calipers. The blood sample was then flash frozen. Increased water retention increases extra-cellular fluid volume (ECFV), which decreases the percent hematocrit (hct) in a centrifuged blood sample (Stallone & Braun 1986). Thus, we use percent plasma (i.e., 1- %hct), hereafter referred to as plasma volume, as a proxy for increased ECFV and water retention. To get a comparable measure of urine concentrating ability between control and salt exposed birds we performed a standard salinity challenge (Sabat et al. 2004). This challenge involved a salt loading trial where birds were force fed 0.02 ml/g of bird of a 0.6 M NaCl solution. Following ingestion of this solution urine samples were collected every 20 min. for 2 hrs. We then euthanized birds to extract whole kidneys, saving the left kidney for histological analyses (e.g. medulla and cortex size).

This experiment was replicated with 14 individuals from a derived tidal marsh population captured from the San Francisco Bay area. These birds were also transported to the University of Montana and kept under identical conditions (mean temp- 23.3ºC; mean humidity- 41.8%; light:dark cycle- 12:12hrs) with fresh water and food provided *ad libitum* for 36 days. Birds were evenly divided between fresh and salt drinking water (0.2 M NaCl solution). Instead of serial sampling of birds, all were sampled after 15 days (Fig. 1). Preliminary analyses of the experiment performed on Wyoming birds indicated that all significant changes occurred by the 15-day sampling point. We performed identical procedures and collected the same data from these tidal marsh birds.

Physiological data collection: Plasma osmolality was measured using freezing point depression methods. For plasma samples ≥50 µl osmolality was measured using the µOsmette 5004 (Precision Systems, Inc; Natick, MA). For smaller volume samples an Otago nanolitre osmometer (Otago Osmometers; Dunedin, NZ) was used to measure plasma osmolality. We measured osmolality for all urine samples using the Otago nanolitre osmometer. For each individual the peak urine osmolality produced during the two hour procedure was noted (Umax). We also noted the time point at which each individual reached Umax (time to Umax) as a measurement of the rate at which salts were excreted following salt loading. Measurements of kidney length and width were taken before and after embedding tissue in paraffin to account for shrinkage. All kidneys were embedded in paraffin wax using routine procedures (e.g. Casotti & Braun 2000). Using a microtome, 6-10 transverse sections, 5 µm thick and ~1 mm apart, were taken from each kidney sample. Kidney sections were stained with haemotoxylin and eosin. Images of the sections were digitized and volume estimates of the medulla and cortex were made using the Cavalieri point-counting method (Gundersen et al. 1988) in imageJ (Schneider et al. 2012).

Data analysis: To determine whether birds from the ancestral Wyoming population exhibit plastic responses in the expected direction and the time course over which these responses occurred we tested for effects of sampling time, treatment (salt vs. freshwater), and their interaction on variation in each of the physiological traits measured over the course of the Wyoming experiment using two-way ANOVAs. Given that we only analyzed data from individuals sampled at 15 days for Umax and time to Umax, we instead performed two sample t-tests to test for differences between treatments. Secondly, we compared acclimation responses in

each of the physiological traits between Wyoming freshwater and California tidal marsh birds sampled after 15 days of salt exposure. We also tested for an effect of treatment, population, and their interaction within a two-way ANOVA framework. We used an ANCOVA approach to analyze drinking rate data in each population with treatment as a factor and day as covariate. Finally, we tested whether the derived tidal marsh population exhibited reduced phenotypic variance as measured by the coefficient of variation (COV) in response to salinity exposure relative to the interior population. Likewise, we compared COV between each population exposed to freshwater. Evidence for reduced phenotypic variance under salt exposure in the derived tidal marsh population is consistent with the prediction that selection has operated on ancestrally variable reaction norms to canalize acclimation responses and consistently produce adaptive phenotypes in response to the environmental stimulus. To control for a potential influence of demographic history on patterns of variance we also compared COV between the two populations in a putatively neutral trait, tarsus length. If selection and not demographic history has operated on osmoregulatory traits to reduce phenotypic variance then we expect a greater reduction in COV in traits associated with osmoregulation than in tarsus length. All statistical analyses were performed in the open source program R (https://www.r-project.org/).

RESULTS:

Physiological responses to salinity in a freshwater-adapted population:

Within the ancestral, freshwater-adapted population, birds exhibited no significant changes in plasma osmolality in response to salinity over the course of the experiment (Table 1). This suggests that salt-exposed, interior birds could maintain a constant plasma osmolality in the face of a salinity challenge. Maintenance of salt-water balance within freshwater-adapted

sparrows was associated with significant increases in plasma volume, medulla volume, and kidney mass (Table 1; Fig. 2). The maximum urine osmolality (Umax) was not significantly different between treatments at 15 days (t=-0.276; p=0.792); however, the amount of time required to reach Umax following salt loading was significantly reduced in salt exposed birds (t=2.52; p=0.046; Table 1). Although we found no significant effect of sampling time or the interaction between treatment and sampling time on acclimation response (Table 1), for medulla volume and kidney mass there was little apparent difference between treatments following 24-hrs of salt exposure and divergence in these traits appears to have largely occurred within the first seven days of salt exposure (Fig. 2).

Patterns of divergence in acclimation responses within the derived tidal marsh population:

After 15 days of salt exposure, freshwater and saltwater exposed birds from tidal marshes exhibited no difference in plasma osmolality (Table 2; Fig. 3). However, we found that tidal marsh birds constitutively maintain plasma osmolality at a significantly higher level than birds from Wyoming (Table 2; Fig. 3). Similar to the ancestral population, derived tidal marsh birds exhibit significant increases in plasma volume, medulla volume, and the amount of time required to reach Umax following salt loading (Table 2; Fig. 4). In addition to a significant influence of treatment, we also found a significant effect of population on medulla volume (Table 2; Fig. 4b), which is likely due to an increase in the elevation of the entire reaction norm within the derived tidal marsh population. We also found a significant population (but no treatment) effect on Umax, indicating that an increased capacity to excrete salts in the urine has evolved in the derived tidal marsh population despite lack of plasticity in the ancestral population (Table 2; Fig. 4c).

Behavioral responses:

Alteration of drinking rate is another mechanism by which animals can regulate salt ingestion and maintain plasma osmolality at constant levels. Birds from Wyoming exhibited a significant reduction in daily water consumption over the course of the 30-day acclimation period while control birds exhibited no significant decrease in water consumption (Fig. 5). We also detected a significant effect of treatment in the tidal marsh population with salt-exposed birds drinking less (Fig. 5). However, we also found a parallel decrease in drinking rate over the course of the experiment in the freshwater control group (Fig. 5). Freshwater exposed tidal marsh birds also exhibited gradual declines in body mass over the course of the experiment, but results were identical when analyzing patterns of drinking rate without accounting for body mass (day- $F = 19.78$, $p<<0.0001$; treatment- $F = 8.81$, $p=0.003$; day*treatment- $F = 0.165$, $p=0.68$) and when drinking rate was analyzed as a percent of body mass (day- $F = 19.34$, $p<<0.0001$; treatment- $F = 8.78$, $p=0.003$; day*treatment- $F = 0.337$, $p=0.56$). Despite similar trends toward decreasing drinking rate in salt-exposed birds from both populations, visualizing individual reaction norms of drinking rate across time revealed dramatically different initial responses to switching from fresh to salt drinking water between populations. The freshwater-adapted population exhibited a large amount of reaction norm variation within the first 24-hrs with individuals increasing, decreasing, or not changing drinking rate in response to salt; whereas, individuals from the tidal marsh population tended to more consistently decrease drinking rate in response to salt (Fig. 6).

Patterns of variance between populations:

107

If selection has operated on ancestral plasticity to canalize responses in a derived population then we expect to see reduced variance in the plastic responses in a derived population when exposed to the same environmental stimulus. Comparing acclimation responses in salt-exposed birds from Wyoming and California we found the most significant reduction in COV to be in initial responses to drinking rate suggesting selection has operated to canalize drinking responses to different salinities in tidal marsh birds (Fig. 7a). We also found reduced variance in plasma osmolality, plasma volume, and time to Umax, but increased variance in kidney size (mass corrected), medulla volume (mass corrected), and Umax (Fig. 7a). In response to freshwater we found an opposite pattern for many traits with the derived California population actually exhibiting increased variance for all measured traits except plasma volume (Fig. 7b). We found no difference in COV between populations in the neutrally evolving trait, tarsus length, indicating that demographic history likely did not influence patterns of COV between populations (Fig. 7).

DISCUSSION:

The precise role that phenotypic plasticity plays in adaptation to new environments remains a contentious question in evolutionary biology. To gain insight into this question, we compared acclimation responses to fresh and salt-drinking water in individuals sampled from both an ancestral, fresh-water adapted and a derived, tidal marsh population of the Savannah Sparrow. Based on these experiments, we found evidence for ancestral plasticity in the direction of tidal marsh divergence for some traits (e.g. plasma volume, medulla volume), but other traits, such as Umax, exhibited no acclimation response (Table 1). Secondly, we found that derived tidal marsh populations exhibited plastic responses that were similar to the ancestral response for

108

many renal traits. However, salt marsh birds exhibited greater medullary volume in both treatments, suggesting that selection may have operated to increase the elevation of the ancestral reaction norm (Fig. 3; Table 2). Finally, in response to salt exposure tidal marsh birds exhibited clear reductions in variance for changes in drinking rate, and modest reductions in COV for plasma osmolality, plasma volume, and time to Umax (Fig. 7). Based on these results, evidence for accommodation of ancestral plasticity in adaptation to tidal marshes appears to be trait specific. Some traits provided support for all three predictions (e.g. plasma volume, drinking responses), others provided mixed support (e.g. medulla volume), and in other traits evolutionary divergence appears to have proceeded entirely via selection on genotypic variation in the derived environment (e.g. Umax). Idiosyncratic evolutionary responses across these different physiological and behavioral traits that contribute to osmoregulatory performance suggest different evolutionary mechanisms can shape divergence in different components of the same integrated system. To understand how organisms colonize and adapt to different environments thus requires consideration of multiple potential mechanisms operating across hierarchically integrated phenotypes that relate to organismal performance and fitness.

Osmoregulatory flexibility in a fresh-water adapted population:

Maintaining homeostasis in plasma osmolality is critical for survival in most vertebrates (Hill et al 2012). We found that in the face of chronic exposure to saline drinking water, a freshwater-adapted population of the Savannah Sparrow maintained blood plasma osmolality at comparable levels to birds provided fresh drinking water (Table 1; Fig. 3). Maintenance of a constant blood osmolality was consistent with other experiments investigating acclimation responses to salinity in passerine birds (Sabat et al. 2004; Peña-Villalobos et al. 2013), but differs

from mallards, which were previously found to exhibit flexibility in plasma osmolality (Holmes et al. 1968). The ability to maintain a constant osmolality in the face of increased salt loads was associated with a suite of physiological responses. First, we found increases in overall kidney size as well as the renal medulla following salt exposure (Table1; Fig. 2). Hypertrophy of medullary tissue in birds is a commonly observed acclimation response to salinity (e.g. Sabat et al. 2004; Peña-Villalobos et al. 2013), dehydration (Goldstein & Ellis 1991), and high-protein diets (Goldstein et al. 2001). Increases in medullary tissue could either result from greater numbers of medullary cones or the overall size of each individual cone. Although we did not collect data on the number of individual medullary cones, previous work reported no differences in the number of medullary cones in response to salinity, but cone size and length did change (Goldstein et al. 2001; Sabat et al. 2004; Peña-Villalobos et al. 2013). Previous studies measured birds after an acclimation period of two (Sabat et al. 2004) to three weeks (Peña-Villalobos et al. 2013). Here, we show that all increases in medullary tissue occur within the first seven days and increases in kidney mass peaks after 15 days of chronic salt exposure (Fig. 2).

Changes in kidney morphology should be associated with increased ability to retain water and excrete salts from the urine and thus maintain salt-water balance. Indeed, we did find evidence of increased plasma volume, which may indicate increased water retention, following salt exposure (Table1; Fig. 2). This response appears to occur within the first 24-hrs following exposure to salt and remains elevated throughout the time course of the experiment (Fig. 2). This result contrasts with other studies, which do not detect differences in plasma volume in response to chronic salt exposure (mallards- Holmes 1968; Cinclodes- Sabat et al. 2004); however, in response to acute salt loading, increases in plasma volume have been documented in chickens (Stallone & Braun 1986). We did not find differences in the maximal urine concentrating ability

110

between treatments at 15 days (Table 1-2), but the time to maximal urine concentration did decrease after salt exposure (Fig. 4d; Table 2). This result also differs from previous studies. Sabat et al. (2004) used a similar approach to measure Umax and found differences in urine concentrating ability among *Cincolodes* species, but in only one species was there an increased ability to concentrate salts in the urine in response to salt exposure. Although the maximal urine osmolality did not differ between treatments the rate at which Umax was reached post-salt loading did differ. This suggests that while overall abilities to concentrate salts in the urine does not change, chronically salt-exposed birds may likely be primed to excrete salts and can more efficiently process heavy salt loads.

Patterns of divergence in osmoregulatory physiology:

Birds from the California tidal marsh population also maintained a constant osmolality in the face of chronic salt exposure; however, tidal marsh birds maintained a plasma osmolality approximately 20 mOsmol/kg greater than the freshwater-adapted Wyoming population (Table 2; Fig. 3). Tidal marsh Savannah Sparrows were previously found to exhibit greater plasma osmolality relative to interior birds (Goldstein et al. 1990) with plasma osmolality increasing from north to south along the Pacific coast in tidal marsh Savannah Sparrows (Chapter 2). Relatively high plasma osmolality has been reported for the Chilean Seaside Cinclodes (*Cinclodes nigrofumosus*) relative to freshwater-adapted congeners (Sabat et al. 2006), and this elevated plasma osmolality was maintained when *C. nigrofumosus* was exposed to both fresh and salt drinking water (Sabat et al. 2004). These results suggest that an ability to tolerate greater internal osmolality is an important adaptation to high saline environments in birds. Most vertebrates tightly regulate internal osmolality at ~300 mOsmol/kg with deviations leading to

fluctuations in cell volume and reduced protein functioning, which can ultimately lead to death (Hochachka & Somero 2002; Giebisch & Windhager 2012). While it is likely that elevated plasma osmolality is related to an increased tolerance of high saline diets, the mechanisms enabling tidal marsh songbirds to cope with high internal osmolality remains an open question.

Similar to ancestral populations, the derived tidal marsh birds exhibit flexible responses in medulla volume, plasma volume, and time to Umax (Table 2; Fig. 4). However, across treatments tidal marsh birds exhibited elevated medulla volume relative to the freshwater population. The kidneys of tidal marsh Savannah Sparrows from California and Mexico both contain larger amounts of medullary tissue than freshwater-adapted relatives (Chapter 2). While there was no evidence for a plastic response in maximum urine osmolality for either population over the course of the experiment, birds from California exhibited a significantly greater capacity to excrete salts in the urine than Wyoming birds (Table 2; Fig. 4c). Seaside Cinclodes (*Cinclodes nigrofumosus*) have also diverged from freshwater-adapted congeners in percent medulla tissue, number of medullary cones, hematocrit, and maximum urine capacity and did not exhibit plastic responses in any of these traits after 15 days of exposure to fresh or salt drinking water (Sabat et al. 2004). However, closely related species of *Cinclodes* that migrate between freshwater and coastal habitats do exhibit plastic responses. This includes *C. patagonicus,* the sister species to both *C. nigrofumosus* and *C. taczanowskii*, an allospecies from coastal Peru (Sanín et al. 2009; Derryberry et al. 2011). It is probable that the ancestor to *C. nigrofumosus/taczanowskii* exhibited some degree of plasticity in traits that are now canalized. Tidal marsh Savannah Sparrows from California and interior birds exhibit little to no population genetic structure (Chapter 1). Thus, it is possible that recent divergence explains the retained ability of California Savannah Sparrows to exhibit plastic responses in the measured traits. Velotta et al. (2015; 2017)

showed that across populations of landlocked Alewife, older populations exhibited reduced plasticity and tolerance of seawater. Indicating that time since divergence from an anadromous (and plastic) ancestor predicts the degree of trait canalization. Whether a similar trend exists in birds colonizing high salinity environments remains to be seen; however, within sparrows there have been multiple colonizations of tidal marsh environments with different tidal marsh taxa exhibiting extensive variation in divergence time from interior relatives (Greenberg et al. 1999; Chan & Arcese 2002; Klicka et al. 2014; Chapter 1). Comparative acclimation experiments across these different taxa would provide opportunities to understand patterns of evolutionary divergence in ancestrally plastic phenotypes.

Drinking behavior:

Increases in plasma osmolality causes cell shrinkage within brain osmoreceptors, this triggers a thirst response, which will bring more water into the body and return plasma osmolality to normal (McKinley & Johnson 2004). Due to this behavioral regulation of plasma osmolality, birds will commonly increase drinking rates in response to being provided water of increasing salinity (Bartholomew & Cade 1963; Poulson 1969; Basham & Mewaldt 1987). This response is thought to be maladaptive as increased drinking of salt water would exacerbate osmoregulatory stress and has been associated with decreased body mass and increased mortality (Cade & Bartholomew 1959; Poulson & Bartholomew 1962). However, several tidal marsh sparrow taxa exhibit the opposite reaction and reduce drinking rate when exposed to higher salinities, which is thought to be a key adaptation to high salinity environments (Cade & Bartholomew 1959; Poulson & Bartholomew 1962; Johnson & Mugaas1973; Basham & Mewaldt 1987; Goldstein 2006b). We monitored drinking rate over the course of 30 days in the

freshwater-adapted Wyoming population. Although we found high levels of variation in the initial drinking rate response following the switch to salt drinking water (Fig. 6-7), over time salt-exposed birds exhibited significant declines in drinking rate (Fig. 5). This suggests that given longer-term exposure, freshwater-adapted birds do exhibit flexible thirst responses, in contrast to the immediate reactions tested in previous experimental work in Savannah Sparrows (Cade & Bartholomew 1959; Poulson & Bartholomew 1962). Although reductions in water consumption would be an adaptive response, the ability to cope with less water likely depends in part on the plastic responses seen in other traits involved with osmoregulation (i.e. medulla volume, plasma volume).

Tidal marsh birds in California also exhibited significant reductions in drinking rate when provided salt drinking water (Fig. 5) and within the first 24-hrs after switching to salt water exhibited more consistent responses to the changes in salinity (Fig. 6-7). Interestingly, California birds given freshwater throughout the course of the experiment also show significant decreases in drinking rate over the course of the experiment. The reasons for this trend were not entirely clear. One potential explanation is that tidal marsh birds were acclimating to freshwater exposure over the course of the experiment. Past studies monitoring drinking rate in tidal marsh sparrows report exceptionally high rates of distilled water consumption relative to birds of comparable body mass (Cade & Bartholomew 1959; Poulson & Bartholomew 1962; Bartholomew 1963; Poulson 1969). While none of these studies reported decreases in drinking rate through time in tidal marsh birds drinking freshwater, it is unclear whether drinking rates were monitored long enough to detect this trend in previous work.

Patterns of Variance:

114

Although initial exposure to a novel environmental stimulus is predicted to be associated with highly variable reaction norms among individuals, long term exposure to the same stimulus should lead to a reduction of inter-individual reaction norm variance, resulting in more consistent production of adaptive phenotypes among individuals within a derived population (Waddington 1953; Lande 2009; Shaw et al. 2014; Levis & Pfennig 2016). We found evidence for reduced variance in plasma osmolality, plasma volume, time to Umax, and drinking rate responses to salt exposure in tidal marsh sparrows (Fig. 7a). However, tidal marsh sparrows exhibited greater COV in responses for medulla volume, kidney size, and Umax. When exposed to fresh water, the freshwater population exhibited reduced variance in most traits relative to tidal marsh populations (Fig. 7b). While seasonal fluctuations in salinity occur in tidal marshes of the San Francisco Bay area (Peterson et al. 1995), sparrows from that region are likely naïve to freshwater conditions. Thus, it is possible that due to lack of exposure to freshwater, genetic variation associated with responses to freshwater is shielded from selection and has increased in the tidal marsh population relative to the freshwater population.

Patterns of trait variance can also be influenced by the demographic history. For instance, population bottlenecks associated with a small founding population could lead to a general reduction in trait variance. We do not think that similar demographic processes explain the observed patterns of reduced COV of osmoregulatory traits in salt-exposed, tidal marsh birds for several reasons. First, population genomic comparisons between interior and tidal marsh populations from the San Francisco bay area exhibit similar levels of nucleotide diversity (Chapter 2), suggesting that they have not experienced significant, recent population bottlenecks. Second, we did not find a consistent reduction of COV in the measured osmoregulatory traits; some osmoregulatory traits exhibited greater variance upon salt exposure in the tidal marsh birds.

Finally, we observed no difference in COV between populations in a reference trait, tarsus length (Fig. 7). If genetic variation was eroded in association with tidal marsh colonization, then we would expect a general trend of reduced variation in both the osmoregulatory and reference traits. Together, these results suggest that reduced COV in plasma osmolality, plasma volume, time to Umax, and drinking rate within the derived population is due to selection operating to canalize reaction norm variation among individuals rather than an influence of demographic history.

Limitations of experimental design:

Developmental environment and maternal effects can have profound impacts on phenotypic variation in adult organisms (e.g. Dufty et al. 2002; West-Eberhard 2005; Räsänen & Kruuk 2007). In our experiment, we brought adult birds that had developed in different environments into a common garden environment for 36 days before exposing them to different salinities. Whether this common garden period was sufficient to reverse developmental effects is not known, and it is thus not possible to exclude the possibility that (1) traits such as plasma osmolality and/or Umax could exhibit plastic responses to different salinities during development that are not reversible in adults. (2) Differences in drinking rate responses could reflect learned experiences with salt rather than evolutionary divergence. (3) Reduced variance in response to salt exposure in some of the osmoregulatory traits measured could reflect previous exposure to salinity during development in tidal marsh birds. Although these represent potential alternative interpretations, there is little known about how differences in developmental environment influence osmoregulatory physiology and drinking behavior in birds. Studies in bobwhite quail found that dehydration during development led to increased medullary tissue and

renal tubule size (Golstein & Ellis 1991), which corresponded to increased tubule reabsorption (Goldstein 1995). Differences in kidney morphology induced by developmental environment were not found to be reversible (except for surface area in the thick ascending limb of the loop of Henle) when adult quail that developed under dehydration or rehydration regimes were exposed to the opposite treatment. However, experiments on adult birds lasted only 5 days and it is unclear whether more chronic exposure may reverse developmentally induced phenotypes (Goldstein & Ellis 1991). In mammals, salt intake by mothers can influence aspects of kidney development, such as the number of nephrons (Koleganova et al. 2011), a trait known to be irreversible in adult mammals (Little & McMahon 2012). Developmental environment also influenced amount of medullary tissue and urine concentrating ability in leaf-eared mice (*Phyllotis darwini*) with mice reared in warmer, water-restricted environments exhibiting larger medullas and urine concentrating ability than mice raised in cold unrestricted-water environments (Cavieres et al. 2017). These effects were found to be reversible when mice raised in warm environments were transferred to cold treatments as adults, but not vice versa. Considerable research remains to be done to determine whether similar developmental responses influence osmoregulatory physiology in birds, necessitating cautious interpretation of our results.

Despite these caveats, assessing patterns of phenotypic flexibility in adults of relatively long-lived organisms can provide valuable insights into whether accommodation of ancestral plasticity contributed to divergence between different environments. Importantly, we did find evidence for the first prediction that ancestral responses to salinity are in the adaptive direction for a number of osmoregulatory traits. Developmental environment should not muddy interpretation of this result. Additional evidence consistent with our second and third predictions exist for some traits and at least suggests that genetic accommodation of ancestral plasticity may

have contributed to tidal marsh adaptation. However, we do acknowledge that experiments designed to eliminate potential developmental effects will be necessary to generate further support for the hypothesis that genetic accommodation contributed to tidal marsh adaptation. Considering the effects of developmental environment is a considerable hurdle for extending experimental evidence for genetic accommodation from organisms conducive to lab experiments (e.g. Suzuki & Nijhout 2006) to long-lived organisms that are difficult to breed in the lab. Nevertheless, rigorously testing predictions consistent with a history of genetic accommodation will be an essential first step in evaluating the relevance of this process in natural populations. Our work highlights a potential study system that may justify the development of more challenging and time-consuming common garden experiments in which the genetic accommodation hypothesis can be more thoroughly tested.

Conclusions:

　　Whether ancestrally plastic responses play a positive, negative, or no role in adaptation to new environments remains a heavily debated question in evolutionary biology (Wund 2012; Schlichting & Wund 2013; Fischer et al. 2016; Levis & Pfennig 2016; Ho & Zhang 2018). Mixed empirical results suggest that the precise role that plasticity plays in the colonization of new environments depends on population history, the traits under study, and the specific ecological pressures. We assessed support for a series of predictions consistent with the hypothesis that accommodation of ancestral plasticity can facilitate colonization of a new environment across an integrated suite of behavioral and physiological traits that contribute to osmoregulatory performance in tidal marsh environments. Although we did find support for all three predictions in some traits, we found mixed or no support for the three predictions in other

traits. These results support the hypothesis that ancestral plasticity in some traits facilitated

adaptation to tidal marsh environments, but this was not universal across all traits assayed.

Previous work comparing the role of plasticity versus genotypic selection across different traits

within complex physiological systems also found the role of these different mechanisms to be

trait dependent (Storz et al. 2010; Cheviron et al. 2013; Dalziel et al. 2015). Adaptation to new

environments reflects selection targeting multiple traits within complex, integrated systems

underlying performance and fitness differences (Dalziel et al. 2009; Storz & Wheat 2010).

Analyzing acclimation responses within this framework will improve our contextual

understanding of how plasticity facilitates adaptation to new environments.

REFERENCES:

Agrawal, A.A. 2001. Phenotypic plasticity in the interactions and evolution of species. *Science* 294: 321-326.

Aubin-Horth, N., and S.C.P. Renn, 2009. Genomic reaction norms: using integrative biology to understand molecular mechanisms of phenotypic plasticity. *Molecular Ecology* 18: 3763-3780.

Aubret, F., and R. Shine. 2009. Genetic assimilation and the postcolonization erosion of phenotypic plasticity in island tiger snakes. *Current Biology* 19: 1932-1936.

Badyaev, A. V. 2009. Evolutionary significance of phenotypic accommodation in novel environments: an empirical test of the Baldwin effect. *Philosophical Transactions of the Royal Society B: Biological Sciences*, 364: 1125-1141.

Baldwin, J. M. 1896 A new factor in evolution. *American Naturalist,* 30: 441-451.

Barrett, R. D. H., & Schluter, D. 2008. Adaptation from standing genetic variation. *Trends in Ecology and Evolution*, 23: 38-44.

Bartholomew, G. A., & Dawson, W. R. 1954. Body temperature and water requirements in the Mourning Dove, *Zenaida macroura marginella*. *Ecology*, 35: 181-187.

Bartholomew, G. a, & Cade, T. J. 1963. The water economy of land birds. *The Auk*, 80: 504-539.

Basham, M. P., Mewaldt, L. R., & Marin, B. T. 1987. Salt water tolerance and the distribution of South San Francisco Bay song sparrows. *The Condor*, 89: 697-709.

Braun, E.J. 2015. Osmoregulatory systems of birds. *In*: Sturkie's Avian Physiology, 6th edition (C.G. Scanes, ed.). Elsevier, New York, NY.

Cade, T., & Bartholomew, G. A. 1959. Sea-water and salt utilization by Savannah sparrows. *Physiological Zoology*, 32: 230-238.

Casotti, G., & Braun, E. J. 2000. Renal anatomy in sparrows from different environments. *Journal of Morphology*, 243: 283-291.

Chan, Y., & Arcese, P. 2002. Subspecific Differentiation and Conservation of Song Sparrows (*Melospiza melodia*) in the San Francisco Bay Region Inferred by Microsatellite Loci Analysis. *The Auk*, 119: 641-657.

Cheviron, Z. A., Bachman, G. C., & Storz, J. F. 2013. Contributions of phenotypic plasticity to differences in thermogenic performance between highland and lowland deer mice. *Journal of Experimental Biology*, 216: 1160-1166.

Colosimo, P. F. 2005. Widespread Parallel Evolution in Sticklebacks by Repeated Fixation of Ectodysplasin Alleles. *Science*, 307: 1928-1933.

Dalziel, A. C., Rogers, S. M., & Schulte, P. M. (2009). Linking genotypes to phenotypes and fitness: How mechanistic biology can inform molecular ecology. *Molecular Ecology*, 18: 4997-5017.

Dalziel, A. C., Martin, N., Laporte, M., Guderley, H., & Bernatchez, L. 2015. Adaptation and acclimation of aerobic exercise physiology in Lake Whitefish ecotypes (Coregonus clupeaformis). *Evolution*, 69: 2167-2186.

Derryberry, E. P., Claramunt, S., Derryberry, G., Chesser, R. T., Cracraft, J., Aleixo, A., Pérez-Emán, J. Remsen, Jr., J.V., & Brumfield, R. T. 2011. Lineage diversification and morphological evolution in a large-scale continental radiation: The neotropical ovenbirds and woodcreepers (aves: furnariidae). *Evolution*, 65: 2973-2986.

Dewitt, T.J., A. Sih, and D.S. Wilson. 1998. Costs and limits of phenotypic plasticity. *Trends in Ecology & Evolution* 13: 77-81.

Dufty, A. M., Clobert, J., & Møller, A. P. 2002. Hormones, developmental plasticity and adaptation. *Trends in Ecology and Evolution*, *17*(4), 190-196.

Endler, J. A. 1980. Natural Selection on Color Patterns in *Poecilia reticulata*. *Evolution*, *34*: 76-91.

Fischer, E. K., Ghalambor, C. K., & Hoke, K. L. 2016. Can a network approach resolve how adaptive vs nonadaptive plasticity impacts evolutionary trajectories. *Integrative and Comparative Biology*, 1-12.

Ghalambor, C.K., J.K. McKay, S.P. Carroll, & D.N. Reznick. 2007. Adaptive versus non-adaptive phenotypic plasticity and the potential for contemporary adaptation in new environments. *Functional Ecology* 21: 394-407.

Ghalambor, C. K., Hoke, K. L., Ruell, E. W., Fischer, E. K., Reznick, D. N., & Hughes, K. A. 2015. Non-adaptive plasticity potentiates rapid adaptive evolution of gene expression in nature. *Nature*, *525*: 372-375.

Giebisch, G. & E. Windhager. 2012. Integration of salt and water balance. *In: Medical Physiology 2nd ed.* (eds. W.F. Boron & E. L. Boulpaep), pgs. 866-880, Saunders Elsevier, Philadelphia, PA.

Goldstein, D. L., & Ellis, C. C. 1991. Effect of water restriction during growth and adulthood on kidney morphology of bobwhite quail. *The American Journal of Physiology*, 261: R117-25.

Goldstein, D. L. 1995. Effects of Water Restriction During Growth and Adulthood on Renal Function of Bobwhite Quail, Colinus Virginianus. *Journal of Comparative Physiology - B, Biochemical, Systemic, & Environmental Physiology*, 164: 663-670.

Goldstein, D. L. 2006. Regulation of the avian kidney by arginine vasotocin. *General and Comparative Endocrinology*, 147: 78-84.

Goldstein, D.L. 2006b. Osmoregulatory biology of saltmarsh passerines. *Studies in Avian Biology,* 32: 110-118

Goldstein, D. L., Williams, J. B., & Braun, E. J. 1990. Osmoregulation in the field by salt-marsh savannah sparrows *Passerculus sandwichensis beldingi. Physiological Zoology*, 63: 669-682.

Goldstein, D. L. 2001. Renal Response to Dietary Protein in the House Sparrow *Passer domesticus*, 74: 461-467.

Gomulkiewicz, R., Holt, R. D., Gomulkiewicz1and, R., & Holt, R. D. 1995. When does evolution by natural selection prevent extinction? *Evolution*, 49: 201-207.

Greenberg, R., Cordero, P. J., Droege, S., & Fleischer, R. C. 1998. Morphological adaptation with no mitochondrial DNA differentiation in the coastal plain swamp sparrow. *The Auk*, 115: 706-712.

Greenberg, R., Maldonado, J. E., Droege, S., & McDonald, M. V. 2006. Tidal marshes: a global perspective on the evolution and conservation of their terrestrial vertebrates. *BioScience*, 56: 675-685.

Grether, G.F. 2005. Environmental change, phenotypic plasticity, and genetic compensation. *The American Naturalist,* 166: E115–E123.

Gundersen, H. J. G., Bendtsen, T. F., Korbo, L., Marcussen, N., Møller, A., Nielsen, K., … West, M. J. 1988. Some new, simple and efficient stereological methods and their use in pathological research and diagnosis. *Apmis*, *96*: 379-394.

Hill, R. W., Wyse, G. A. & M. Anderson. 2012. *Animal physiology, 3rd ed.* Sinauer Associates, Inc., Sunderland, MA.

Ho, W.-C., & Zhang, J. 2018. Evolutionary adaptations to new environments generally reverse plastic phenotypic changes. *Nature Communications*, 9: 350.

Hochachka, P.W. & G.N. Somero 2002. *Biochemical adaptation: mechanism and process in physiological evolution.* Oxford University Press, Oxford, UK.

Holmes, W. N., Fletcher, G. L., & Stewart, D. J. 1968. The patterns of renal electrolyte excretion in the duck (Anas platyrhynchos) maintained on freshwater and on hypertonic saline. *J Exp Biol*, 48: 487-508.

Johnson, O. W., & Mugaas, J. N. 1970. Quantitative and Organizational Features of the Avian Renal Medulla. *The Condor*, 72: 288-292.

Johnson, O. W., & Ohmart, R. D. 1973. Some Features of Water Economy and Kidney Microstructure in the Large-Billed Savannah Sparrow (*Passerculus sandwichensis rostratus*). *Physiological Zoology*, 46: 276-284.

Klicka, J., Keith Barker, F., Burns, K. J., Lanyon, S. M., Lovette, I. J., Chaves, J. A., & Bryson, R. W. 2014. A comprehensive multilocus assessment of sparrow (Aves: Passerellidae) relationships. *Molecular Phylogenetics and Evolution*, 77: 177-182.

Koleganova, N., Piecha, G., Ritz, E., Becker, L. E., Müller, A., Weckbach, M., … Gross-Weissmann, M.-L. 2011. Both high and low maternal salt intake in pregnancy alter kidney development in the offspring. *American Journal of Physiology. Renal Physiology*, 301: F344-354.

Kozak, K. H., & Wiens, J. J. 2010. Accelerated rates of climatic-niche evolution underlie rapid species diversification. *Ecology Letters*, 13: 1378-1389.

Lande, R. 2009. Adaptation to an extraordinary environment by evolution of phenotypic plasticity and genetic assimilation. *Journal of Evolutionary Biology* 22: 1435-1446.

Langerhans, R. B. 2018. Predictability and Parallelism of Multitrait Adaptation. *Journal of Heredity*, 109: 59-70.

122

Laporte, M., Dalziel, A. C., Martin, N., & Bernatchez, L. 2016. Adaptation and acclimation of traits associated with swimming capacity in Lake Whitefish (*Coregonus clupeaformis*) ecotypes. *BMC Evolutionary Biology*, 16: 1-13.

Levis, N. A., & Pfennig, D. W. 2016. Evaluating "Plasticity-First" evolution in nature: key criteria and empirical approaches. *Trends in Ecology and Evolution*, 7: 563-574.

Little, M. H., & McMahon, A. P. 2012. Mammalian kidney development: principles, progress, and projections. *Cold Spring Harbor Perspectives in Biology*, 4: a008300–a008300.

Louthan, A. M., Doak, D. F., & Angert, A. L. 2015. Where and when do species interactions set range limits? *Trends in Ecology and Evolution*, 30: 780-792.

Masel, J., & Maughan, H. 2007. Mutations leading to loss of sporulation ability in Bacillus subtilis are sufficiently frequent to favor genetic canalization. *Genetics*, 175: 453-457.

Masel, J., King, O. D., & Maughan, H. 2007. The loss of adaptive plasticity during long periods of environmental stasis. *The American Naturalist*, 169: 38-46.

Mayr, E. 1947. Ecological Factors in Speciation. *Evolution*, 1: 263-288.

McKinley, M. J., & Johnson, A. K. 2004. The physiological regulation of thirst and fluid intake. *News in Physiological Sciences*, 19: 1-6.

Murren, C. J., Auld, J. R., Callahan, H., Ghalambor, C. K., Handelsman, C. A., Heskel, M. A., ... & Pfennig, D. W. 2015. Constraints on the evolution of phenotypic plasticity: limits and costs of phenotype and plasticity. *Heredity*, 115: 293

Orr, H. A., & Unckless, R. L. 2008. Population extinction and the genetics of adaptation. *The American Naturalist*, 172: 160-169.

Peña-Villalobos, I., F. Valdés-Ferranty, and P. Sabat. 2013. Osmoregulatory and metabolic costs of salt excretion in the Rufous-collared sparrow *Zonotrichia capensis*. *Comparative Biochemistry and Physiology Part A* 164: 314-318.

Peterson, D., Cayan, D., Dileo, J., Noble, M., & Dettinger, M. 1995. The role of climate variability in   estuarine variability. *American Scientist*, 83: 58-67.

Pigliucci, M., and C.J. Murren. 2003. Perspective: genetic assimilation and a possible evolutionary paradox: can macroevolution sometimes be so fast as to pass us by? *Evolution,* 57: 1455-1464.

Pigliucci, M., C.J. Murren, and C.D. Schlichting 2006. Phenotypic plasticity and evolution by genetic assimilation. *Journal of Experimental Biology,* 209: 2362-2367.

Pigot, A. L., Phillimore, A. B., Owens, I. P. F., & Orme, C. D. L. 2010. The shape and temporal dynamics of phylogenetic trees arising from geographic speciation. *Systematic Biology*, 59: 660-673.

Poulson, T. L., & Bartholomew, G. A. 1962. Salt balance in the Savannah Sparrow. *Physiological Zoology*, 35: 109-119.

Poulson, T. 1969. Salt and water balance in Seaside and Sharp-tailed Sparrows. *The Auk*, 86: 473-489.

Price, T.D., A. Qvarnstrom, & D.E. Irwin. 2003. The role of phenotypic plasticity in driving genetic evolution. *Proceedings of the Royal Society B: Biological Sciences* 270: 1433-1440.

Räsänen, K., & Kruuk, L. E. B. 2007. Maternal effects and evolution at ecological time-scales. *Functional Ecology*, 21: 408-421.

Sabat, P., Maldonado, K., Rivera-Hutinel, A., & Farfan, G. 2004. Coping with salt without salt glands: osmoregulatory plasticity in three species of coastal songbirds (ovenbirds) of the genus Cinclodes (Passeriformes: Furnariidae). *Journal of Comparative Physiology. B, Biochemical, Systemic, and Environmental Physiology*, 174: 415-420.

Sabat, P., Maldonado, K., Canals, M., & Del Rio, C. M. 2006. Osmoregulation and adaptive radiation in the ovenbird genus Cinclodes (Passeriformes: Furnariidae). *Functional Ecology*, 20: 799-805.

Sanín, C., Cadena, C. D., Maley, J. M., Lijtmaer, D. A., Tubaro, P. L., & Chesser, R. T. 2009. Paraphyly of Cinclodes fuscus (Aves: Passeriformes: Furnariidae): Implications for taxonomy and biogeography. *Molecular Phylogenetics and Evolution*, 53: 547-555.

Schlichting, C. D., & Wund, M. A. 2014. Phenotypic plasticity and epigenetic marking: An assessment of evidence for genetic accommodation. *Evolution*, 68: 656-672.

Schneider, C. A., Rasband, W. S., & Eliceiri, K. W. 2012. NIH Image to ImageJ: 25 years of image analysis. *Nature Methods*, 9: 671-675.

Scoville, A.G., & M.E. Pfrender. 2010. Phenotypic plasticity facilitates recurrent rapid adaptation to introduced predators. *Proceedings of the National Academy of Sciences* 107: 4260-4263.

Shaw, J.R., T.H. Hampton, B.L. King, A. Whitehead, F. Galvez, R.H. Gross, N. Keith, E. Notch, D. Jung, S.P. Glaholt, C.Y. Chen, J.K. Colbourne, & B.A. Stanton. 2014. Natural Selection Canalizes Expression Variation of Environmentally Induced Plasticity-Enabling Genes. *Molecular Biology and Evolution* 31: 3002-3015.

Skadhauge, E. 1981. *Osmoregulation in birds.* Springer-Verlag, Berlin, Germany.

Srinivasan, U., Elsen, P. R., Tingley, M. W., & Wilcove, D. S. 2018. Temperature and competition interact to structure Himalayan bird communities. *Proceedings of the Royal Society B: Biological Sciences*, 285: 20172593.

Stallone, J. N., & Braun, E. J. 1986. Osmotic and volemic regulation of plasma arginine vasotocin in conscious domestic fowl. *American Journal of Physiology- Regulatory Integrative and Comparative Physiology*, 250: R644-R657.

Storz, J. F., & Wheat, C. W. 2010. Integrating evolutionary and functional approaches to infer adaptation at specific loci. *Evolution*, 64: 2489-2509.

Storz, J. F., Scott, G. R., & Cheviron, Z. A. 2010. Phenotypic plasticity and genetic adaptation to high-altitude hypoxia in vertebrates. *The Journal of Experimental Biology*, 213: 4125-4136.

Suzuki, Y., & H.F. Nijhout. 2006. Evolution of a polyphenism by genetic accommodation. *Science,* 311: 650-652.

Velotta, J. P., Mccormick, S. D., & Schultz, E. T. 2015. Trade-offs in osmoregulation and parallel shifts in molecular function follow ecological transitions to freshwater in the Alewife. *Evolution*, 69: 2676-2688.

Velotta, J. P., Wegrzyn, J. L., Ginzburg, S., Kang, L., Czesny, S., O'Neill, R. J., … Schultz, E. T. 2017. Transcriptomic imprints of adaptation to fresh water: parallel evolution of osmoregulatory gene expression in the Alewife. *Molecular Ecology*, 26: 831-848.

Via, S., Gomulkiewicz, R., De Jong, G., Scheiner, S. M., Schlichting, C. D., & Van Tienderen, P. H. 1995. Adaptive phenotypic plasticity: consesus and controversy. *Trends in Ecology & Evolution*, 10: 212-217.

Waddington, C.H. 1953. Genetic assimilation of an acquired character. *Evolution,* 7: 118-126.

West-Eberhard, M. J. 2005. Developmental plasticity and the origin of species differences. *Proceedings of the National Academy of Sciences,* 102: 6543-6549.

Wheelwright, N.T., and J.D. Rising. 2008. Savannah Sparrow (*Passerculus sandwichensis*). *in* Birds of North American Online (A. Poole, Ed.). Cornell Lab of Ornithology, Ithaca, NY.

Whitehead, A., J.L. Roach, S. Zhang, and F. Galvez. 2011. Genomic mechanisms of evolved physiological plasticity in killifish distributed along an environmental salinity gradient. *Proceedings of the National Academy of Science,* 108: 6193-6198.

Wiens, J. J., & Graham, C. H. 2005. Niche conservatism: integrating evolution, ecology, and conservation biology. *Annual Review of Ecology, Evolution, and Systematics*, 36: 519-539.

Wiens, J. J. (2011). The niche, biogeography and species interactions. *Philosophical Transactions of the Royal Society B: Biological Sciences*, 366: 2336-2350.

Wund, M.A. 2012. Assessing the impacts of phenotypic plasticity on evolution. *Integrative and Comparative Biology* 52: 5-15.
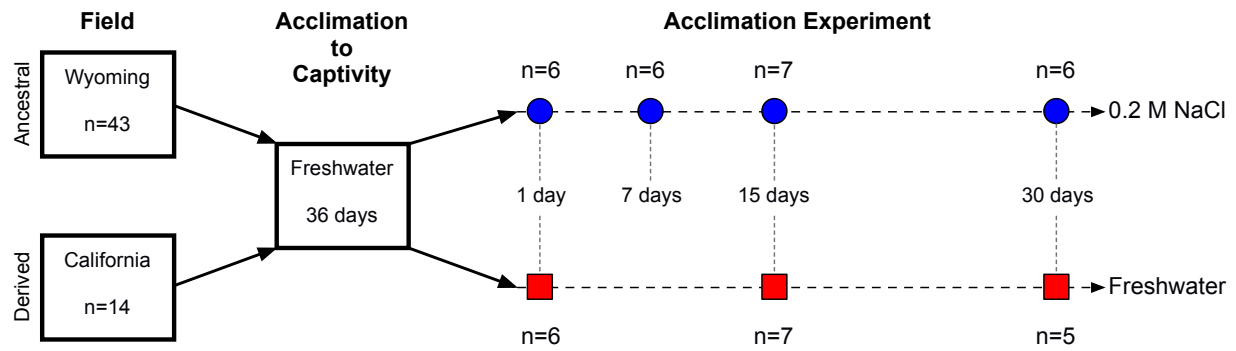
Figure 1: Overview of experimental design. Only birds from the Wyoming population were sampled at all time points. The 14 birds from California were split evenly between the two treatments and all of them were sampled on day 15.
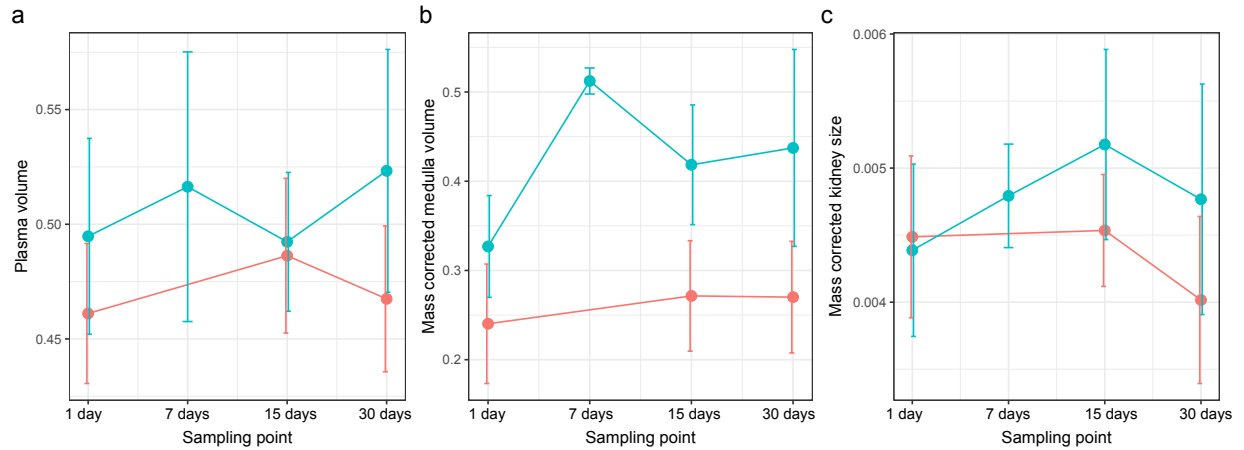
Figure 2: Acclimation responses within the ancestral, freshwater-adapted population in (a) plasma volume, (b) medulla volume corrected for body mass, and (c) kidney size corrected for body mass. Responses within the group exposed to salt drinking water is shown in blue and within the fresh drinking water group shown in red. Circles represent group mean for each trait at each time point with error bars equaling ± 1 SD. For all traits there was a significant effect of treatment (Table 1).
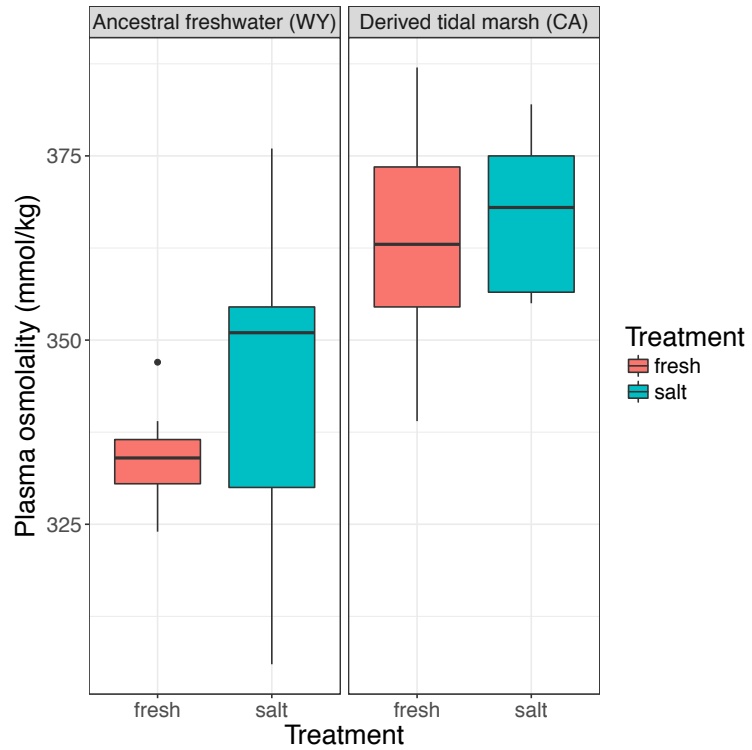
Figure 3: Differences in plasma osmolality (mmol/kg) between treatments for both the ancestral and derived populations sampled at 15 days.
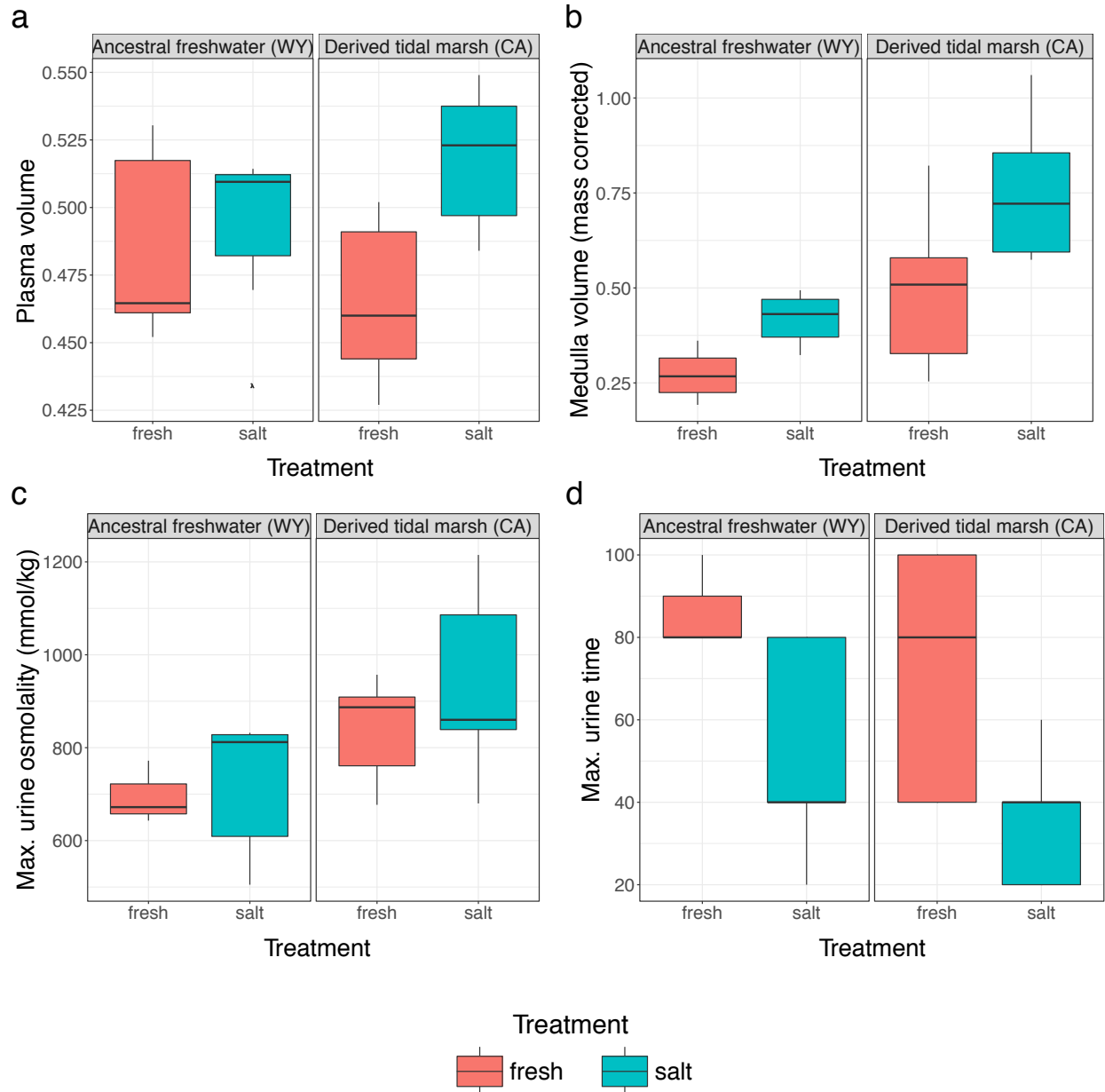
Figure 4: Comparison of acclimation responses in (a) plasma volume, (b) medulla volume corrected for body size, (c) Umax, and (d) time to reach Umax between the two populations for birds sampled at 15 days. See table 2 for results of two-way ANOVA testing for effects of population, treatment, and population*treatment.
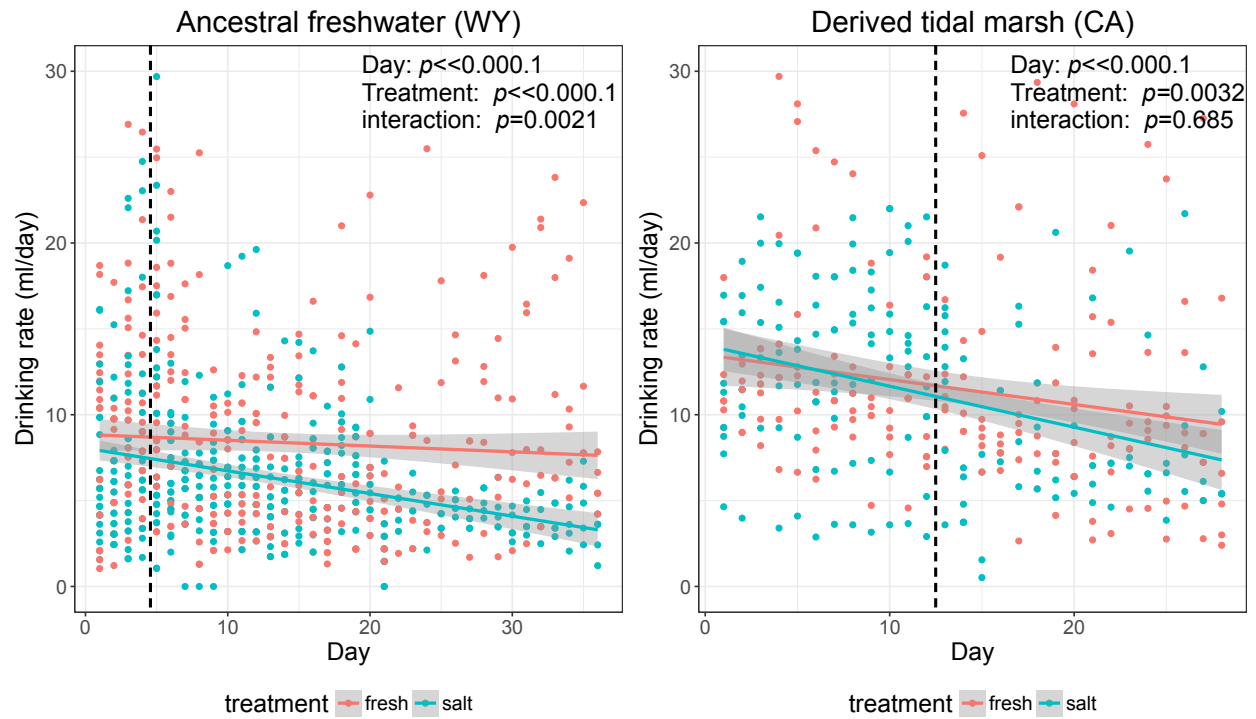
Figure 5: Changes in daily drinking rate throughout the course of the experiment for both populations. Trendlines from linear regression with gray shading the 95% confidence intervals around the slope. Statistics based on ANCVOA analysis with treatment as factor and day as the covariate.
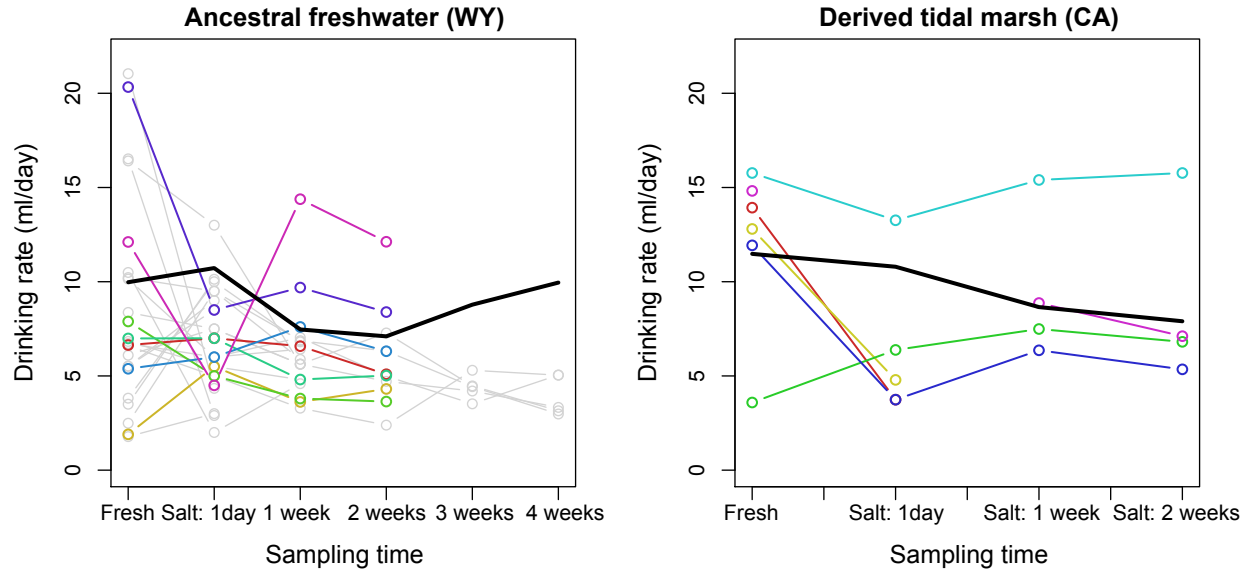
Figure 6: Individual level reaction norms for drinking rate changes in response to increased length of exposure to salt drinking water. Different colored lines and points correspond to different individuals from salt group. In the ancestral freshwater (WY) population only birds sampled at 15 days are shown in color to make a comparable visual comparison to derived tidal marsh birds. All other birds from the ancestral population are in light gray. Bold black line is the mean at each point for the freshwater group.
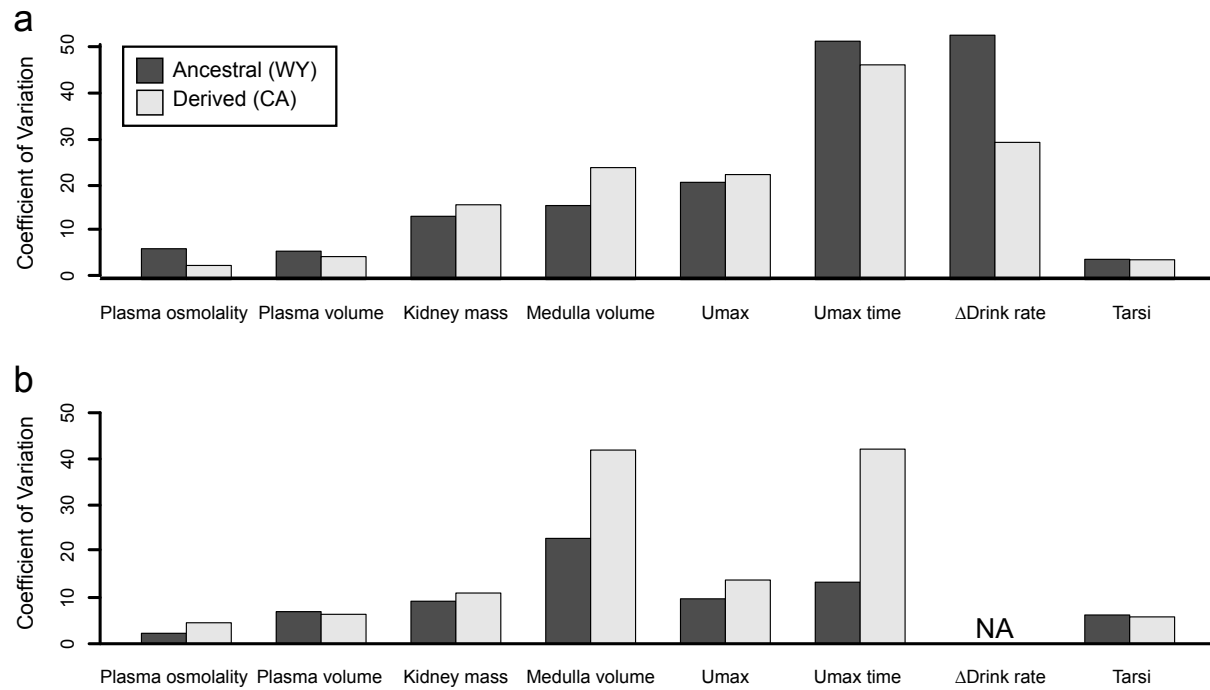
Figure 7: Comparisons of the coefficient of variation (COV) for each physiological trait between (a) salt-exposed birds from each population, and (b) freshwater-exposed birds from each population. ΔDrink rate is the change in drinking rate within the first 24 hours post-salt exposure. Data for changes in drinking rate are for the salt-exposed group only as we did not collect comparable data for the freshwater group. Tarsus length was measured as a reference trait that is assumed to be evolving neutrally between populations and allows us to account for the influence of population demography on trait variance.

Table 1: Responses to salt drinking water in the ancestral, freshwater adapted population. Presented are the mean values (± 1 SD) for each sampling time and treatment. p-values from two-way ANOVA analysis are presented for effects of treatment (fresh/salt), sampling time (1day-30days), and the interaction between treatment and sampling time. Statistical results for Umax and Utime are based on t-tests given that only data from 15 days was analyzed.

| trait | treat. | Sampling time | | | | effects | | |
		1 day	7 days	15 days	30 days	treatment	time	int.
Plasma osmo	fresh	328.83 ± 9.89	NA	334.14 ± 7.56	343.0 ± 9.38	0.232	0.481	0.501
(mmol/kg)	salt	351.17 ± 19.36	327.83 ± 36.21	343.14 ± 22.93	347 ± 19.64			
Plasma vol	fresh	0.461 ± 0.031	NA	0.486 ± 0.034	0.467 ± 0.032	0.015	0.336	0.936
	salt	0.495 ± 0.043	0.516 ± 0.059	0.492 ± 0.030	0.523 ± 0.053			
Kidney mass	fresh	0.0045 ± 0.0006	NA	0.0045 ± 0.0004	0.0040 ± 0.0006	0.0396	0.861	0.135
	salt	0.0044 ± 0.0006	0.0048 ± 0.0004	0.0052 ± 0.0007	0.0048 ± 0.0009			
Medulla	fresh	0.240 ± 0.0669	NA	0.271 ± 0.062	0.270 ± 0.062	<<0.0001	0.107	0.570
volume	salt	0.326 ± 0.057	0.512 ± 0.015	0.418 ± 0.067	0.437 ± 0.110			
Urine osmo	fresh	NA	NA	694.14 ± 189.16	NA	0.792	NA	NA
(mmol/kg)	salt	NA	NA	682 ± 139.70	NA			
Utime (min.)	fresh	NA	NA	86.67 ± 11.55	NA	0.046	NA	NA
	salt	NA	NA	52.0 ± 26.83	NA			

Table 2: Comparative acclimation responses for ancestral Wyoming and derived California populations following 15-days of exposure to salt drinking water. Presented are the mean values (± 1 SD) for each population and treatment. Results of two-way ANOVA reported as p-values for effects of treatment, locality, and interaction (int.) between treatment and locality.

| Trait | Wyoming | | California | | effects | | |
	fresh	salt	fresh	salt	treat.	loc.	int.
Plasma osmo	334.14 ± 7.56	343.14 ± 22.93	363.57 ± 16.51	366.86 ± 11.21	0.31	0.0001	0.63
Plasma vol.	0.486 ± 0.034	0.492 ± 0.030	0.466 ± 0.030	0.518 ± 0.026	0.017	0.83	0.053
Kidney size	0.0045 ± 0.0004	0.0052 ± 0.0007	0.0051 ± 0.0006	0.0052 ± 0.0008	0.14	0.18	0.34
Medulla vol	0.271 ± 0.062	0.418 ± 0.067	0.485 ± 0.203	0.751 ± 0.182	0.0009	<0.0001	0.29
Umax	695.67 ± 67.68	717.2 ± 150.98	838.2 ± 115.6	936 ± 212.75	0.39	0.029	0.62
Utime (min.)	86.67 ± 11.55	52.0 ± 26.83	72.0 ± 30.33	36.0 ± 16.73	0.007	0.35	0.95

APPENDIX 1: List of samples used in study

Table 1.1: Tissue samples and vouchers for specimens included in this study. Voucher numbers with asterisk refer to blood samples only, all other samples were extracted from muscle tissue. † denotes individuals included in SFS. § signifies birds included in analyses for second chapter.

Species	Voucher Number[1]	Locality
Ammodramus henslowi	FMNH 482581	ILLINOIS: Cook Co; Chicago, Prudential Building
Ammodramus leconteii	FMNH 493778	ILLINOIS: Cook Co; Chicago, McCormack Place
Melospiza melodia	FMNH 498516	ILLINOIS: Cook Co; Chicago, McCormack Place
Pooecetes gramineus	FMNH 476629	MINNESOTA: Cass Co; Sylvan Township
P. s. alaudinus	FMNH 499933[§]	CALIFORNIA: Humboldt Co; Mad River Slough Wildlife Area
P. s. alaudinus	FMNH 499934[§]	CALIFORNIA: Humboldt Co; Mad River Slough Wildlife Area
P. s. alaudinus	FMNH 499935[†§]	CALIFORNIA: Humboldt Co; Mad River Slough Wildlife Area
P. s. alaudinus	FMNH 499936[§]	CALIFORNIA: Humboldt Co; Mad River Slough Wildlife Area
P. s. alaudinus	FMNH 499937[§]	CALIFORNIA: Humboldt Co; Mad River Slough Wildlife Area
P. s. alaudinus	UWBM 79363	CALIFORNIA: Marin Co; Point Reyes National Seashore
P. s. alaudinus	MVZ 180638	CALIFORNIA: San Benito Co; Little Panoche and Panoche Rd
P. s. alaudinus	MB1*[§]	CALIFORNIA: San Luis Obispo Co; Morro Bay State Park
P. s. alaudinus	MB3*[§]	CALIFORNIA: San Luis Obispo Co; Morro Bay State Park
P. s. alaudinus	MB4*[§]	CALIFORNIA: San Luis Obispo Co; Morro Bay State Park
P. s. alaudinus	MB5*[§]	CALIFORNIA: San Luis Obispo Co; Morro Bay State Park
P. s. alaudinus	MB6*[§]	CALIFORNIA: San Luis Obispo Co; Morro Bay State Park
P. s. alaudinus	MB7*[§]	CALIFORNIA: San Luis Obispo Co; Morro Bay State Park
P. s. alaudinus	MB8*[§]	CALIFORNIA: San Luis Obispo Co; Morro Bay State Park
P. s. alaudinus	MB9*[§]	CALIFORNIA: San Luis Obispo Co; Morro Bay State Park
P. s. alaudinus	FMNH 499928[§]	CALIFORNIA: Santa Clara Co; San Francisco Bay NWR
P. s. alaudinus	FMNH 499929[†§]	CALIFORNIA: Santa Clara Co; San Francisco Bay NWR
P. s. alaudinus	FMNH 499930[§]	CALIFORNIA: Santa Clara Co; San Francisco Bay NWR
P. s. alaudinus	FMNH 499931[§]	CALIFORNIA: Santa Clara Co; San Francisco Bay NWR
P. s. alaudinus	FMNH 499932[§]	CALIFORNIA: Santa Clara Co; San Francisco Bay NWR
P. s. alaudinus	GIWA1*[§]	CALIFORNIA: Solano Co; Grizzly Island Wildlife Area
P. s. alaudinus	GIWA2*[§]	CALIFORNIA: Solano Co; Grizzly Island Wildlife Area
P. s. alaudinus	GIWA3*[§]	CALIFORNIA: Solano Co; Grizzly Island Wildlife Area
P. s. alaudinus	GIWA4*[§]	CALIFORNIA: Solano Co; Grizzly Island Wildlife Area
P. s. alaudinus	GIWA7*[†§]	CALIFORNIA: Solano Co; Grizzly Island Wildlife Area
P. s. alaudinus	GIWA8*[§]	CALIFORNIA: Solano Co; Grizzly Island Wildlife Area
P. s. alaudinus	ROM JR11429[†§]	CALIFORNIA: Solano Co; Grizzly Island, 20 km SSE Suisun City
P. s. alaudinus	ROM JR11430[§]	CALIFORNIA: Solano Co; Grizzly Island, 20 km SSE Suisun City
P. s. alaudinus	ROM JR11431[§]	CALIFORNIA: Solano Co; Grizzly Island, 20 km SSE Suisun City
P. s. alaudinus	ROM JR11432[§]	CALIFORNIA: Solano Co; Grizzly Island, 20 km SSE Suisun City
P. s. alaudinus	ROM JR11433[§]	CALIFORNIA: Solano Co; Grizzly Island, 20 km SSE Suisun City
P. s. alaudinus	FMNH 499924[§]	CALIFORNIA: Solano Co; Napa-Sonoma Marshes Wildlife Area

Species	Voucher Number[1]	Locality
P. s. alaudinus	FMNH 499925[†§]	CALIFORNIA: Solano Co; Napa-Sonoma Marshes Wildlife Area
P. s. alaudinus	FMNH 499926[†§]	CALIFORNIA: Solano Co; Napa-Sonoma Marshes Wildlife Area
P. s. alaudinus	FMNH 499927[§]	CALIFORNIA: Solano Co; Napa-Sonoma Marshes Wildlife Area
P. s. anthinus	USNM 640087	ALASKA: Anchorage
P. s. anthinus	YPM 141657	ALASKA: Black Rapids, E Bank Delta River
P. s. anthinus	MSB 222766[†]	ALASKA: Denali HWY
P. s. anthinus	MSB 222767	ALASKA: Denali HWY
P. s. anthinus	UAM 7444	ALASKA: Fairbanks
P. s. anthinus	YPM 141833	ALASKA: Fairbanks Borough; Taylor HWY, Mt. Fairplay
P. s. anthinus	USNM 601765[†]	ALASKA: Fairbanks, Eielson Air Force Base, Ski Resort
P. s. anthinus	USNM 622691	ALASKA: Fairbanks, Eielson Air Force Base, Ski Resort
P. s. anthinus	USNM 622692	ALASKA: Fairbanks, Eielson Air Force Base, Ski Resort
P. s. anthinus	USNM 622693	ALASKA: Fairbanks, Eielson Air Force Base, Ski Resort
P. s. anthinus	USNM 601708[†]	ALASKA: Fairbanks, Fort Wainwright Military Reservation
P. s. anthinus	USNM 601829	ALASKA: Fairbanks, Fort Wainwright Military Reservation
P. s. anthinus	UAM 15235[†]	ALASKA: Ketchikan, Tongass HWY
P. s. anthinus	UWBM 53866	ALASKA: Lake Louise State Recreation Area
P. s. anthinus	UWBM 53875[†]	ALASKA: Lake Louise State Recreation Area
P. s. anthinus	UWBM 53876	ALASKA: Lake Louise State Recreation Area
P. s. anthinus	USNM 638948	ALASKA: Mt. Fairplay at Taylor Highway
P. s. anthinus	UWBM 66281	ALASKA: North Slope Borough; Toolik Field Station
P. s. anthinus	UWBM 66288	ALASKA: North Slope Borough; Toolik Field Station
P. s. anthinus	UWBM 78648	ALASKA: North Slope Borough; Toolik Field Station
P. s. anthinus	YPM 142424	ALASKA: North Slope; Dalton HWY Mi. 296
P. s. anthinus	UWBM 53962	ALASKA: Paxon, along Denali Highway near Maclaren Summit
P. s. anthinus	UWBM 53971	ALASKA: Paxon, along Denali Highway near Maclaren Summit
P. s. anthinus	MSB 222765[†]	ALASKA: Seward Peninsula, Nome
P. s. anthinus	UWBM 53840	ALASKA: Valdez, along trans-Alaskan pipeline near terminal
P. s. anulus	ROM JR401991[§]	BAJA CALIFORNIA SUR; Guerrero Negro
P. s. anulus	ROM JR401992[§]	BAJA CALIFORNIA SUR; Guerrero Negro
P. s. anulus	ROM JR401993[§]	BAJA CALIFORNIA SUR; Guerrero Negro
P. s. anulus	ROM JR402992[§]	BAJA CALIFORNIA SUR; Guerrero Negro
P. s. anulus	ROMJR423991[†§]	BAJA CALIFORNIA SUR; Guerrero Negro
P. s. anulus	ROMJR423994[†§]	BAJA CALIFORNIA SUR; Guerrero Negro
P. s. anulus	ROM JR423995[§]	BAJA CALIFORNIA SUR; Guerrero Negro
P. s. anulus	FMNH 496773[§]	BAJA CALIFORNIA SUR; Mpio. Mulegé, Puerto Viejo
P. s. anulus	FMNH 496774[§]	BAJA CALIFORNIA SUR; Mpio. Mulegé, Puerto Viejo
P. s. anulus	FMNH 496775[§]	BAJA CALIFORNIA SUR; Mpio. Mulegé, Puerto Viejo
P. s. anulus	MZFC 27471[†§]	BAJA CALIFORNIA SUR; Mpio. Mulegé, Puerto Viejo
P. s. anulus	MZFC 27472[§]	BAJA CALIFORNIA SUR; Mpio. Mulegé, Puerto Viejo
P. s. anulus	MZFC 27474[§]	BAJA CALIFORNIA SUR; Mpio. Mulegé, Puerto Viejo

Species	Voucher Number[1]	Locality
P. s. atratus	UWBM 90711[§]	SINALOA: Mpio. Ahome, El Carrizo
P. s. atratus	UWBM 90712[§]	SINALOA: Mpio. Ahome, El Carrizo
P. s. atratus	UWBM 90732[†§]	SINALOA: Mpio. Ahome, El Carrizo
P. s. atratus	UWBM 90733[†§]	SINALOA: Mpio. Ahome, El Carrizo
P. s. atratus	MZFC 27480[§]	SONORA: Mpio. Bacum; Couplejo Acuicola "La Atanasia"
P. s. atratus	MZFC 27481[§]	SONORA: Mpio. Bacum; Couplejo Acuicola "La Atanasia"
P. s. atratus	MZFC 27482[§]	SONORA: Mpio. Bacum; Couplejo Acuicola "La Atanasia"
P. s. atratus	MZFC 27483[†§]	SONORA: Mpio. Bacum; Couplejo Acuicola "La Atanasia"
P. s. atratus	FMNH 496783[†§]	SONORA: Mpio. Bacum; Couplejo Acuicola "La Atanasia"
P. s. atratus	FMNH 496784[§]	SONORA: Mpio. Bacum; Couplejo Acuicola "La Atanasia"
P. s. atratus	FMNH 496785[§]	SONORA: Mpio. Bacum; Couplejo Acuicola "La Atanasia"
P. s. beldingi	ROM JR330991[§]	BAJA CALIFORNIA: 2 km W El Papalote, Bahia San Quintin
P. s. beldingi	ROM JR330992[§]	BAJA CALIFORNIA: 2 km W El Papalote, Bahia San Quintin
P. s. beldingi	ROMJR330994[†§]	BAJA CALIFORNIA: 2 km W El Papalote, Bahia San Quintin
P. s. beldingi	ROMJR330995[†§]	BAJA CALIFORNIA: 2 km W El Papalote, Bahia San Quintin
P. s. beldingi	ROM JR330997[§]	BAJA CALIFORNIA: 2 km W El Papalote, Bahia San Quintin
P. s. beldingi	ROM JR330998[§]	BAJA CALIFORNIA: 2 km W El Papalote, Bahia San Quintin
P. s. beldingi	SDNHM 489[†§]	CALIFORNIA: San Diego Co.; San Elijo Lagoon
P. s. beldingi	SDNHM 692[†§]	CALIFORNIA: San Diego Co.; Santa Margarita River Mouth
P. s. brooksi	FMNH 499938[§]	CALIFORNIA: Del Norte Co; Lake Earl Wildlife Area
P. s. brooksi	FMNH 499939[§]	CALIFORNIA: Del Norte Co; Lake Earl Wildlife Area
P. s. brooksi	FMNH 499940[†§]	CALIFORNIA: Del Norte Co; Lake Earl Wildlife Area
P. s. brooksi	FMNH 499941[†§]	CALIFORNIA: Del Norte Co; Lake Earl Wildlife Area
P. s. brooksi	FMNH 499942[§]	CALIFORNIA: Del Norte Co; Lake Earl Wildlife Area
P. s. brooksi	FMNH 499943[§]	CALIFORNIA: Del Norte Co; Lake Earl Wildlife Area
P. s. brooksi	UWBM 79578[†]	WASHINGTON: King Co; SeaTac Airport
P. s. brooksi	UWBM 79831	WASHINGTON: Clallam Co; Sequim
P. s. brooksi	LSUMZ 19131[†]	WASHINGTON: Gray's Harbor Co.; Ocean Shores
P. s. brooksi	UWBM 86202	WASHINGTON: Island Co; Coupeville, Naval Landing Field
P. s. brooksi	UWBM 79555	WASHINGTON: Kitsap Co; Port Gamble
P. s. brooksi	UWBM 79663[†]	WASHINGTON: Klickitat Co; BZ Corner, Kreps Ranch
P. s. brooksi	UWBM 79664	WASHINGTON: Klickitat Co; BZ Corner, Kreps Ranch
P. s. brooksi	UWBM 79665	WASHINGTON: Klickitat Co; BZ Corner, Kreps Ranch
P. s. brooksi	UWBM 79634	WASHINGTON: Thurston Co; Lacey, 300 Desmond Ave.
P. s. guttatus	MZFC 27476[§]	BAJA CALIFORNIA SUR: Mpio. Mulegé; Punta Abreojos
P. s. guttatus	FMNH 496778[†§]	BAJA CALIFORNIA SUR: Mpio. Mulegé; Punta Abreojos
P. s. guttatus	MZFC 27477[§]	BAJA CALIFORNIA SUR: Mpio. Mulegé; Punta Abreojos
P. s. guttatus	FMNH 496779[§]	BAJA CALIFORNIA SUR: Mpio. Mulegé; Punta Abreojos
P. s. guttatus	FMNH 496780[§]	BAJA CALIFORNIA SUR: Mpio. Mulegé; Punta Abreojos
P. s. labradorius	UWBM 110765	NEWFOUINDLAND: 25 Km N Burgeo
P. s. magdalanae	ROM JR411991[§]	BAJA CALIFORNIA SUR: 4 km SE Puerto Lopez Mateos

Species	Voucher Number[1]	Locality
P. s. magdalanae	ROM JR411993[§]	BAJA CALIFORNIA SUR: 4 km SE Puerto Lopez Mateos
P. s. magdalanae	ROMJR411994[†§]	BAJA CALIFORNIA SUR: 4 km SE Puerto Lopez Mateos
P. s. magdalanae	FMNH 496781[†§]	BAJA CALIFORNIA SUR: Mpio. Comondu; Lopez Mateos
P. s. magdalanae	FMNH 496782[§]	BAJA CALIFORNIA SUR: Mpio. Comondu; Lopez Mateos
P. s. magdalanae	MZFC 27478[§]	BAJA CALIFORNIA SUR: Mpio. Comondu; Lopez Mateos
P. s. magdalanae	MZFC 27479[§]	BAJA CALIFORNIA SUR: Mpio. Comondu; Lopez Mateos
P. s. nevadensis	UWBM 116194	ALBERTA: Zama City
P. s. nevadensis	UWBM 116195	ALBERTA: Zama City
P. s. nevadensis	MVZ 182308[§]	CALIFORNIA: Lassen Co; Eagle Lake
P. s. nevadensis	MVZ 182309[§]	CALIFORNIA: Lassen Co; Eagle Lake
P. s. nevadensis	FMNH 499944[§]	CALIFORNIA: Lassen Co; Lassen NF, Pine Creek Valley
P. s. nevadensis	FMNH 499945[§]	CALIFORNIA: Lassen Co; Lassen NF, Pine Creek Valley
P. s. nevadensis	FMNH 499946[†§]	CALIFORNIA: Lassen Co; Lassen NF, Pine Creek Valley
P. s. nevadensis	FMNH 499947[†§]	CALIFORNIA: Lassen Co; Lassen NF, Pine Creek Valley
P. s. nevadensis	FMNH 499948[§]	CALIFORNIA: Lassen Co; Lassen NF, Pine Creek Valley
P. s. nevadensis	FMNH 499949[§]	CALIFORNIA: Lassen Co; Lassen NF, Pine Creek Valley
P. s. nevadensis	FMNH 499950[§]	CALIFORNIA: Lassen Co; Lassen NF, Pine Creek Valley
P. s. nevadensis	SDNHM 2723[§]	CALIFORNIA: Riverside Co; Lake Hemet
P. s. nevadensis	FMNH 499951[§]	CALIFORNIA: San Bernardino Co; San Bernardino NF, Baldwin Lake
P. s. nevadensis	FMNH 499952[†§]	CALIFORNIA: San Bernardino Co; San Bernardino NF, Baldwin Lake
P. s. nevadensis	FMNH 499953[§]	CALIFORNIA: San Bernardino Co; San Bernardino NF, Baldwin Lake
P. s. nevadensis	FMNH 499954[§]	CALIFORNIA: San Bernardino Co; San Bernardino NF, Baldwin Lake
P. s. nevadensis	AMNH 7770[§]	CALIFORNIA: Shasta Co; Redding
P. s. nevadensis	USNM 636882	CALIFORNIA: Tulare Co; Sequoia National Forest, Big Meadow West
P. s. nevadensis	USNM 636883	CALIFORNIA: Tulare Co; Sequoia National Forest, Big Meadow West
P. s. nevadensis	UWBM 56357	COLORADO: Park Co; 5 mi SW Jefferson
P. s. nevadensis	UWBM 56358	COLORADO: Park Co; 5 mi SW Jefferson
P. s. nevadensis	UWBM 70319	COLORADO: Park Co; 5 mi SW Jefferson
P. s. nevadensis	UWBM 70320	COLORADO: Park Co; 5 mi SW Jefferson
P. s. nevadensis	UWBM 70321	COLORADO: Park Co; 5 mi SW Jefferson
P. s. nevadensis	MSB 23807[†]	NEW MEXICO: Rio Arriba Co; 1.5 Mi. N, 11.6 Mi. E Chama
P. s. nevadensis	UWBM 80586	NORTH DAKOTA: Bottineau Co; Antler
P. s. nevadensis	USNM 647160[†]	NORTH DAKOTA: Bottineau, 7.1 km NNE of Newburg
P. s. nevadensis	UWBM 80607	NORTH DAKOTA: Slope Co; Amidon
P. s. nevadensis	UWBM 80845	NORTH DAKOTA: Towner Co; Egeland
P. s. nevadensis	UWBM 90442[†]	OREGON: Crook Co; Hampton, Crooked River
P. s. nevadensis	UWBM 90447	OREGON: Crook Co; Hampton, Crooked River
P. s. nevadensis	UWBM 90459	OREGON: Crook Co; Hampton, Crooked River
P. s. nevadensis	UWBM 90479	OREGON: Crook Co; Hampton, Crooked River
P. s. nevadensis	UWBM 90513	OREGON: Crook Co; Hampton, Crooked River
P. s. nevadensis	UWBM 90514	OREGON: Crook Co; Hampton, Crooked River

Species	Voucher Number[1]	Locality
P. s. nevadensis	UWBM 62271	WASHINGTON: Grant Co; Electric City, Banks Lake
P. s. nevadensis	LSUMZ 3959	WYOMING: Medicine Bow National Forest, N Platte River
P. s. oblitus	ROM JR10979	ONTARIO
P. s. oblitus	ROM JR11043	ONTARIO
P. s. oblitus	ROM JR11048[†]	ONTARIO
P. s. oblitus	ROM JR11044[†]	ONTARIO: Moosonee
P. s. oblitus	ROM JR11052	ONTARIO: Moosonee
P. s. oblitus	ROM JR11053	ONTARIO: Moosonee
P. s. oblitus	ROM JR11056	ONTARIO: Moosonee
P. s. rostratus	ROM JR11413	SONORA; 8 km E Puerto Peñasco
P. s. rostratus	ROM JR11414	SONORA; 8 km E Puerto Peñasco
P. s. rostratus	ROM JR11415	SONORA; 8 km E Puerto Peñasco
P. s. rostratus	ROM JR11416	SONORA; 8 km E Puerto Peñasco
P. s. rostratus	ROM JR11417	SONORA; 8 km E Puerto Peñasco
P. s. sanctorum	ROM JR425992	BAJA CALIFORNIA SUR; Islas San Benito
P. s. sanctorum	ROM JR425993	BAJA CALIFORNIA SUR; Islas San Benito
P. s. sanctorum	ROM JR425994[†]	BAJA CALIFORNIA SUR; Islas San Benito
P. s. sanctorum	ROM JR425995[†]	BAJA CALIFORNIA SUR; Islas San Benito
P. s. sanctorum	ROM JR425997	BAJA CALIFORNIA SUR; Islas San Benito
P. s. sanctorum	ROM JR426993	BAJA CALIFORNIA SUR; Islas San Benito
P. s. sanctorum	ROM JR426994	BAJA CALIFORNIA SUR; Islas San Benito
P. s. sandwichensis	SDNHM 2976	ALASKA; Aleutian Islands, Akun Island, Lost Harbor
P. s. savana	FMNH 498592	ILLINOIS: Stephenson Co; 2 Mi. S Loran
P. s. savana	FMNH 498593	ILLINOIS: Stephenson Co; 2 Mi. S Loran
P. s. savana	FMNH 498594	ILLINOIS: Stephenson Co; 2 Mi. S Loran
P. s. savana	CUMV 54897	NEW YORK: Orleans Co; Holley, Howard Rd.
P. s. savana	AMNHDOT5968	NEW YORK: Queens Co; JFK Airport
P. s. savana	CUMV 53399	NEW YORK: Tompkins Co; Dryden, Mineah Rd.
P. s. savana	CUMV 53435	NEW YORK: Tompkins Co; Dryden, Mineah Rd.
P. s. savana	CUMV 52283	NEW YORK: Tompkins Co; Dryden, Mt. Pleasant Rd
P. s. savana	CUMV 53072	NEW YORK: Tompkins Co; Ithaca, Mt. Pleasant Rd.
P. s. savana	USNM 602031	VIRGINIA: Fauquier Co; Rectortown Road at Rt 710

[1]American Museum of Natural History (AMNH); Cornell University Museum of Vertebrates (CUMV); Field Museum of Natural History (FMNH); Louisiana State University Museum of Natural History (LSUMZ); Museum of Southwestern Biology (MSB); Museum of Vertebrate Zoology at Berkeley (MVZ); El Museo de Zoología de la Facultad de Ciencias de la Universidad Nacional de Autónoma de México (MVFZ); Royal Ontario Museum (ROM); San Diego Natural History Museum (SDNHM); University of Alaska Museum of the North (UAM); Smithsonian National Museum of Natural History (USNM); University of Washington Burke Museum (UWBM); Yale Peabody Museum of Natural History (YPM).

APPENDIX 2: Supplemental methods chapter 1.

mtDNA sequencing:

We used the same primers as Zink et al. (2005) [L5215 (Hackett 1996) and H1064 (S.V. Drovetski)] and amplified the *ND2* locus using 25 µl reactions [2.5 µL DNA (~20-30 ng/µl); 17.1 µL H2O; 0.75 µL 50 mM MgCl2; 2.5 µL GeneAmp 10× PCR buffer; 0.5 µL 10 mM dNTP; 0.75 µL of 10 mM reverse and forward primer; and 0.15 µL (5 units/µL) Invitrogen *Taq* DNA Polymerase (ThermoFisher Scientific, Waltham, MA, USA)] with the following PCR protocol: initial denaturation at 94°C for 3 min; 35 cycles of denaturation at 94 °C for 45 sec, annealing at 58°C for 1 min, and extension at 72 °C for 1 min; and final extension at 72 °C for 5 min. Following PCR, sequences were cleaned using 0.5 µL/5 µL product of exonuclease I and 1 µL/5 µL product of FastAP thermosensitive alkaline phosphotase with the recommended thermal cycler protocol (ThermoFisher Scientific, Waltham, MA, USA). Finally, we performed 14 µl sequencing reactions [2.5 µl DNA (~20-30 ng/µl); 0.4 µl ABI BigDye terminator v. 3.1 (Applied Biosystems); 2.25 µl 10 mM MgCl2; 3 µl 5x sequencing buffer; 1 µl PCR primer; 5.85 µl H2O] and then sequenced both the forward and reverse strands on an ABI 3130 automated sequencer.

STACKS parameter optimization:

A number of parameters within the stacks pipeline can significantly impact the resulting number of RAD-loci and SNP calling, including the minimum depth of coverage (*m*), maximum distance between stacks (*M*), and the maximum distance to align secondary reads to primary stacks (*n*) (Catchen et al. 2011). Misspecification of these parameters can result in systematic under- or over-merging of RAD-loci and an inability to distinguish SNPs from sequencing error (Mastretta-Yanes et al. 2014). To optimize these parameters in our dataset we performed multiple runs of STACKS on a subset of 24 individuals randomly selected from the entire dataset, but spanning the geographic scope of the study. In each STACKS run we varied *m* from 2-10 (with *M*=2, *n*=2), *M* from 2-8 (with *m*=3, *n*=2), and *n* from 1-5 (with *m*=3, *M*=2). Only *m* had a major influence on the resulting number of RAD-loci and SNPs obtained, with increasing *m* corresponding to a rapid decrease in loci. There was a slight increase in the number of loci and SNPs obtained with increasing *M,* but no change with varying *n* (Appendix 3: Fig. 3.1). In addition to examining the impact of parameter variation on the number of loci and SNPs we assessed whether patterns of genetic structure were robust to this variation. We performed principal components analysis on each of the 21 resulting datasets in the R-package ADGENET v. 2.0 (Jombart & Ahmed 2011) and constructed a neighbor-joining tree using the r-package APE (Paradis 2004). We found patterns of genetic structure to be robust across a wide range of parameter settings with both PCA and NJ-tree supporting the presence of two clusters in all datasets (Appendix 3: Fig. 3.2).

Site frequency spectrum generation:

To generate the SFS from our dataset we restricted the number of individuals included to maximize the number of SNPs that are shared across all individuals. Individuals were included in the final dataset based on two criteria: (1) they must have been one of the 73 individuals included within the catalog used to call SNPs in the Stacks pipeline to ensure that rare polymorphisms were included in the dataset; and (2) the percent missing data for each individual was below the 50th percentile for all individuals. The final dataset included 25 individuals from the nominate population and 16 from the Mexican population. To remove any Z-linked loci from this dataset

we first removed any reads that aligned to the Zebra Finch (*Taeniopygia guttata*) Z-chromosome; and second, given the evolutionary distance between these species and potential lack of synteny, we removed loci that exhibited excess heterozygosity in females (Brelsford et al. 2016) and did not map anywhere on the Zebra Finch genome. Variant sites that deviated from Hardy-Weinberg equilibrium (α set to 0.05) and had a minimum individual read depth <10 were removed in VCFtools (Danecek et al. 2011). This resulted in a final dataset of 24,382 SNPs from 8,614 loci (mean: 2.8 and median: 2 SNPs per locus; Appendix 3: Fig. 3.3). The resulting vcf file was converted to $\partial a \partial i$ input file format using the vcf2dadi function in the r package stackr v. 0.2.6 (Gosselin & Bernatchez 2016) and within $\partial a \partial i$ analyses were based on a folded SFS due to the lack of quality outgroup data to polarize the SFS. Observed folded-SFS for the nominate clade shown in Appendix 3: Fig. 3.4 and joint SFS for both clades in Fig. 6b.

REFERENCES:

Brelsford, A., G. Lavanchy, R. Sermier, A. Rausch, and N. Perrin. 2016. Identifying homomorphic sex chromosomes from wild-caught adults with limited genomic resources. Molecular Ecology Resources, 1-8.

Catchen, J. M., A. Amores, P. Hohenlohe, W. Cresko, J. H. Postlethwait, and D. J. De Koning. 2011. Stacks: building and genotyping loci de novo from short-read sequences. G3: Genes, Genomes, Genetics 1: 171-182.

Danecek, P., A. Auton, G. Abecasis, C. A. Albers, E. Banks, M. A. DePristo, R. Handsaker, G. Lunter, G. Marth, S. T. Sherry, G. McVean, R. Durbin, and 1000 Genomes Project Analysis Group. 2011. The variant call format and VCFtools. Bioinformatics 27: 2156-2158.

Hackett, S. J. 1996. Molecular phylogenetics and biogeography of tanagers in the genus Ramphocelus (Aves). Mol. Phylogenet. Evol. 5: 368-82.

Jombart, T., and I. Ahmed. 2011. Adegenet 1.3-1: New tools for the analysis of genome-wide SNP data. Bioinformatics 27: 3070-3071.

Mastretta-Yanes, A., N. Arrigo, N. Alvarez, T. H. Jorgensen, D. Piñero, and B. C. Emerson. 2015. Restriction site-associated DNA sequencing, genotyping error estimation and de novo assembly optimization for population genetic inference. Molecular Ecology Resources 15: 28-41.

Paradis, E., J. Claude, and K. Strimmer. 2004. APE: analyses of phylogenetics and evolution in R language. Bioinformatics 20: 289-290.

TABLE 3.1: Number of SNPs output from STACKS for phylogenetic and population analysis with different levels of missing data allowed.

% missing	# SNPs with outgroups	# SNPS without outgroups
5%	13,058	6,709
10%	54,519	22,608
15%	103,629	37,324
25%	200,791	66,705
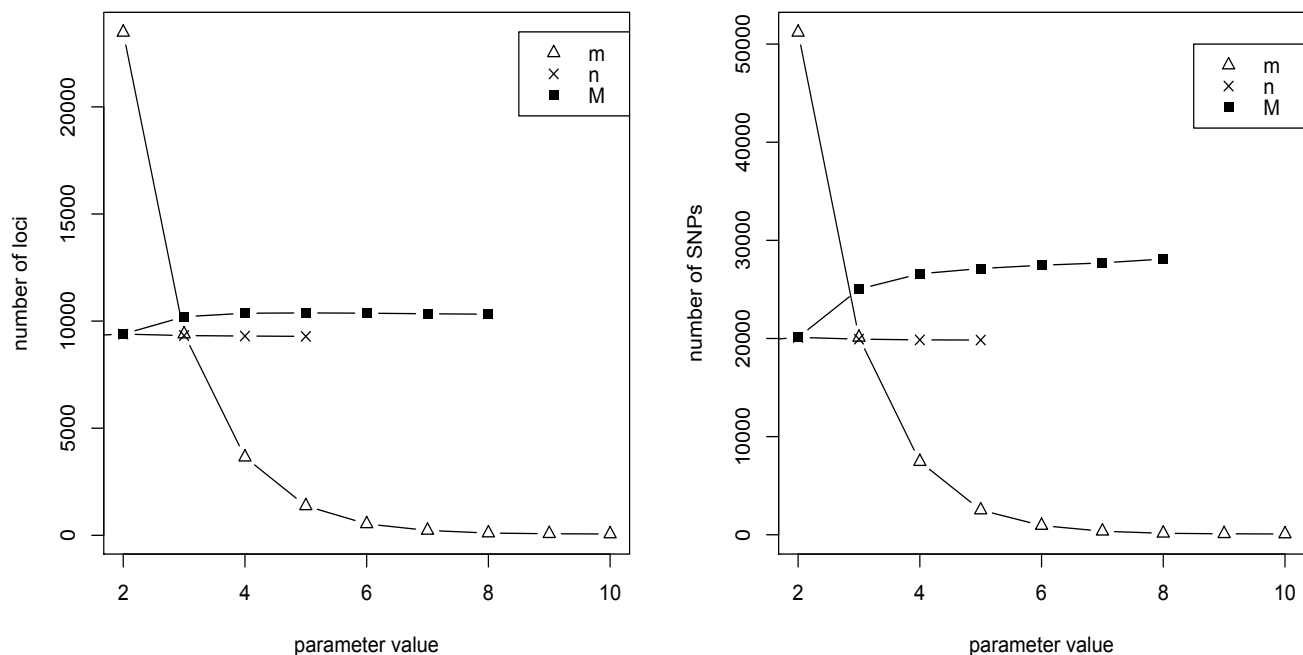
Figure 3.1: The influence of different ustacks and cstacks parameter settings on the resulting number of loci and SNPs. The parameters varied were: minimum depth of coverage (*m*), maximum distance allowed between stacks (*M*), and number of mismatches allowed between sample tags in catalog (*n*). We ran the stacks pipeline for *m* 2-10 (while setting *M* to 2 and *n* to 2); *M* 2-8 (with *m* 3 and *n* 2); and *n* 1-5 (with *M* 2 and *n* 2).
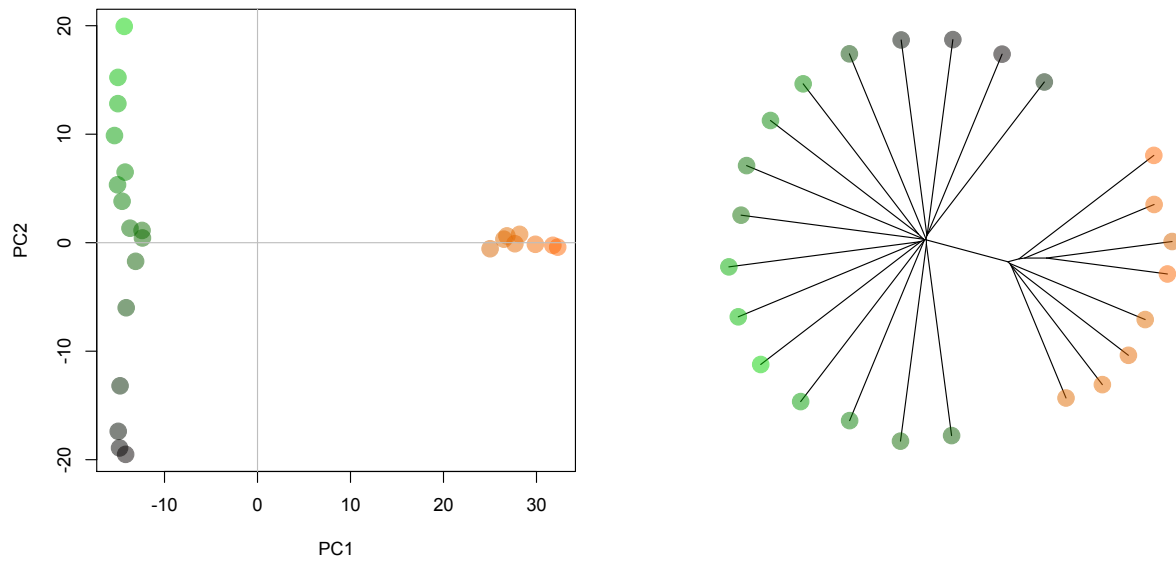
Figure 3.2: Principal components analysis and NJ tree for the 24 sample panel used for parameter optimization. Orange corresponds to samples from Mexico and green Nominate *Passerculus sandwichensis.* This plot was generated with output for *m*3*M*3*n*3
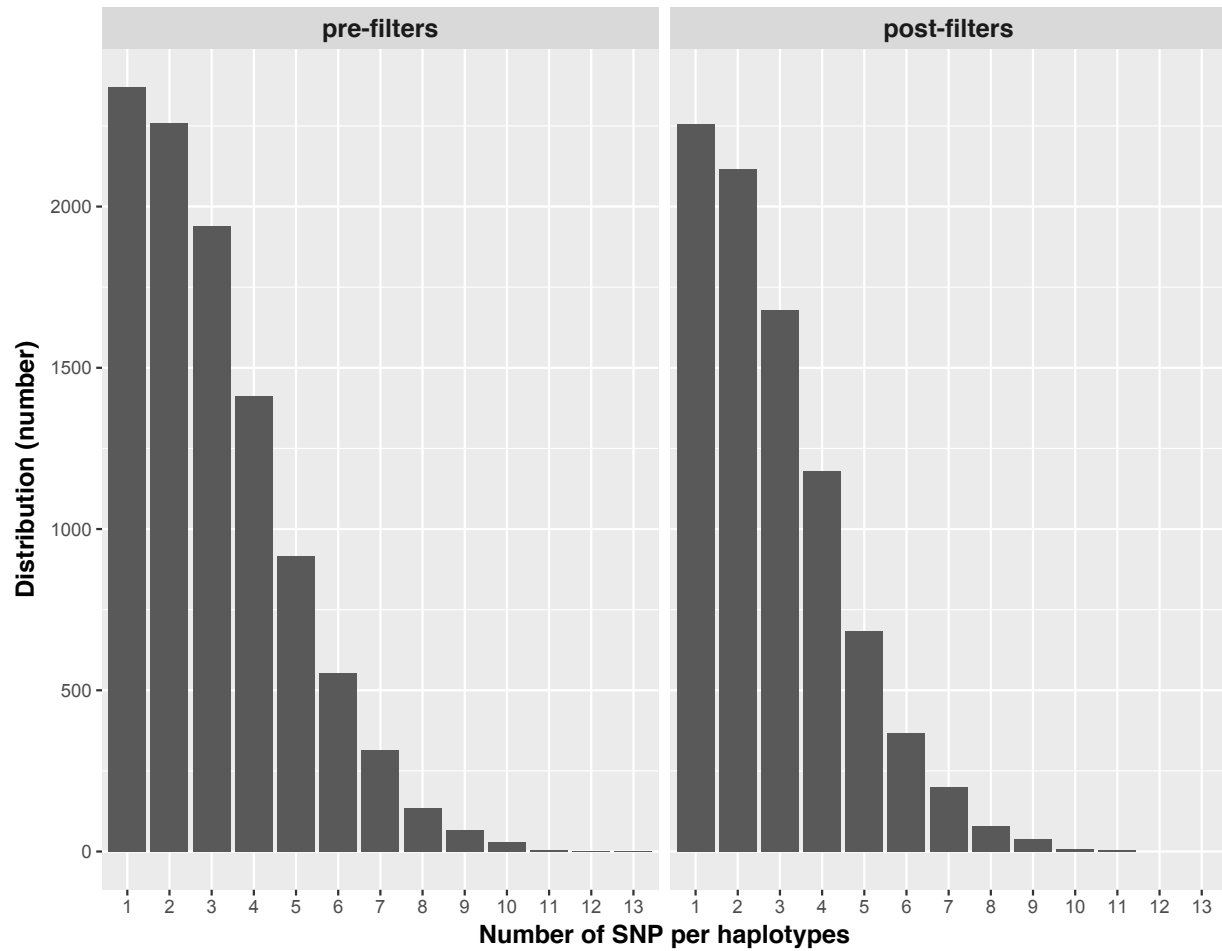
Figure 3.3: Distributions of the number of SNPs per 89bp RAD locus. Plot on the left shows distribution before filtering based on Hardy-Weinberg equilibrium and read depth. Plot on the right shows SNP distribution following filtering. After filtering there was a mean of 2.8 and median of 2 SNPs per locus.
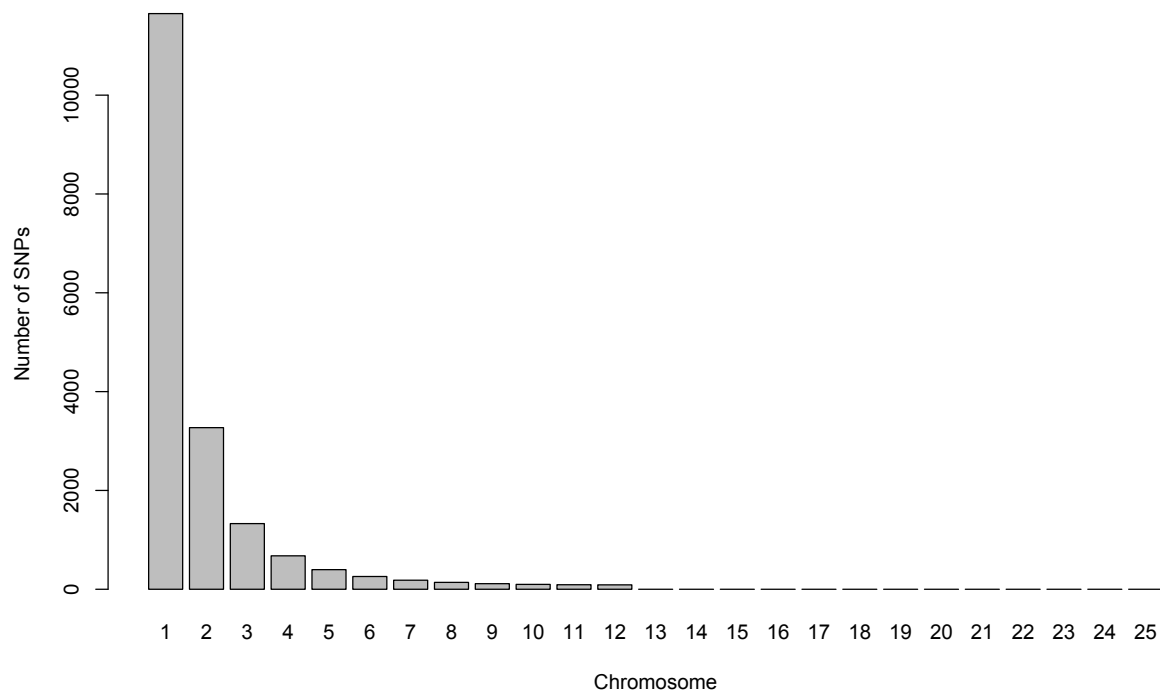
Figure 3.4: Folded site frequency spectrum for the nominate clade of Savannah Sparrows used in ∂a∂i analyses.
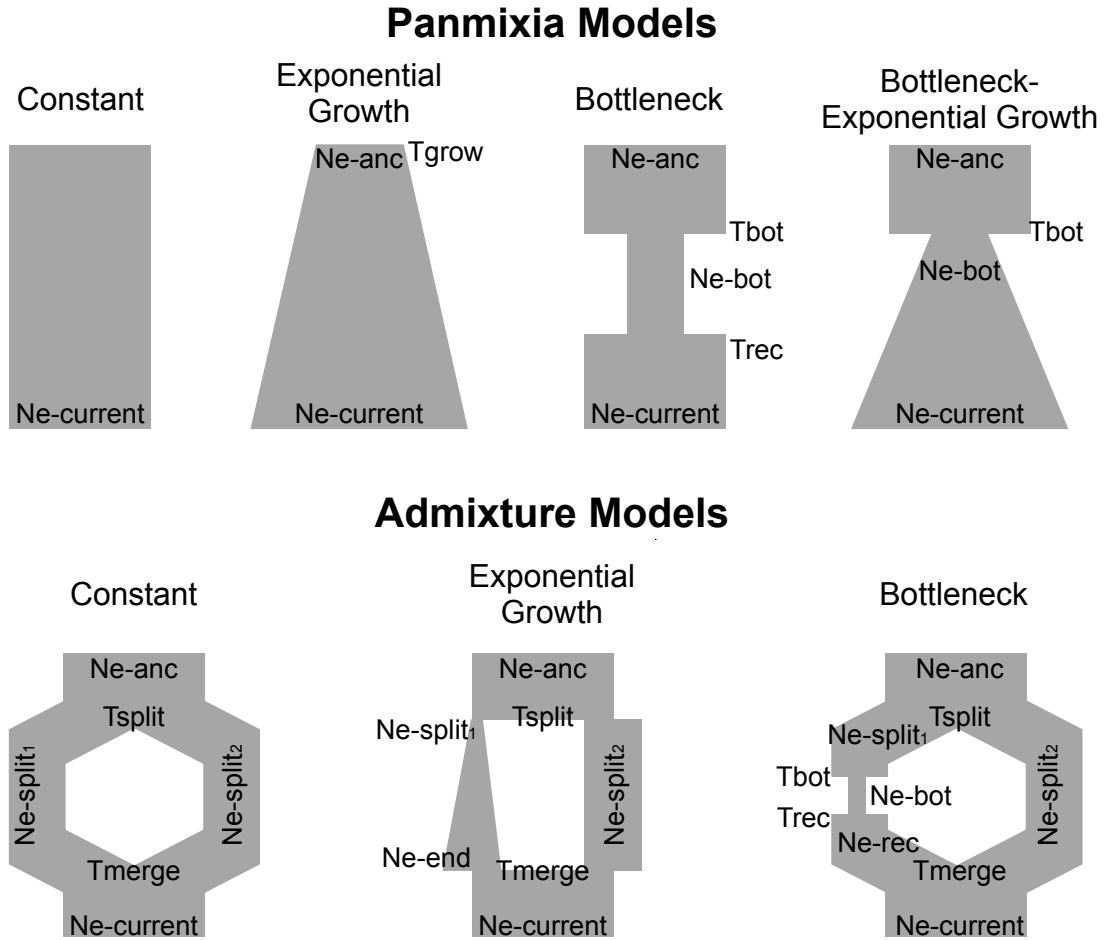
Figure 3.5: Demographic models fit to the site frequency spectrum of the nominate population in ∂a∂i. Changes in width of the gray bars represent changes in population size. The same admixture models were fit to a "ghost" population or SFS based on mtDNA haplotypes. Parameters estimated are labeled on each model. Population sizes (Ne) during different events are labeled: current (Ne-current); ancestral (Ne-anc); bottleneck (Ne-bot); end bottleneck (Ne-rec); end growth (Ne-end); in isolation (Ne-split). Labeling for time parameters: beginning of growth period (Tgrow); bottleneck start (Tbot); bottleneck end (Trec); divergence time (Tsplit); and merger time (Tmerge).
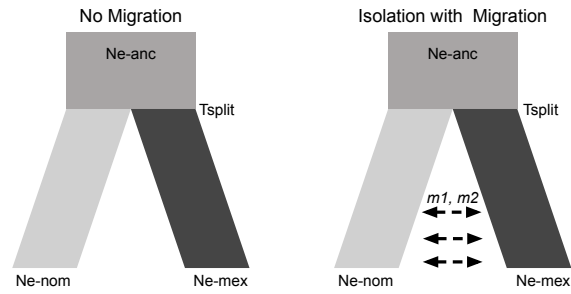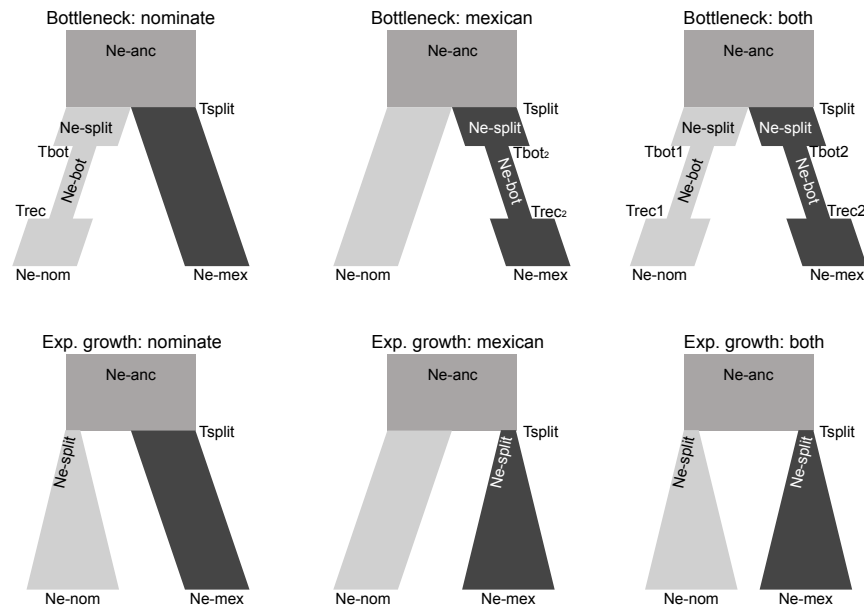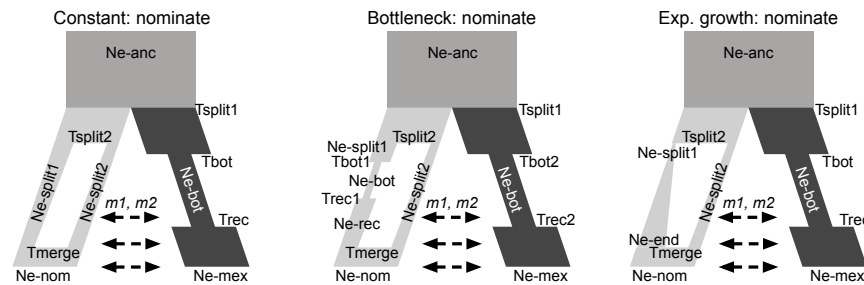
Figure 3.6: Models fit to joint site frequency spectrum of nominate (light gray) and Mexican populations (dark gray). We fit models with and without migration (*m1, m2)* between the two populations for all panmixia models (n=7). For admixture models, initial analyses suggested that a bottleneck in the Mexican population and a history of isolation with migration were the best fit models. Thus, we only vary the demographic model for one of the nominate populations while it is in isolation prior to admixture. Parameters estimated are labled on each model. Population sizes (Ne) during different events are labeled: current (Ne-current); ancestral (Ne-anc); bottleneck (Ne-bot); end bottleneck (Ne-rec); end growth (Ne-end); in isolation (Ne-split). Labeling for time parameters: beginning of growth period (Tgrow); bottleneck start (Tbot); bottleneck end (Trec); divergence time (Tsplit); and merger time (Tmerge).

Figure 3.7: The influence of each level of missing data (5%, 10%, 15%, 25%) on principal components analysis. Results are presented for the full dataset (n=191); Mexican dataset (n=56); and continental/'typical' dataset (n=135).

150
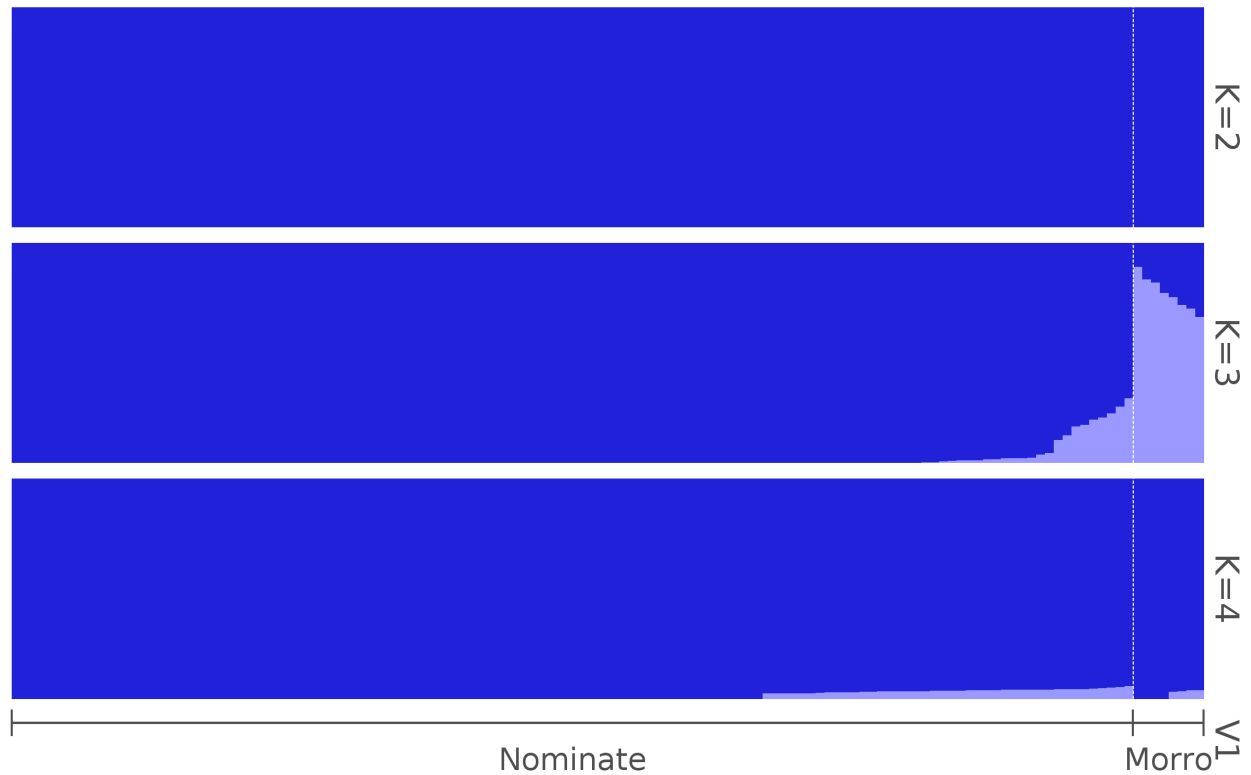
Figure 3.8: FastStructure results for the nominate clade of Savannah Sparrows with a logistic prior. K=1 was found to be the best-supported model and the results plotted for K=2-4 also show little structure across the range. Only individuals from Morro Bay exhibit some structure at K=3. Barplots were generate in the r-package pophelper v. 1.1.6 (Francis 2016).
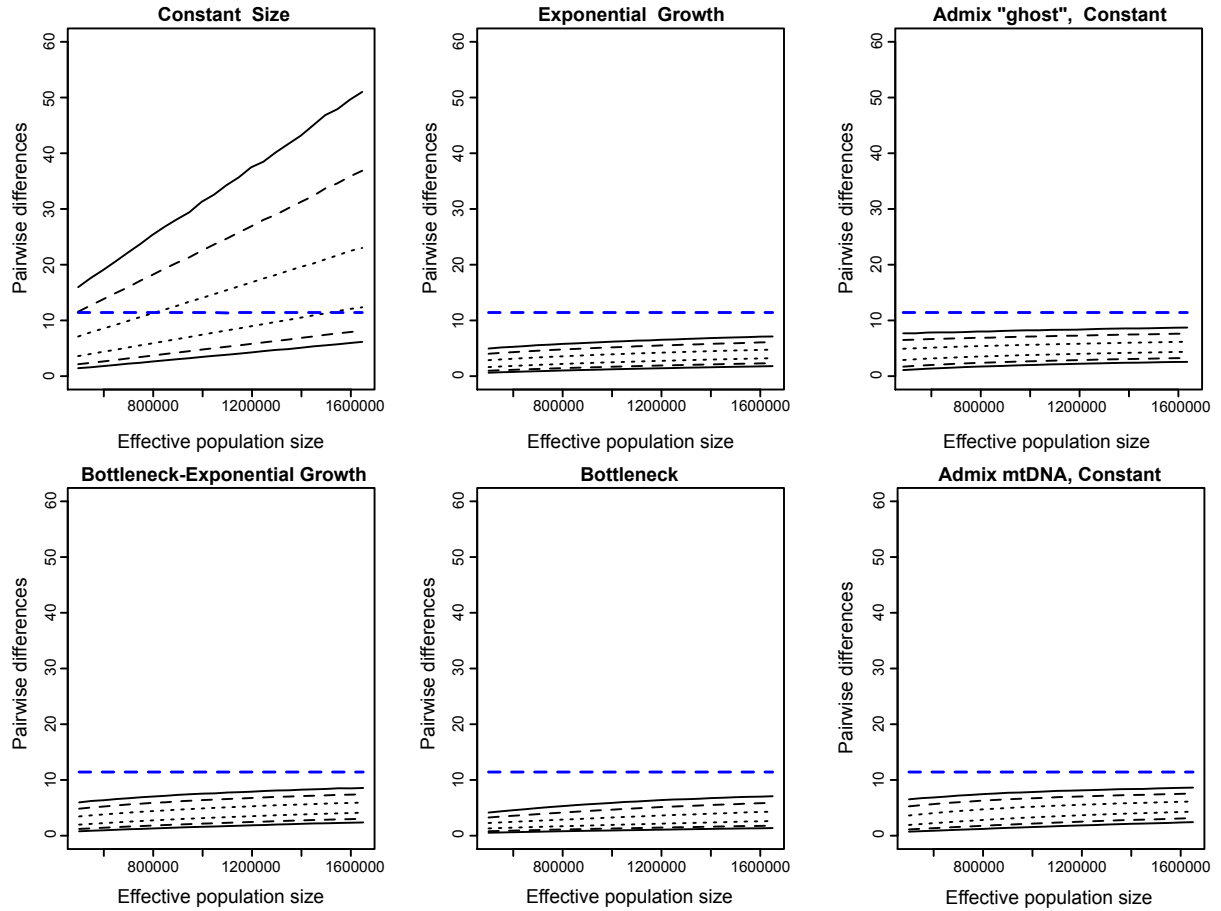
Figure 3.9: Simulation results from *ms* that were designed to relate estimated demographic histories for the nominate population in ∂a∂i to observed level of average pairwise differences (pi) in Savannah Sparrow mtDNA. For each of these six different models all parameters are based on estimates from ∂a∂i except for effective population size. Rather than assume that mtDNA Ne was equal to 1/4 nuclear Ne, we directly estimated a range of Ne for *ND2* based on upper and lower bounds ($\pm$ 1 sd of the mean) of nucleotide diversity (0.011 $\pm$ 0.006) divided by μ (1.1×10^{-8}/site/generation). This gave bounds on Ne from 500,000 to 1,650,000 and we ran sets of simulations for each 50,000 increment (24 total). For each of the 24 Ne values we ran 100,000 simulations with all other model parameters remaining the same. Blue dashed line shows the observed value of pi for Savannah Sparrow mtDNA estimated in Arlequin 3.5. Black solid, dashed, and dotted lines represent the 99th, 95th and 75th percentiles, respectively, of pi distributions generated from the 100,000 simulations performed for each parameter set.
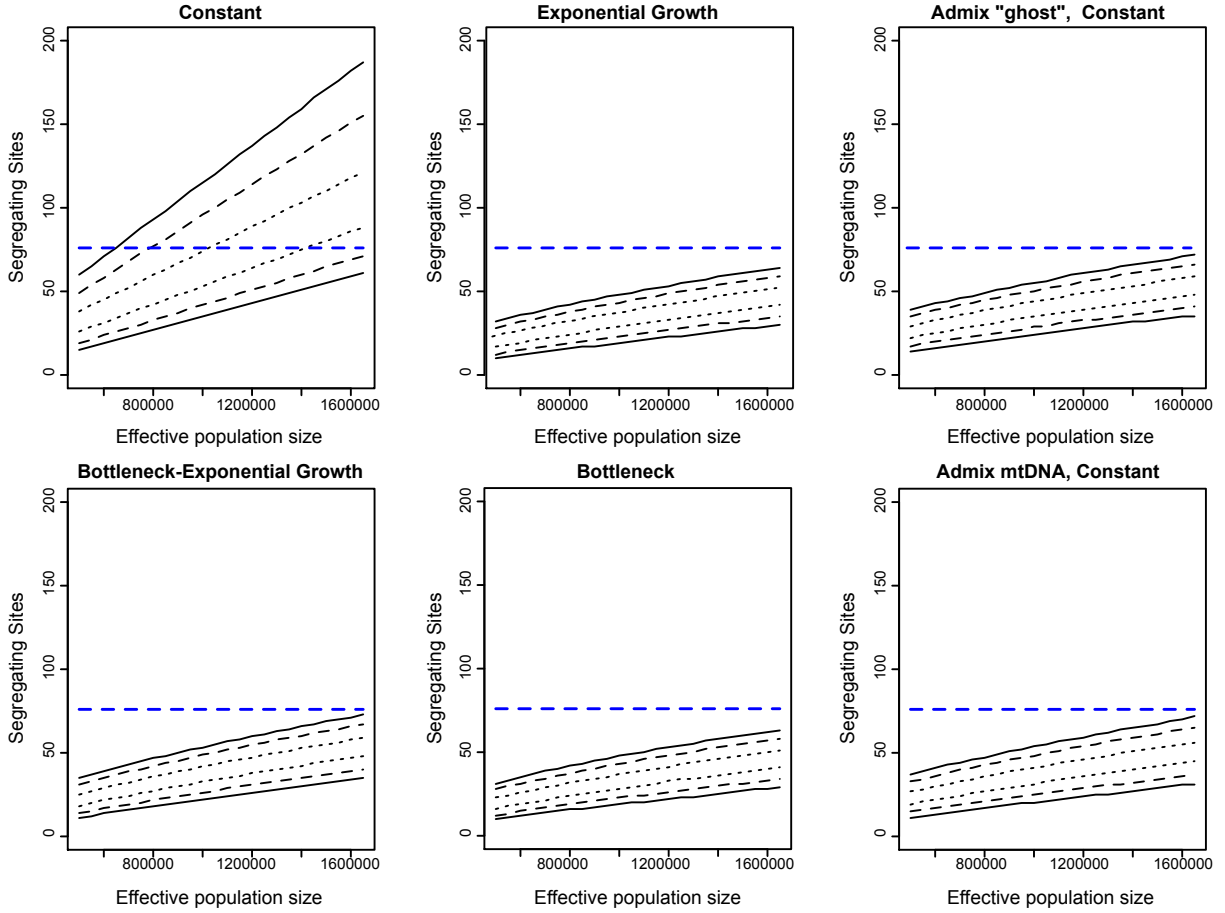
Figure 3.10: Simulation results from *ms* that were designed to relate estimated demographic histories for the nominate population in ∂a∂i to observed level of segregating sites (SS) in Savannah Sparrow mtDNA. For each of these six different models all parameters are based on estimates from ∂a∂i except for effective population size. Rather than assume that mtDNA Ne was equal to 1/4 nuclear Ne, we directly estimated a range of Ne for *ND2* based on upper and lower bounds ($\pm$ 1 sd of the mean) of nucleotide diversity (0.011 $\pm$ 0.006) divided by μ (1.1x10^{-8}/site/generation). This gave bounds on Ne from 500,000 to 1,650,000 and we ran sets of simulations for each 50,000 increment (24 total). For each of the 24 Ne values we ran 100,000 simulations with all other model parameters remaining the same. Blue dashed line shows the observed value of SS for Savannah Sparrow mtDNA estimated in Arlequin 3.5. Black solid, dashed, and dotted lines represent the 99th, 95th and 75th percentiles, respectively, of SS distributions generated from the 100,000 simulations performed for each of the 24 parameter sets.
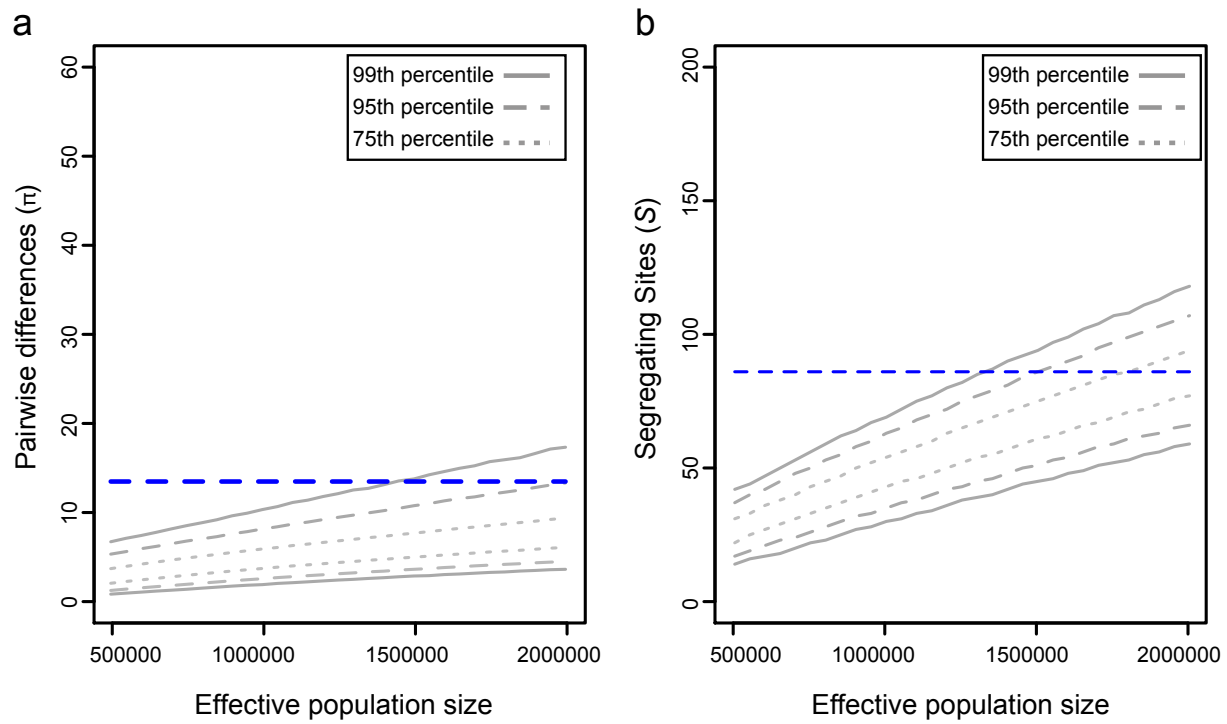
Figure 3.11: Results from *ms* simulations based on lower bound (95% CI) parameter estimates from the best-supported demographic model in ∂a∂i analyses (Fig. 6). Simulations are based on 204 individuals (163 nominate clade and 41 Mexican clade) across a range of effective population sizes relevant to empirical estimates of mtDNA Ne with the range of Ne based on variance in nucleotide diversity. For average pairwise differences (a) and number of segregating sites (b) solid, dashed, and dotted gray lines represent 99%, 95%, and 75% quantiles, respectively, of these summary statistics calculated from across 100,000 simulations for each effective population size. Blue line represents empirical estimate of mtDNA average pairwise differences (13.48) and number of segregating sites (86).
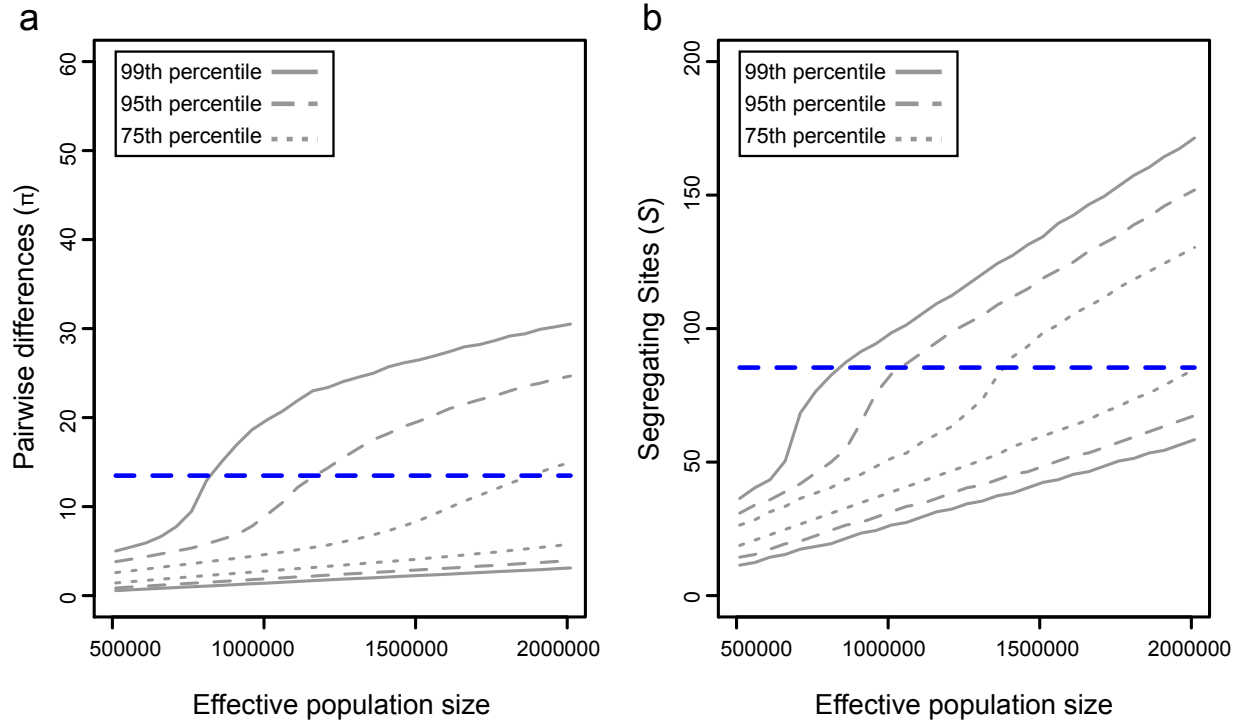
Figure 3.12: Results from *ms* simulations based on upper bound (95% CI) parameter estimates from the best-supported demographic model in ∂a∂i analyses (Fig. 6). Simulations are based on 204 (163 nominate clade and 41 Mexican clade) individuals across a range of effective population sizes relevant to empirical estimates of mtDNA Ne with the range of Ne based on variance in nucleotide diversity. For average pairwise differences (a) and number of segregating sites (b) solid, dashed, and dotted gray lines represent 99%, 95%, and 75% quantiles, respectively, of these summary statistics calculated from across 100,000 simulations for each effective population size. Blue line represents empirical estimate of mtDNA average pairwise differences (13.48) and number of segregating sites (86).
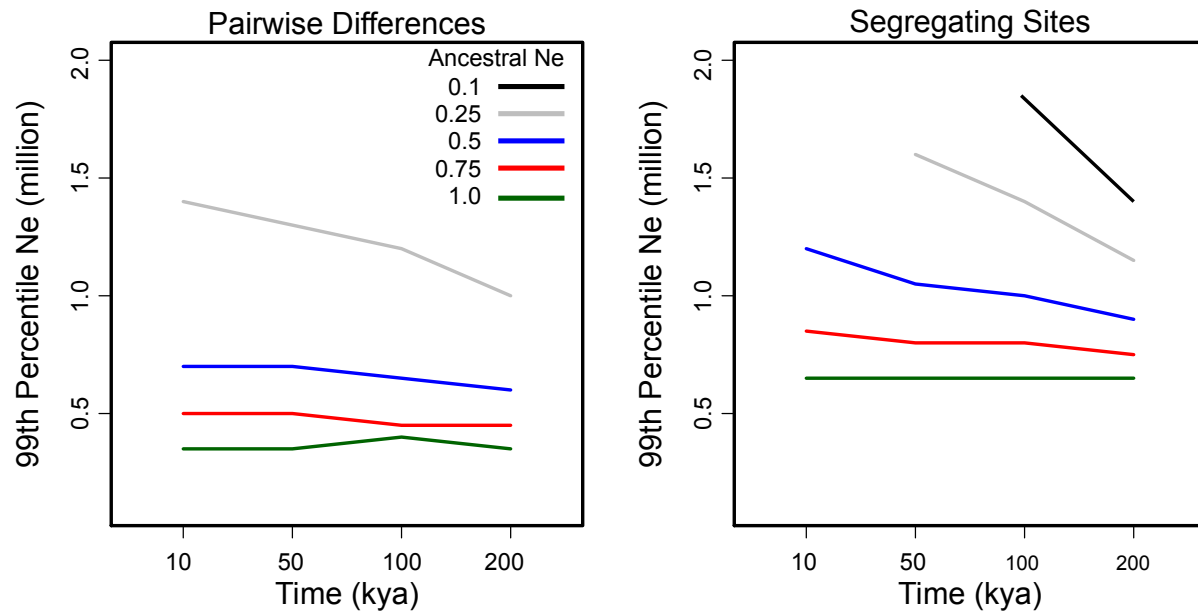
Figure 3.13: Summary of simulation results from a panmixia with constant population size (Ne) model. Shows the influence of variation in ancestral Ne and time since change from ancestral Ne on the 99th percentile Ne (in millions). The 99th percentile Ne represents the lowest simulated current Ne where observed mtDNA statistics (pi and SS) fall within the 99th percentile of the 25,000 iterations performed for each Ne. Different colors represent varying values for the ancestral Ne parameter with each value representing the proportion of ancestral Ne relative to current Ne. For each parameter set Ne was varied from 100,000 to 2 million and under some conditions the Ne required to match observed mtDNA diversity exceeded 2 million and is thus not encompassed on the graph (e.g. ancestral Ne = 0.1).
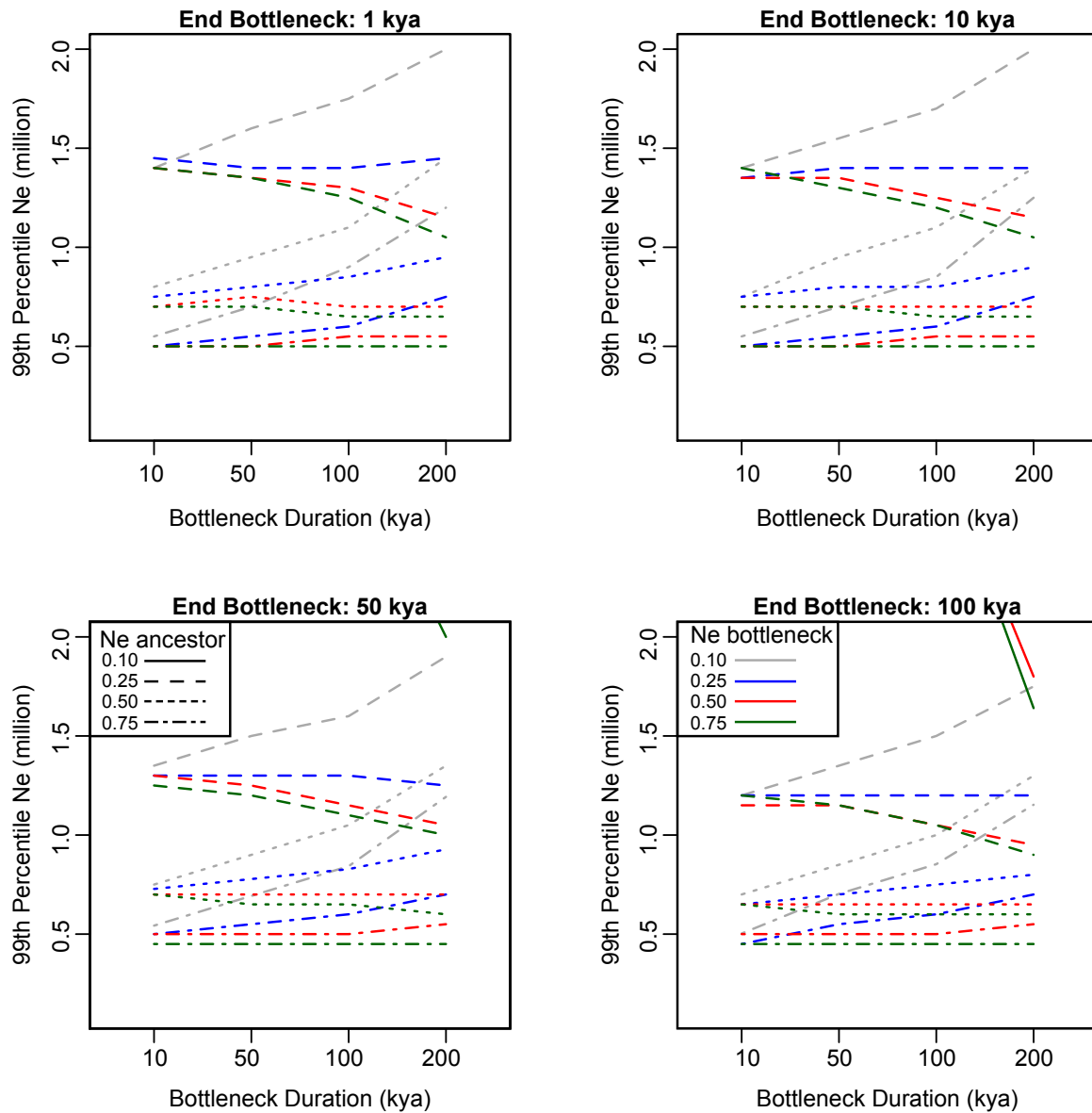
Figure 3.14: Summary of simulation results from a panmixia with bottleneck model. Shows the influence of variation in ancestral Ne, bottleneck Ne, duration of bottleneck and time since the end of the bottleneck on the 99th percentile Ne (in millions). The 99th percentile Ne represents the lowest simulated current Ne where observed mtDNA average pairwise differences (pi) fall within the 99th percentile of the 25,000 iterations performed for each Ne. Different colors represent varying values for the bottleneck Ne parameter with each value the proportion of bottleneck Ne relative to current Ne and different line types corresponding to the different simulated values for ancestral Ne. For each parameter set Ne was varied from 100,000 to 2 million and under some conditions the Ne required to match observed mtDNA diversity exceeded 2 million and is thus not encompassed on the graph (e.g. ancestral Ne = 0.1).
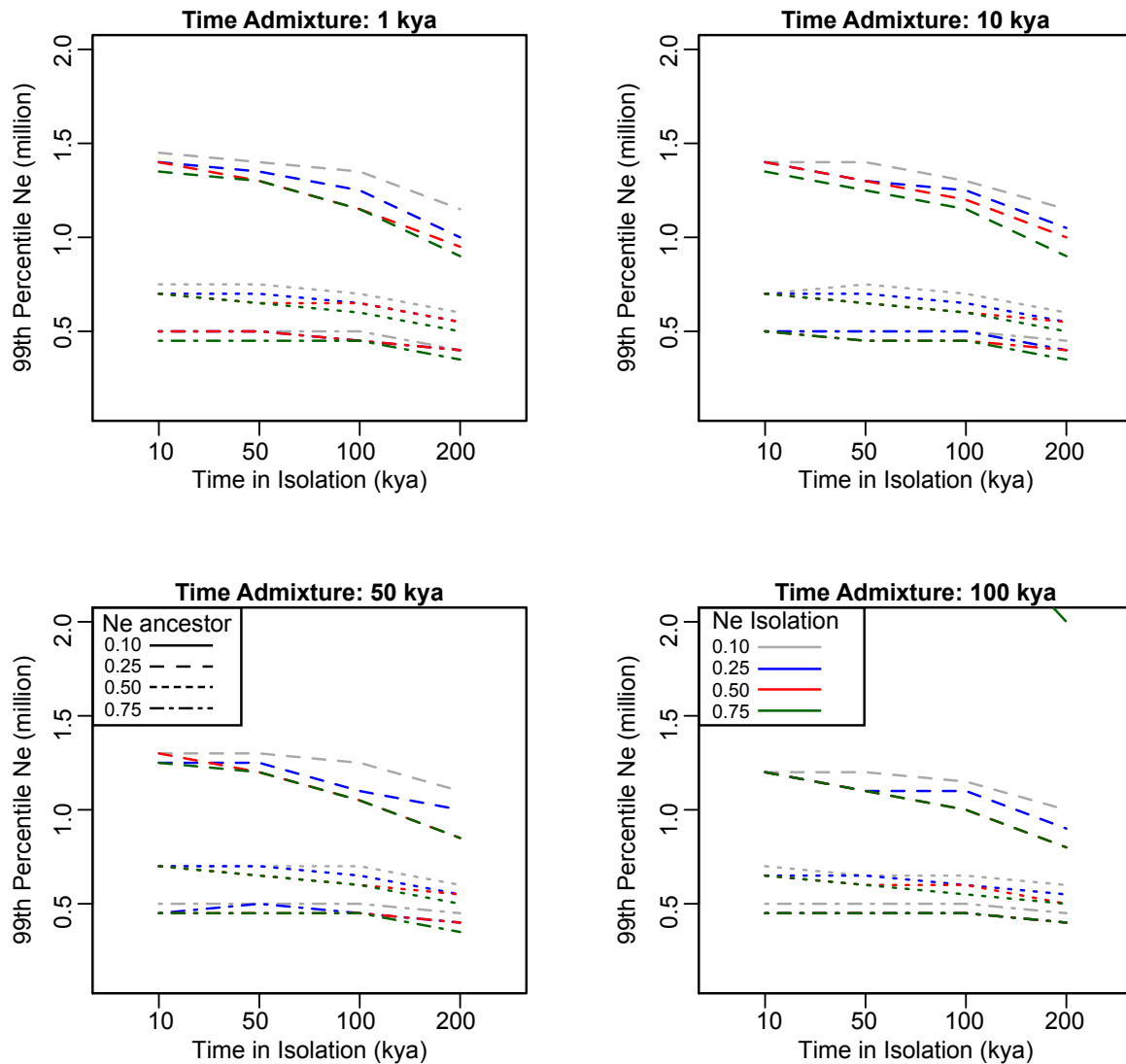
Figure 3.15: Summary of simulation results from a model where two populations diverge, evolve in isolation, and then merge into a single population via admixture. The plot shows the influence of variation in ancestral Ne, Ne for each population during isolation, the length of time populations remain isolated, and time since admixture of the two populations on the 99th percentile Ne (in millions). The 99th percentile Ne represents the lowest simulated current Ne where observed mtDNA average pairwise differences (pi) fall within the 99th percentile of the 25,000 iterations performed for each Ne. The admixture proportion (f) was set to 0.5. Different colors represent varying values for the isolation Ne parameter with each value the proportion of isolation Ne relative to current Ne and different line types corresponding to the different simulated values for ancestral Ne (i.e. Ne before population divergence). For each parameter set Ne was varied from 100,000 to 2 million and under some conditions the Ne required to match observed mtDNA diversity exceeded 2 million and is thus not encompassed on the graph (e.g. ancestral Ne = 0.1).
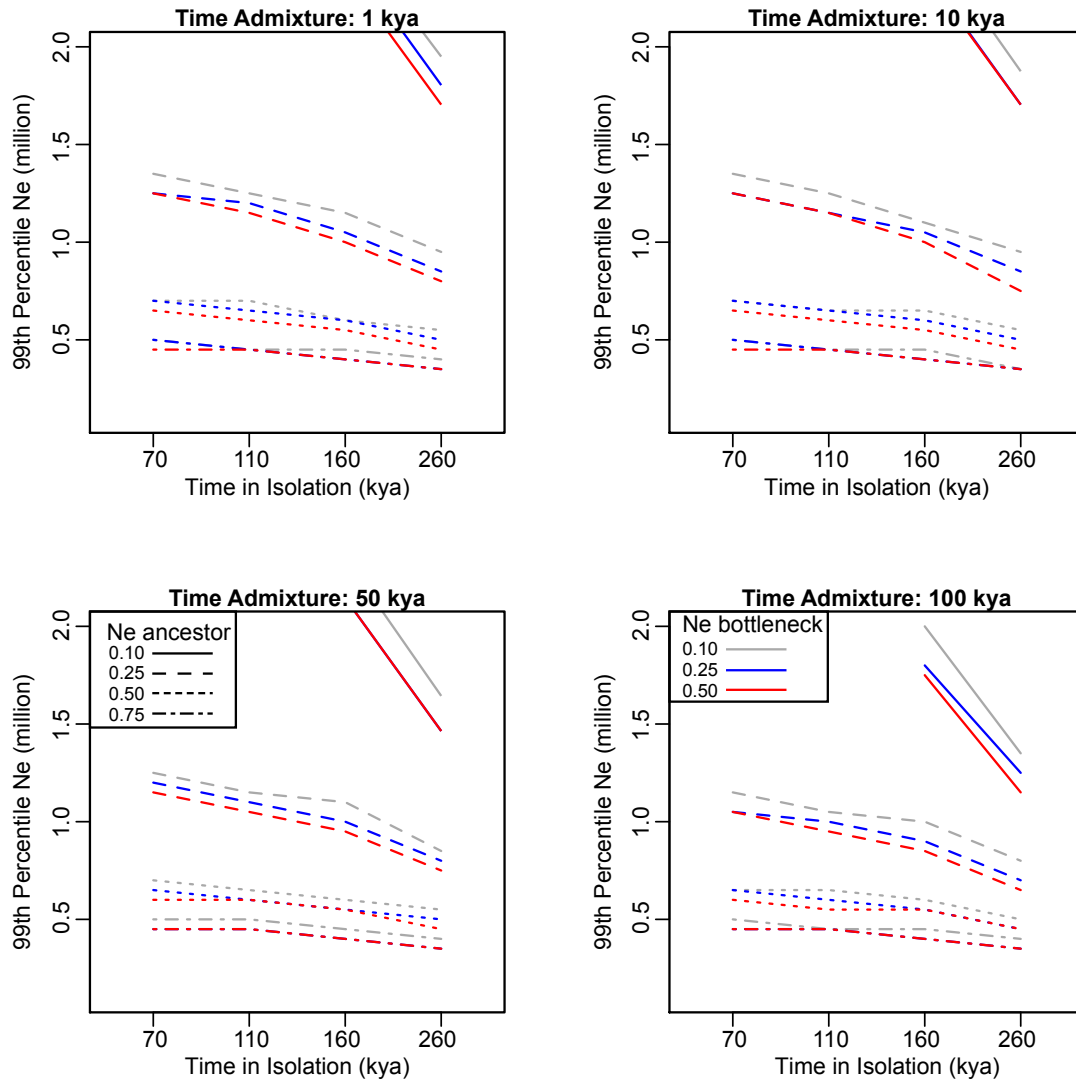
Figure 3.16: Summary of simulation results from a model where two populations diverge, evolve in isolation, both isolated populations experience a bottleneck, and then merge into a single population via admixture. The plot shows the influence of variation in ancestral Ne, bottleneck Ne for each population, the length of time populations remain isolated, and time since admixture of the two populations on the 99th percentile Ne (in millions). The 99th percentile Ne represents the lowest simulated current Ne where observed mtDNA average pairwise differences (pi) fall within the 99th percentile of the 25,000 iterations performed for each Ne. For both populations the isolation Ne before and after the bottleneck was set to 0.75, admixture proportion (f) was 0.5, duration of the bottleneck was 50 kyr, and admixture occurred 10 kyr following the end of the bottleneck. Different colors represent varying values for the isolation Ne parameter with each value the proportion of isolation Ne relative to current Ne and different line types corresponding to the different simulated values for ancestral Ne (i.e. Ne before population divergence). For each parameter set Ne was varied from 100,000 to 2 million and under some conditions the Ne required to match observed mtDNA diversity exceeded 2 million and is thus not encompassed on the graph (e.g. ancestral Ne = 0.1).